

## 1.22 Deep Earth Structure: Lower Mantle and D''

T Lay, University of California Santa Cruz, Santa Cruz, CA, USA

© 2015 Elsevier B.V. All rights reserved.

<b>1.22.1</b>	<b>Lower Mantle and D'' Basic Structural Attributes</b>	684
1.22.1.1	Elastic Parameters, Density, and Thermal Structure	684
1.22.1.2	Mineralogical Structure	685
<b>1.22.2</b>	<b>One-Dimensional Lower Mantle Structure</b>	686
1.22.2.1	Body-Wave Travel Time and Slowness Constraints	687
1.22.2.2	Surface-Wave/Normal-Mode Constraints	688
1.22.2.3	Attenuation Structure	688
<b>1.22.3</b>	<b>Three-Dimensional Lower Mantle Structure</b>	689
1.22.3.1	Seismic Tomography	689
1.22.3.2	Dynamic Structures	691
<b>1.22.4</b>	<b>D'' Region</b>	693
1.22.4.1	Large-Scale Seismic Velocity Attributes	693
1.22.4.2	Thermal Boundary Layer Aspect	694
<b>1.22.5</b>	<b>D'' Discontinuities</b>	695
1.22.5.1	Seismic Wave Tripliations	695
1.22.5.2	Phase Change in Perovskite	697
<b>1.22.6</b>	<b>Large Low-Shear-Velocity Provinces</b>	699
1.22.6.1	Seismic Velocity Properties	699
1.22.6.2	Thermal-Chemical Interpretations	701
<b>1.22.7</b>	<b>Ultralow-Velocity Zones</b>	701
1.22.7.1	Seismic Phases Used for Detection	702
1.22.7.2	Partial Melting and Chemical Anomalies	703
<b>1.22.8</b>	<b>Lower Mantle Anisotropy</b>	704
1.22.8.1	Shear-Wave Splitting Observations	704
1.22.8.2	Mineralogical/Dynamic Implications	704
<b>1.22.9</b>	<b>Small-Scale Heterogeneities</b>	705
1.22.9.1	Scattering in D''	706
1.22.9.2	Core-Mantle Boundary Topography	706
<b>1.22.10</b>	<b>Conclusions</b>	706
<b>Acknowledgment</b>		707
<b>References</b>		707

### Glossary

**Attenuation** Loss of signal amplitude during propagation. Intrinsic attenuation involves irreversible anelastic losses; scattering attenuation involves partitioning of energy into separate waves.

**CMB** The core–mantle boundary is the surface defined by the contrast in composition between mantle rocks and core molten alloy. A huge density contrast and change in physical properties make this a sharp boundary, with very limited mass flux across it at present.

**D''** Designation for the lowermost 200–300 km of the lower mantle. This region is distinct from the overlying mantle in that the seismic velocity variations are not consistent with homogeneous material under self-compression and adiabatic temperature gradient.

**LLSVP** Large low-shear-velocity province, used to describe broad regions beneath Africa and the South Atlantic and

beneath the southern Pacific, which have anomalously low shear velocities, less pronounced compressional velocity decreases, sharp lateral boundaries, and indications of higher than average densities. These features have often been labeled superplumes, but the seismic data favor them being chemically distinct, dense piles of material possibly entrained by surrounding mantle flow.

**P wave** Elastic wave involving compressional and dilatational motion of the medium as the wave propagates and the faster of the two seismic waves. Can transit both solid and fluid media.

**S wave** Elastic wave involving shearing motion of the medium with no volumetric change as the wave propagates and the slower of the two seismic waves. Can only transit solid media.

### 1.22.1 Lower Mantle and D'' Basic Structural Attributes

Earth's lower mantle is a thick layer of rock extending downward more than 2000 km from the transition zone to the core-mantle boundary (CMB) at an average depth of 2891 km. Seismology provides the basis for defining the lower mantle, as it was evident from the consideration of even the earliest global P-wave and S-wave travel time curves that this region of the interior has relatively smoothly increasing seismic velocities with depth, with an overall velocity gradient significantly reduced from that in the overlying transition zone.

The upper limit of the lower mantle has various definitions; many geophysicists associate it with the 650 km deep seismic velocity discontinuity, while others prefer to designate it at a greater depth of about 800 km, where there tends to be a reduction in radial velocity gradients in detailed seismic velocity models, as well as intermittent reports of a seismic discontinuity (e.g., [Datt and Muirhead, 1976](#); [Revenaugh and Jordan, 1991](#)). The variety of phase transformations for upper mantle minerals olivine, enstatite, and garnet to their high-pressure polymorphs that characterize the transition zone all culminate in transitions to magnesium silicate perovskite  $[(\text{Mg},\text{Fe})\text{SiO}_3]$ , ferropericlase  $[(\text{Mg},\text{Fe})\text{O}]$ , and calcium perovskite  $[\text{CaSiO}_3]$ . The latter transitions should largely go to completion by about 800 km depth, which can thus be viewed as the base of the transition zone. The subsequent stability of the abundant magnesium silicate perovskite mineral over great pressure and temperature ranges is the probable explanation for the relatively smooth velocity gradients observed across the lower mantle, with self-compression and a nearly adiabatic thermal gradient resulting in smoothly increasing density, rigidity, incompressibility, and associated P-wave and S-wave seismic velocities down to near the CMB.

A few hundred kilometers above the CMB seismic velocities have more complex structure, with abrupt increases or discontinuities in velocity occurring in regions of relatively high seismic velocity, likely as a result of a phase transition from magnesium silicate perovskite to the postperovskite phase ([Hirose, 2006](#); [Murakami et al., 2004](#); [Shim, 2008](#)), along with enhanced lateral variations that indicate the presence of thermal and chemical heterogeneities in a boundary layer above the CMB (e.g., [Garnero, 2000](#); [Garnero and McNamara, 2008](#); [Lay and Garnero, 2004](#); [Trønnes, 2009](#)). Based on the seismic evidence for inhomogeneity in the structure, the lowermost few hundred kilometers of the lower mantle is called the D'' region (harkening back to an early nomenclature in which the lower mantle was labeled the D shell and then subdivided into D' and D''; see [Bullen, 1949](#)). At the base of the lower mantle, there are localized regions with very strong seismic velocity reductions that may be explained by the presence of a melt component or strong iron enrichment within the lower mantle rock. The CMB separates the silicate and oxide minerals of the lower mantle from the molten iron alloy of the core, with the contrasts in physical properties such as density, viscosity, and rigidity across the CMB being as large or larger than those at the surface of the Earth.

Despite its generally simple overall seismological structure, the lower mantle appears to be undergoing large-scale dynamic processes. These are revealed by second-order features of the

seismological models that have only begun to be resolved over the past 30 years or so. The great pressures existing in the lower mantle suppress the sensitivity of seismic wave velocities to variations in temperature and composition, muting the detectable effects. Progress in imaging the few percent three-dimensional variations in seismic velocities is unveiling the dynamic complexity of the lower mantle and indicates regions of convective upwellings, downwellings, and large-scale chemical heterogeneities that may have accumulated over time in the deep mantle. While current understanding of the dynamic regime remains limited, it appears that the lower mantle plays a major role in regulating heat flux from the core, in cycling heat out of the interior, and in segregating chemical heterogeneities for long intervals of time, giving rise to geochemical anomalies observed at surface volcanic sites.

#### 1.22.1.1 Elastic Parameters, Density, and Thermal Structure

P-wave and S-wave velocities and density increase smoothly across the lower mantle to the D'' region in all one-dimensional seismic velocity models for the Earth. [Figure 1](#) shows the variations in these properties as given by the Preliminary Reference Earth Model (PREM), which was based on a large number of body-wave travel times and free-oscillation eigenfrequencies ([Dziewonski and Anderson, 1981](#)). Below the abrupt seismic velocity and density increases near 650–670 km deep, which are primarily attributed to the dissociative phase transition of  $(\text{Mg},\text{Fe})_2\text{SiO}_4$   $\gamma$ -spinel (ringwoodite) to  $(\text{Mg},\text{Fe})\text{SiO}_3$  perovskite plus  $(\text{Mg},\text{Fe})\text{O}$  ferropericlase (e.g., [Ito and Takahashi, 1989](#); [Ito et al., 1990](#); [Yu et al., 2007](#)), all the way down to the CMB, there are no abrupt changes in properties that demand global large-scale layering of the lower mantle (e.g., [Green and Falloon, 1998](#)). The bounds on the seismic velocity models given in [Figure 1](#) indicate the range of velocities that are admissible for one-dimensional models, based on observed travel time fluctuations for seismic body waves. The relatively tight range of velocity bounds indicate that if there are any velocity discontinuities in the deep mantle, they are less than a few percent or there are strong lateral variations in the depths of the structure such that it is not well represented by a one-dimensional model.

In fact, there are many studies inferring the presence of localized reflectors or scatterers in the depth range 650–1200 km depth (e.g., [Kaneshima and Helffrich, 2009](#); [Muirhead and Hales, 1980](#); [Niu and Kawakatsu, 1997](#); [Vinnik et al., 1998a](#)), but the observations are intermittent, and there is, as yet, no agreed upon globally extensive discontinuity below 650-km depth that would be warranted in a one-dimensional Earth model. This fact is often invoked to support the idea that the lower mantle is chemically uniform, but one should keep in mind that chemical layering is likely to involve rather subtle changes in seismic velocities and details of the density structure are not well resolved by normal-mode observations. Thus, it is possible that the lower mantle is chemically stratified, perhaps with depth variations in Si or Fe content, with substantial topography on any chemical contrasts (e.g., [Anderson, 1991, 1998](#); [Kellogg et al., 1999](#); [Murakami et al., 2012](#)). Assessing this possibility requires consideration of three-dimensional velocity structures, but even then, it may

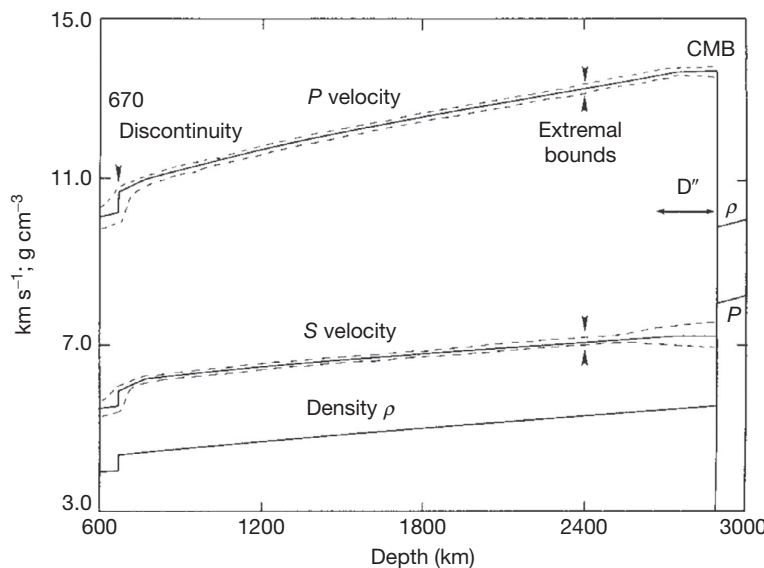


**Figure 1** Variation of seismic velocities and density through the lower mantle for model Preliminary Reference Earth Model (PREM) (Dziewonski and Anderson, 1981), along with the extremal bounds that indicate the confidence intervals for spherically averaged models based on travel time data (Lee and Johnson, 1984). The D'' region is the lowermost 200–300 km of the lower mantle overlying the core–mantle boundary (CMB). Reproduced from Lay T (1989) Structure of the core–mantle transition zone: A chemical and thermal boundary layer. *Eos, Transactions of the American Geophysical Union* 70: 49, 54–55, 58–59.

be difficult because velocity discontinuities associated with any chemical contrasts are likely to be relatively small.

The bounds on one-dimensional S-wave velocity models tend to flare in the lower 300 km of the mantle, indicating larger variability in S-wave travel times for waves traversing the D'' region above the CMB. In this region, seismic waveform modeling has resulted in localized velocity models with 1–3% abrupt increases in shear velocity and large-scale regions with 3–6% low shear velocity. There is no average one-dimensional model that represents the D'' structure well, and the lateral variations must be characterized with three-dimensional structures in order to assess their significance. P-wave observations also indicate abrupt increases in P-wave velocity in some regions, but in general, the P-wave structure is less heterogeneous than for S waves. At the very base of the lower mantle, within tens of kilometers above the CMB, there are localized regions with very pronounced reductions in both P-wave velocity and S-wave velocity, which are called ultralow velocity zones (ULVZs). ULVZs may represent a transition zone from mantle to core, but they must be undetectably thin ( $<\sim 5$  km) or not present in many regions.

### 1.22.1.2 Mineralogical Structure

The composition and mineralogy of the lower mantle is not directly determined from seismic observations and must be deduced based on models for the bulk composition of the Earth along with experimental and theoretical mineral physics that reproduces observed density and elastic velocity profiles for appropriate pressures and temperatures. Given the experimental determination of stability of the magnesium silicate perovskite phase (Liu, 1974) as the polymorph of predominant upper mantle minerals subjected to lower

mantle conditions, along with the chondritic Earth model, there is high confidence that  $(\text{Mg}_x\text{Fe}_{1-x})\text{SiO}_3$  perovskite is the primary mineral form in the lower mantle (e.g., Fiquet et al., 2000; Gong et al., 2004; Knittle and Jeanloz, 1987; Shim et al., 2001, 2004; Wentzcovitch et al., 2004). The value of  $x$  (the magnesium number) is probably in the range 0.8–0.9, although some aluminum substitution is very likely to exist in lower mantle perovskites as well. The experimental and chondritic model constraints on mineralogy also favor the presence of  $(\text{Mg}_x\text{Fe}_{1-x})\text{O}$ , with  $x$  again in the range 0.8–0.9 overall, although it could be much lower in some cases, as well as some Ca perovskite. Other minor phases are likely to exist, but constraints on their abundance are very limited.

Extensive theoretical and experimental mineral physics research continues to characterize the equations of state, effects of minor components like Al, element partitioning, and physical properties of the following primary lower mantle minerals (or low-pressure analog minerals): magnesium silicate perovskite (e.g., Aizawa and Yoneda, 2006; Andrault et al., 2007; Auzende et al., 2008; Boffa Ballaran et al., 2012; Carrez et al., 2007a; Cordier et al., 2004; Deng et al., 2008; Dorfman et al., 2012; Ferré et al., 2007; Irfune et al., 2010; Ito and Toriumi, 2010; Jackson and Kung, 2008; Jackson et al., 2005; Jung et al., 2010; Katsura et al., 2009; Lundin et al., 2008; Miyajima et al., 2009; Mosenfelder et al., 2009; Murakami et al., 2007a; Nishio-Hamane et al., 2008; Nishiyama et al., 2007; Ono et al., 2006a,b; Panero et al., 2006; Ricolleau et al., 2009; Saikia et al., 2009; Sakai et al., 2009a; Tange et al., 2009, 2012; Vanpeteghem et al., 2006a,b; Xu et al., 2011; Yamazaki et al., 2009), MgO and ferropericlase (e.g., de Koker, 2010; Fukui et al., 2012; Gleason et al., 2011; Jackson et al., 2006; Komabayashi et al., 2010; Marquardt et al., 2009b; Murakami et al., 2009; Speziale et al., 2007a,b).

Tsujino and Nishihara, 2010; Wu et al., 2008), and calcium perovskite (e.g., Adams and Oganov, 2006; Jung and Oganov, 2005; Kojitani et al., 2009; Komabayashi et al., 2007; Kudo et al., 2012; Li et al., 2006b,c; Miyagi et al., 2006, 2009; Stixrude et al., 2007; Sueda et al., 2006).

Transport properties for the major minerals such as electrical conductivity are also being addressed (e.g., Ono et al., 2006b; Tarits and Mandéa, 2010; Velimsky, 2010). With the possibility of lithospheric slabs sinking into the lower mantle, the deep mantle properties for mid-ocean ridge basalt (MORB) compositions (in the high-pressure eclogitic phase and in lower mantle polymorphs) are also being explored (e.g., Hirose et al., 2005a; Kono et al., 2007; Mookherjee, 2011; Ohta et al., 2008a, 2010b; Ricolleau et al., 2010; Tsuchiya, 2011). Other minor phases such as poststishovite (e.g., Bolfan-Casanova et al., 2009; Lakshtanov et al., 2007; Nomura et al., 2010; Wang et al., 2012) and various carbonates (e.g., Boulard et al., 2012; Lavina et al., 2009, 2010; Litasov et al., 2008; Mao et al., 2011a; Oganov et al., 2006, 2008) are likely to exist in the lower mantle, but constraints on their small abundances are very limited. This huge outpouring of experimental and theoretical mineral physics results reflects great advances made in the last decade in both laboratory measurements and first-principles computations of mineral phase equilibria and material properties. Comparisons of predictions with seismic observations are still not uniquely diagnostic of the lower mantle composition due to many trade-offs and uncertainties in mineral composition, accompanied by new discoveries in material properties (e.g., Matas et al., 2007).

Recent experimental and first-principles work (Badro et al., 2003, 2004; Hofmeister, 2006; Li et al., 2004, 2005; Lin and Tsuchiya, 2008; Lin et al., 2005; Speziale et al., 2005; Sturhahn et al., 2005; Zhang and Oganov, 2006) has established that at high pressure, Fe, normally in its high-spin state for both  $\text{Fe}^{2+}$  and  $\text{Fe}^{3+}$  in perovskite and ferropericlase in the shallow lower mantle, will prefer to be in a denser, low-spin state in the lowermost mantle. This so-called spin transition can influence thermal, electric, elastic, and viscous properties of the lower mantle, and there has been a huge surge of research in the past few years to characterize the attributes of the iron spin transition and its implications. Computational and experimental efforts are quantifying the spin crossovers in ferropericlase (e.g., Ammann et al., 2011; Antonangeli et al., 2011; Cammarano et al., 2010; Chen et al., 2012a,b; Crowhurst et al., 2008; Fei et al., 2007; Kantor et al., 2006; Lin et al., 2006a,b, 2007a,b; Mao et al., 2011a,b; Persson et al., 2006; Saha et al., 2011, 2013; Speziale et al., 2007b; Tsuchiya et al., 2006a,b; Wentzcovitch et al., 2009; Wu et al., 2009; Yoshino et al., 2011) and magnesium silicate perovskite (Bengtson et al., 2008, 2009; Caracas et al., 2010; Catalli et al., 2010b, 2011; Fang and Ahuja, 2008; Fujino et al., 2012; Grocholski et al., 2009; Hsu et al., 2010, 2011; Li et al., 2006a; McCammon et al., 2008, 2010; Narygina et al., 2011; Nomura et al., 2011; Stackhouse et al., 2006b, 2007; Umemoto et al., 2008, 2010).

Implications of the spin transition for mixing dynamics and plume formation are also being considered (e.g., Bower et al., 2009; Shahnas et al., 2011), as well as effects on electrical conductivity (Ohta et al., 2007, 2010a). The various studies are not in full agreement, but most favor substantial pressure

ranges for the various spin transitions and relatively subtle effects on seismic velocities, making it difficult to directly confirm the presence of spin transitions with seismic observations.

Properties of melts in the lower mantle are critical to understanding mantle chemical evolution, and theoretical and experimental studies have addressed issues of melt density and iron fractionation and Si and O partitioning between liquids and perovskite and ferropericlase in the deep mantle (e.g., de Koker and Stixrude, 2009; de Koker et al., 2013; Fiquet et al., 2010; Frost et al., 2004; Liebske and Frost, 2012; Mosenfelder et al., 2007; Seagle et al., 2008; Stixrude et al., 2009; Terasaki et al., 2007; Zhang and Fei, 2008; Zhang and Guo, 2009).

When one considers the mineralogy of the lower mantle, it is essential to keep in mind that there has undoubtedly been extensive chemical processing, melting, and mixing. This would have occurred during the energetic processes of accretion and core formation, as a result of early large impacts, and as an ongoing consequence of mantle convection and chemical differentiation involving crustal formation and recycling. The huge density increase at the CMB, larger than that at Earth's surface, provides an environment favorable for the accumulation of dense silicate and oxide materials, a region toward which dense iron-rich materials may settle, and a chemically active environment in which mantle rocks and core alloys may exchange elements over time. Geophysical constraints on the precise mineralogy and chemistry are quite limited, and we lack direct access to samples of lower mantle rocks, so various mineralogical scenarios for the lower mantle, particularly for minor components, can be considered as long as they are shown to agree overall with the seismological information available for the region. While high viscosity of the lower mantle may allow chemical heterogeneities to persist for long intervals of time, the notion of a primitive, unprocessed lower mantle composition is at odds with prevailing notions of Earth's formation and evolution. Presumably huge amounts of iron have separated from the mantle, and there has been extensive melting, which likely would lead to volatile depletion of the deep mantle and chemical stratification that may or may not have survived subsequent entrainment.

## 1.22.2 One-Dimensional Lower Mantle Structure

The most direct constraints on lower mantle structure are provided by seismic waves that traverse the interior. The main observables of importance are the travel times of P waves and S waves, any waveform complexities arising from interactions with contrasts in properties in the rocks, S-wave splitting produced by anisotropy, and frequency-dependent amplitude behavior of the seismic waves that can constrain the anelasticity of the lower mantle. The average lower mantle seismic velocities have been determined by both classical arrival time inversion and normal-mode analysis, with the latter also refining early estimates of the density structure that had been based on velocity-density systematics, integral constraints provided by Earth's mass and moment of inertia, and piecewise integration of seismic velocity models using the Adams–Williamson equation (Adams and Williamson, 1923). With the early

recognition of the general simplicity of lower mantle structure, most research prior to 1980 focused on developing robust one-dimensional models for lower mantle structure.

### 1.22.2.1 Body-Wave Travel Time and Slowness Constraints

Observations of travel times of seismic waves at varying distances from earthquake and explosion sources for which the source locations and origin times are either known or solved for are plotted in travel time curves, as shown for shallow focus events in [Figure 2](#). This classic display of seismic observations immediately reveals two defining attributes of the Earth: The deep structure must be largely radially symmetrical, as that is required for having tightly defined travel time branches for each path through the Earth, and the travel times of major phases such as P, PP, S, and SS are smoothly increasing functions in the angular distance ( $\Delta$ ) range 30–100°, which corresponds to the range where the seismic wave fronts turn in the lower mantle. The smooth, continuous curves obtained by fitting the observations can be inverted for one-dimensional models of seismic velocity versus depth using classic methods such as the Herglotz–Wiechert inversion or by computer modeling (see [Lay and Wallace, 1995](#)). The slope of a travel time curve at a given angular distance,  $\Delta T/d\Delta$ ,

gives the seismic ray parameter and its inverse the apparent velocity. These are related to the geometry of the wave front as it sweeps through the Earth and the velocity at the depth in the Earth where the wave turns back toward the surface causing it to arrive at a particular distance. The smooth, concave downward curvature of P-wave and S-wave travel time curves beyond 30° directly implies smoothly increasing velocities with depth in the lower mantle. The ray parameter can be estimated either from a smoothed travel time curve or by direct measurement of relative arrival times of a given seismic phase across an array of closely spaced receivers.

Global observations of body-wave travel times and measurements of slopes of the travel time curves by seismic array analyses proliferated in the 1960–1990s, with many radially symmetrical Earth models for the lower mantle being produced (e.g., [Chinnery and Toksöz, 1967](#); [Dziewonski and Anderson, 1981](#); [Hales and Roberts, 1970](#); [Hales et al., 1968](#); [Herrin, 1968](#); [Johnson, 1969](#); [Kennett and Engdahl, 1991](#); [Morelli and Dziewonski, 1993](#); [Randall, 1971](#); [Sengupta and Julian, 1978](#); [Uhrhammer, 1978](#)). While the variations in lower mantle velocities at a given depth among these models are <1%, there is still great importance in having an accurate reference model both for earthquake location procedures and for use as a background model in tomographic analyses. Thus, efforts to improve the average lower mantle parameters continue, with increasing quantities of data and variety of phase types being incorporated into the analysis ([Masters et al., 1999](#)). All of these one-dimensional lower mantle models have smooth velocity gradients like those in the PREM model ([Figure 1](#)).

The small variations between lower mantle radial velocity models have still received much attention because any departure from homogeneity (as expected for self-compression of uniform composition material) would have major implications for possible chemical layering or phase changes. P and S velocities throughout the lower mantle above the D'' region are bounded to within about  $\pm 0.1 \text{ km s}^{-1}$  in terms of an average model (e.g., [Lee and Johnson, 1984](#)). This tight bound ([Figure 1](#)) is consistent with the finding by [Burdick and Powell \(1980\)](#) that small features in ray parameter estimates from seismic arrays tend to vary azimuthally, but are not globally representative, with on average very smooth structure in the lower mantle being preferred for a one-dimensional model. There have been observations of reflections and converted phases from a velocity or impedance contrast near 900 km depth near subduction zones (e.g., [Kawakatsu and Niu, 1994](#); [Revenaugh and Jordan, 1991](#)), but this appears to be a strongly laterally varying structure ([Shearer, 1993](#)) and may be associated with steeply dipping mantle heterogeneities that are likely associated with deeply penetrating subducted slabs ([Castle and Creager, 1999](#); [Kaneshima, 2009](#); [Kaneshima and Helffrich, 1998, 2009](#); [Niu and Kawakatsu, 1997](#); [Vanacore et al., 2006](#); [Vinnik et al., 1998a](#)). Reports of arrivals reflected or scattered from other depths in the upper third of the lower mantle are numerous ([Courtier and Revenaugh, 2008](#); [Courtier et al., 2007](#); [Kito et al., 2008](#); [Rost et al., 2008](#); [Vinnik et al., 2010](#)), but at this time, there is no compelling evidence for significant laterally extensive layering of the lower mantle except near the top of the D'' region.

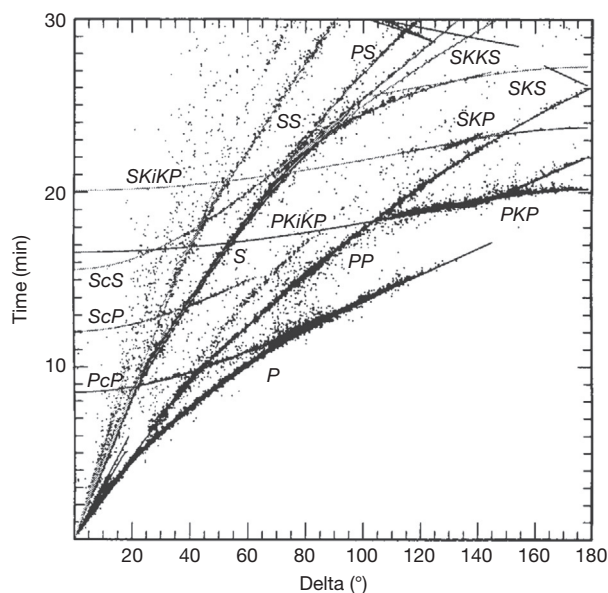


**Figure 2** Observed travel time measurements for P and S seismic phases as a function of epicentral distance in the Earth for shallow earthquake sources, along with the predicted (labeled) travel time curves for a radially symmetrical model of P-wave and S-wave velocity variations with depth. P and S are direct phases; P<sub>c</sub>P, S<sub>c</sub>P, and S<sub>c</sub>S reflect from the core–mantle boundary; PK<sub>i</sub>KP and SK<sub>i</sub>KP reflect from the inner core–outer core boundary; PP, SS, and PS reflect once from Earth's surface; and PKP, SKP, SKS, and SKKS are phases that traverse Earth's core. Reprinted from Kennett BLN and Engdahl ER (1991) Travel times for global earthquake location and phase identification. *Geophysical Journal International* 105: 429–465, with permission from the Royal Astronomical Society.

### 1.22.2.2 Surface-Wave/Normal-Mode Constraints

In addition to body-wave travel times, measurements of normal-mode eigenfrequencies play a major role in defining one-dimensional seismic velocity and, most importantly, density models for the lower mantle (see also Chapter 1.04). Normal modes correspond to standing patterns of P-wave and S-wave motions and provide constraints on the structure appropriate for relatively long-period motions compared to body-wave arrival times. The motions of normal modes involve large volumes of rock, and the varying depth sensitivity of different modes readily allows for the construction of one-dimensional models of the lower mantle. The large-scale motions allow the density structure to be sensed as well, particularly when a variety of modes are analyzed together to obtain velocity and density models. Important early one-dimensional models for lower mantle structure based largely on normal-mode observations include those of [Jordan and Anderson \(1974\)](#), [Gilbert and Dziewonski \(1975\)](#), [Dziewonski et al. \(1975\)](#), and [Dziewonski and Anderson \(1981\)](#). These models are compatible in basic structure with those obtained from body-wave analyses, but it was observed early on that there is some difference in absolute velocities between body-wave and normal mode-based models. In the late 1970s, this baseline discrepancy was recognized to be the effect of dispersion due to intrinsic attenuation as waves traverse the Earth. Attenuation causes shorter-period signals to sense slightly higher seismic velocities than longer-period signals. The development of phenomenological models for attenuation in the mantle allows an anelastic Earth model, such as PREM ([Figure 1](#)), to vary systematically in velocity as a function of wave period, reconciling body-wave and normal-mode observations (e.g., [Anderson et al., 1977](#); [Dziewonski and Anderson, 1981](#); [Kanamori and Anderson, 1977](#); [Liu et al., 1976](#)).

By far, the most important contribution to lower mantle structure from normal modes is the resolution of density structure. Body-wave travel times provide indirect sensitivity to density, and only through the use of the Adams–Williamson approach can body-wave seismic velocities be used to infer the density structure (reflected and converted phases can provide some information on density contrasts at internal boundaries). The large volume of rock in motion during normal-mode oscillations provides direct sensitivity to gravitational effects on the waves and hence to density. Thus, the development of one-dimensional seismic models from normal-mode observations explicitly involves density structure. As for the seismic velocity models, the density structure in the lower mantle involves simple increase with depth ([Figure 1](#)), with density increasing from about  $4.8 \text{ g cm}^{-3}$  at 800 km depth to  $5.56 \text{ g cm}^{-3}$  just above the CMB. The normal-mode sensitivity is limited in terms of resolving any small discontinuities but can bound the absolute levels over several hundred kilometer thickness to less than about 0.5% uncertainty for a one-dimensional model. This places some constraint on the degree of admissible lower mantle layering due to chemical density differences, although the likelihood that any deep layering may have large topographic variations induced by mantle flow complicates the interpretation of such normal-mode constraints.

### 1.22.2.3 Attenuation Structure

The Earth is not perfectly elastic, and as seismic waves travel through the interior, they undergo anelastic attenuation that gradually diminishes their amplitudes at a rate greater than that caused by geometric spreading. The mechanisms responsible for anelastic losses are generally thermally activated microscale processes such as dislocation motions and grain boundary interactions (e.g., [Anderson, 1967](#); [Minster, 1980](#); [Minster and Anderson, 1981](#)). Lacking resolution of the microscale processes, seismologists use phenomenological models that account for the macroscopic effects of anelasticity, parameterizing the corresponding departures of wave behavior from that for a purely elastic medium. The most common parameterization of attenuation is in the form of a quality factor,  $Q$ , defined as the inverse of the fractional loss of energy,  $E$ , per cycle of oscillation:  $1/Q = -\Delta E/(2\pi E)$ . Lower values of  $Q$  correspond to stronger anelastic loss or more attenuation. Infinite  $Q$  would correspond to elastic behavior. The finite  $Q$  encountered by a seismic wave in the lower mantle may vary from frequency to frequency because different mechanisms are activated for different timescales. Over a finite range of frequencies, there will be a dispersive effect, with higher frequencies sensing an unrelaxed effective modulus relative to lower frequencies. This results in physical dispersion, the reason that short-period body waves sense slightly higher seismic velocities than long-period normal modes. The magnitude of this effect depends on the absolute value and frequency dependence of  $Q$  appropriate for a given wave motion.

The lower mantle has relatively high  $Q$  values for seismic waves, and determining the structure is rather difficult due to regional variations of strong attenuation in the overlying upper mantle that must be traversed by all wave motions observed at the surface. Normal modes and averaged body-wave attenuation measurements place some constraints on the average  $Q$  values, but it is possible to satisfy most data with extremely simple models (e.g., [Anderson and Hart, 1978](#); [Dziewonski and Anderson, 1981](#); [Masters and Gilbert, 1983](#); [Widmer et al., 1991](#)). For example, the PREM model has S-wave quality factor,  $Q_{\mu} = 312$ , throughout the lower mantle, while P-wave quality factor,  $Q_s$ , increases from 759 at 670 km depth to 826 at the CMB. While there is some evidence for a low- $Q$  zone at the base of the mantle, this is not well resolved because of strong trade-offs with velocity gradients in the D'' region. The detailed frequency dependence of attenuation in the lower mantle is not yet well resolved, and there have been some recent efforts to develop new attenuation models for the lower mantle (e.g., [Ford et al., 2012](#); [Hwang and Ritsema, 2011](#); [Lawrence and Wysession, 2006](#)).

To give a sense for the anelastic dispersive effect associated with lower mantle structure, we consider the PREM S-wave velocities at a depth of 2271 km for periods of 1 s ( $7.055 \text{ km s}^{-1}$ ) and 200 s ( $7.017 \text{ km s}^{-1}$ ). The respective P-wave velocities are  $13.131$  and  $13.103 \text{ km s}^{-1}$ . The dispersive effects are small but physically must be present. Over long path lengths in the attenuating lower mantle, the small velocity differences integrate to give observable differences in body-wave and normal-mode observations that have to be accounted for. Thus, a realistic one-dimensional model of the

lower mantle must include a seismic wave attenuation structure, and that intrinsically leads the velocity model to have frequency dependence. PREM is the primary one-dimensional model with this physical dispersion explicitly being included, although Montagner and Kennett (1996) considered frequency-dependent effects. Other single-frequency models, such as ak135 (Kennett et al., 1995), have improved the travel time fit to certain seismic phases, notably core phases, but such models have not explicitly been reconciled across a broad frequency range so they are useful for earthquake location procedures, but not as a Earth model for interdisciplinary applications.

### 1.22.3 Three-Dimensional Lower Mantle Structure

One-dimensional Earth models are remarkably successful in predicting seismic wave travel times for paths traversing the lower mantle, typically accurate within a fraction of a percent for teleseismic P and S waves. This is a manifestation of the importance of gravity and chemical differentiation in producing a strongly radially stratified planet. Nonetheless, there are observable systematic travel time fluctuations at a given distance range that indicate deviations from a one-dimensional structure. Such fluctuations are particularly evident for waves traversing only the crust and upper mantle, where there are relatively strong heterogeneities. After suppressing the contributions from strong upper mantle heterogeneity either by using laterally varying models or by computing differential travel times between phases observed at a given station, the scatter in P-wave travel times relative to predictions for a one-dimensional lower mantle model is generally within  $\pm 1\text{--}2$  s (for paths with travel times of 600–700 s), while for S waves, scatter is typically  $\pm 4\text{--}6$  s (for paths with travel times of 1000–1200 s). There are some regions like that in the lowermost mantle under Africa and the central Pacific, with late S-wave arrival time anomalies of up to 15–20 s attributed to particularly anomalous lower mantle paths (e.g., Ni and Helmberger, 2003a). These variations in travel times indicate that minor aspherical elastic velocity structure exists in the lower mantle, and many seismological studies have attempted to constrain either global or regional heterogeneities in the lower mantle.

#### 1.22.3.1 Seismic Tomography

Initial investigations of aspherical structure in the lower mantle utilized moderate-sized (hundreds to a few thousand) sets of travel time anomalies (e.g., Sengupta and Toksoz, 1976) or differential travel time observations (e.g., Jordan and Lynn, 1974; Lay, 1983) to detect systematic variations relative to standard one-dimensional models. The main challenges in resolving lower mantle heterogeneity involve the uncertainty in earthquake source locations (typically, these are approximated by solving the location problem assuming a one-dimensional velocity structure, which intrinsically leads to an incorrect location estimate and consequent artifacts in the residual arrival times) and the strength of upper mantle heterogeneities (particularly near-source structures such as subducting slabs). These remain vexing problems, and it is reasonable to believe that current estimates of deep mantle heterogeneity are still biased by

incomplete suppression of event location effects and upper mantle heterogeneities. While strategies such as computing differential time anomalies (e.g., ScS-S, SKS-S, or Pcp-P differential arrival times relative to one-dimensional model predictions are commonly used) can reduce source mislocation and near-source and near-receiver structural effects due to the similarity of the ray-paths for the two phases in these regions, it remains possible that failure to account for strong lateral gradients in shallow structure causes erroneous interpretation of differential time anomalies as being due to deep mantle heterogeneity. The long-term solution to this problem is the development of very accurate models for upper mantle structure (including 3D slab and mid-ocean ridge structures) used in a self-consistent way with event locations. In general, this is still not done in most of today's large-scale tomographic inversions, but progress is gradually being made toward this goal (see also Chapters 1.06 and 1.09).

Given large numbers of observations of seismic phases with good azimuthal and ray parameter coverage from an earthquake, the effects of source mislocation can be suppressed even if a one-dimensional model or low-resolution upper mantle aspherical model is used. This can never be a perfect process unless one invokes precise *a priori* near-source information (the process of estimating the origin time always removes a baseline term from the travel times leading to anomalies with fluctuating sign even when the true anomalies should be one-sided). Seismic tomography uses the arrival time anomalies from many source–receiver combinations to invert for a parameterized version of mantle heterogeneity, ideally for well-sampled event populations where location effects are suppressed by coverage. In this case, the crossing coverage from multiple paths can build up the image of spatially varying velocity structure, although in almost every case, the amplitude of the actual heterogeneity will be intrinsically underestimated by the inversion model. This is the primary approach to imaging lower mantle heterogeneity on large and small scales; although the requirement of well-resolved source locations is seldom met in practice, approximations in ray tracing are commonly made, and iteration to attain self-consistent event locations and aspherical models is performed in only a minority of studies (e.g., Mégnin and Romanowicz, 2000). All results of lower mantle seismic tomography must thus be viewed as having limited resolution at this time, and there is significant inconsistency in small-scale structures between models. Even with these limitations, the implications of the current generation of models are profound.

One of the earliest fundamental contributions of global seismic tomography was the demonstration that coherent structure exists in the lower mantle on scale lengths of several thousand kilometers and that this unexpected configuration of large-scale deep heterogeneity can account for previously unexplained long-wavelength features in Earth's geoid (e.g., Clayton and Comer, 1983; Dziewonski, 1984; Dziewonski et al., 1977; Hager et al., 1985; Masters et al., 1982). Establishing this connection required both the development of global models and the improved understanding of how mantle heterogeneities induce flow and deflection of boundaries that affect the geoid (Hager, 1984; Richards and Hager, 1984). While the early low-resolution tomographic models for the lower mantle have relatively strong spherical harmonic components from degrees 2 to 5, and proved remarkably successful

in accounting for the long-wavelength geoid (see review by Hager and Richards, 1989), there has been continuing debate about the spectrum of lower mantle heterogeneity. Are the long-wavelength patterns the result of truly diffuse structures or are they in part due to smoothed sampling of smaller scale but very heterogeneous features such as slabs embedded in the lower mantle? If the latter is the case, the long-wavelength distribution of heterogeneity in the lower mantle is more a consequence of the last few hundred million years of surface tectonics and associated plate subduction than a very long-term aspect of the lower mantle convective regime (e.g., McNamara and Zhong, 2005). Similarly, if the long-wavelength patterns in surface hot spots reflect swarms of thermal plumes rising from the CMB, then the distribution of recent D'' boundary layer instabilities may contribute to the present long-wavelength structure of the deep mantle.

Imaging of deep mantle structure has advanced in resolution by steadily increasing the size and raypath coverage of the data sets and by using improved measurement and inversion approaches. There is significant convergence in large-scale structures in recent deep mantle tomographic shear velocity models (e.g., Antolik et al., 2003; Grand, 2002; Grand et al., 1997; Gu et al., 2001; Houser et al., 2008; Kustowski et al., 2008; Lekic et al., 2012; Li and Romanowicz, 1996; Liu and Dziewonski, 1998; Masters et al., 1996, 2000; Mégard and Romanowicz, 2000; Panning and Romanowicz, 2006; Panning et al., 2010; Ritsema et al., 1999, 2011; Simmons et al., 2007, 2009, 2010; Takeuchi, 2007), all of which have dominant long-wavelength heterogeneities. The same is true for large-scale P velocity models, although there is still less agreement between models and somewhat less complete coverage of lower mantle regions (e.g., Antolik et al., 2003;

Bijwaard and Spakman, 1999; Bijwaard et al., 1998; Boschi and Dziewonski, 1999, 2000; Fukao et al., 1992, 2001; Houser et al., 2008; Karason and van der Hilst, 2001; Lei and Zhao, 2006; Li et al., 2008; Myers et al., 2011; Simmons et al., 2011, 2012; van der Hilst and Károly, 1999; Vasco and Johnson, 1998; Widjiantoro and van der Hilst, 1996; Zhao, 2001).

As the resolution of large-scale lower mantle 3D structure has improved with each new generation of global tomographic models, it has become clear that there are significant intermediate-scale features in the lower mantle. This had previously been deduced for localized regions by array studies or by analyses of differential travel times for phase pairs sensitive to lower mantle structure (e.g., Jordan and Lynn, 1974; Lay, 1983), but the geometry and lateral extent of such features could not be resolved until large-scale tomographic models were produced. Recent high-resolution S-wave velocity (e.g., Grand, 2002; Simmons et al., 2010) and P-wave velocity (Ren et al., 2007; van der Hilst et al., 1997) models resolve a high-velocity quasitabular structure extending nearly vertically in the lower mantle beneath North America and South America and a similar elongate body beneath southern Eurasia, both of which extend to at least 1300–1600 km depth (Figure 3). The width of these features is not tightly resolved, but appears to be at least 500 km, and the anomalies are 1–2%, which is relatively high for this depth range in the mantle. These features are usually interpreted as relatively cold, sinking slab material that has penetrated into the lower mantle as the Americas moved westward and as the Tethys Sea closed, respectively. The aspherical seismic velocity structure in the mid-mantle near 1300 km depth is dominated by these elongate tabular high-velocity features, and it is likely that these contribute significantly to the strong long-wavelength patterns in spherical

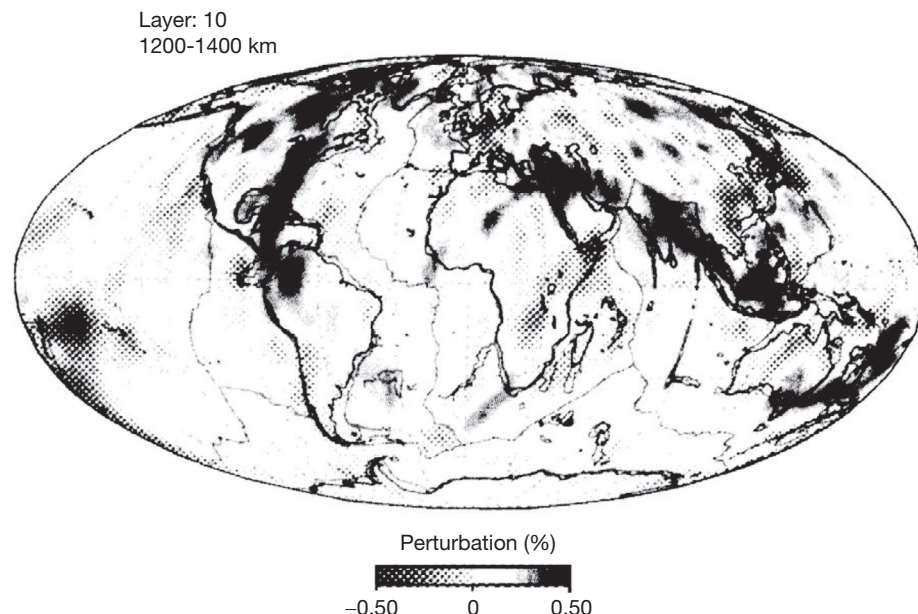


**Figure 3** Horizontal section through a tomographic model of P-wave velocity structure near 1300 km deep in the lower mantle, obtained by inversion of ISC arrival times after careful processing for depth determination. Solid dark areas correspond to relatively high velocities, with two major coherent features that correspond to tabular structures extending semivertically below southern Asia and eastern North America. These are inferred to be subducted slab material that has penetrated into the lower mantle. Reproduced from van der Hilst RD, Widjiantoro S, and Engdahl ER (1997) Evidence for deep mantle circulation from global tomography. *Nature* 386: 578–584.

harmonic models that have lower resolution (see corresponding features in the early lower-resolution models discussed by Dziewonski et al., 1993). While there may be contributions to these structures from inadequately suppressed shallow mantle structures, particularly strong near-source slab anomalies, the high-velocity regions do appear in models with different data sets, different model parameterizations, and varying source-receiver geometries, so it is very difficult to dismiss them as artifacts.

Below about 1600 km depth, tomographic models show less coherence, relatively weak velocity anomalies, and tabular structures are not clearly imaged (e.g., Grand et al., 1997; Simmons et al., 2012). Instead, the models tend to become dominated by horizontally extensive regions of high and low velocity with strong degree 2 and 3 patterns in the lowermost mantle (Figure 4). The strength of the velocity heterogeneity increases in the lowermost 300–500 km of the mantle, particularly for shear waves (Figure 5). Lateral variations of  $\pm 4\%$  in S-wave velocity and  $\pm 1.5\%$  in P-wave velocity are observed. High shear velocities in the lowermost mantle are found beneath circum-Pacific margins, although only in a few places is there apparent continuity of high-velocity features from the mid-mantle all the way to the CMB. The aspherical S-wave velocity models all display two large low-shear-velocity provinces (LLSVPs) located below the central Pacific and the southern Atlantic/southern Africa/southern India Ocean region. The latter two low-velocity regions appear to extend upward above the D'' region, possibly as much as 800–1000 km. These features have sometimes been called ‘superplumes,’ given than their scale greatly exceeds that expected for isolated D'' boundary layer instabilities, and Dziewonski et al. (1993) called them the ‘Equatorial Pacific Plume Group’ and the ‘Great African Plume,’ respectively. Attributing dynamic significance to these features with the ‘plume’ label is complicated and very uncertain; low velocities may be caused by high temperatures or by chemical differences. It is preferable to use the dynamically neutral label of LLSVPs, as discussed later.

### 1.22.3.2 Dynamic Structures

While the geoid and some attributes of subduction zone morphology provide geodynamic constraints on lower mantle dynamics, most of what we know about dynamic processes in the deep Earth derives from interpretations of seismic tomography. This is not a trivial undertaking because there are limitations in the spatial resolution of the tomographic models and possible contributions from both thermal and chemical heterogeneities that are difficult to separate. Any

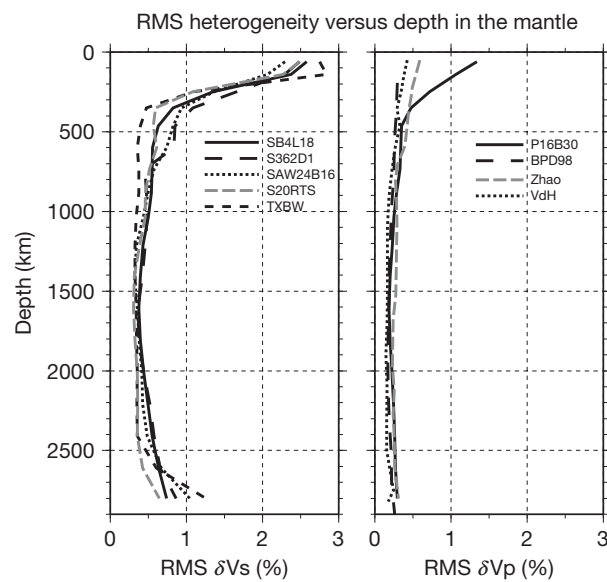


**Figure 5** RMS velocity fluctuations at various depths in the mantle shear velocity models SB4L18 (Masters et al., 2000), S362D1 (Gu et al., 2001), SAW24B16 (Mégnin and Romanowicz, 2000), S20RTS (Ritsema and van Heijst, 2000), and TXBW (Grand, 2002) and in the mantle compressional velocity models P16B30 (Bolton, 1996), BPD98 (Boschi and Dziewonski, 1999), Zhao (Zhao, 2001), and VdH (Karáson and van der Hilst, 2001).

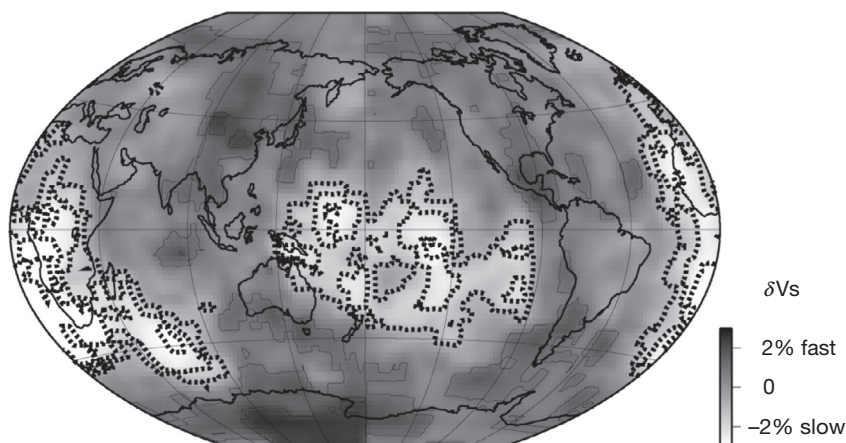


**Figure 4** Representative large-scale mantle tomography for S-wave velocity structure (Grand, 2002) near the base of the mantle. Note the long-wavelength patterns of high velocities beneath the circum-Pacific and low velocities beneath the central Pacific and Africa. 1% contours are shown, with dotted lines highlighting the internal variations in the two large low-shear-velocity provinces. Variations of  $\pm 3\%$  are imaged by this and other models with similar spatial patterns. Note the contrast in scale length of predominant heterogeneities with the mid-mantle pattern in Figure 3.

interpretation of tomography requires a foundation in mineral physics characterization of material property dependence on temperature and composition for the high-pressure conditions of the deep Earth. It also requires geodynamic analysis to assess the deformation processes taking place, guided by the seismological and mineral physics constraints on structure.

Seismological resolution of overall lower mantle structure has to be achieved by using different data types that provide distinct control on spatial and depth variations of structure. Overtones and multiple surface reflections provide sampling of structure near and below the transition zone, direct body-wave phases including core phases provide spatially nonuniform sampling of deep mantle corridors, diffracted waves extend coverage of structure near the CMB, and normal modes provide control on the large-scale even harmonics of the structure. One of the main challenges is that differences in how inversions of various data sets are regularized have large effects on how structural characterizations are interpolated and extrapolated in the various models (e.g., [Boschi and Dziewonski, 1999](#)). The very large-scale, degrees 2 and 3 patterns of heterogeneity are pronounced and well resolved now, and one of the key issues is whether weaker shorter-wavelength features are independent of or linked to the causes of the long-wavelength patterns.

While the lower mantle does not appear to have pronounced internal layering, it has been proposed that the downward transition in heterogeneity pattern from a mid-mantle dominated by slablike structures to a deep mantle dominated by large-scale high-velocity and low-velocity features is caused by compositional stratification. The stratification could be in a thin layer essentially confined to D'' (e.g., [Davies and Gurnis, 1986](#)) or in a much thicker layer. In the latter model (see [Kellogg et al., 1999; van der Hilst and Káráson, 1999](#)), the lowermost mantle is compositionally distinct, being composed of undifferentiated, possibly 'primordial' mantle material that is then invoked as the source of isotopic anomalies sampled by upwelling thermal plumes that produce distinctive surface hot spot volcanism. Downwelling slabs can depress the conjectured chemical boundary by hundreds of kilometers, deflecting it from a depth of around 2000 km. The chemical boundary is not expected to be a strong reflector and does not give rise to coherent features in the radially averaged mantle model. The density increase of the deep layer could be due to enrichment in iron or silica, which has competing effects on the velocity structure. This is a highly speculative model, but it can begin to reconcile the current observations of the deep mantle seismic structure with geochemical observations. An alternative to chemical layering is the presence of distinct blobs of chemically distinct mantle mixed into the lower mantle, in the so-called plum-pudding model ([Davies, 1984](#)). An intermediate scenario, motivated by recent seismic observations, of discrete piles of chemically distinct material in the LLSVP regions is discussed later.

Significant improvement of our understanding of the lower mantle will come with reliable determination of density heterogeneity directly from simultaneous inversion of normal modes and gravity observations. A first step in this direction has been presented by [Ishii and Tromp \(1999\)](#). While preliminary, that study found that high-density material may be piled up in the regions of low shear velocity, presumably hot material beneath the Pacific and Africa. A significant chemical heterogeneity density effect is needed to offset any thermal

buoyancy of the upwellings. Until the models improve, it may thus be premature to associate the low shear velocities with upwellings, for chemical heterogeneity is likely to be important in the deep mantle.

The existence of large-scale lower mantle features enables the formulation of simultaneous or iterative inversions for dynamic features such as the geoid and dynamic topography, and this has emerged as a new area of research (e.g., [Dziewonski et al., 1993; Forte and Mitrovica, 2001; Forte et al., 1993, 1994; Hager and Clayton, 1989; Hager et al., 1985; Mitrovica and Forte, 2004; Phipps Morgan and Shearer, 1993; Simmons et al., 2009, 2010; Soldati et al., 2012; Tackley, 2012](#)). The primary additional parameter that is constrained in such geodynamic models is the viscosity structure, and it is generally found in geoid inversions and contemporary studies of glacial rebound processes that the viscosity of the lower mantle is one to two orders of magnitude higher on average than that of the average upper mantle (e.g., [Mitrovica and Forte, 1997, 2004](#)). This may be a consequence of lower mantle mineralogy, or it may represent the effect of devolatilization of the lower mantle during extensive melting early in Earth history. The simultaneous interpretation of thermal, chemical, and dynamic structures based on probabilistic tomographic velocity structures has been expanded to statistical approaches that recognize the uncertainties and correlations among thermal and compositional parameters (e.g., [Cobden et al., 2009, 2012; Deschamps and Tackley, 2008; Deschamps and Trampert, 2003; Hernlund and Houser, 2008; Mosca et al., 2012; Trampert et al., 2004](#)).

Resolving small-scale structures in the lower mantle by seismic imaging is a complementary approach to imaging the dynamic system. Essentially, seismologists look for the strong patterns expected to accompany mantle convection that is extensively driven by boundary layer flow. The primary elements of this are expected to be cold, sinking lithospheric slabs, which should have relatively high seismic velocities and tabular geometries, and hot, rising thermal plumes, which should have relatively low seismic velocities and cylindrical geometries. Extensive work has addressed lower mantle penetration by subducting oceanic lithosphere, which clearly penetrates down through at least the transition zone in some regions, given the occurrence of deep earthquakes in subduction zones. [Jordan \(1977\)](#) introduced a residual sphere modeling formalism for seeking patterns in travel time residuals from individual earthquakes in subduction zones, which was further developed by [Creager and Jordan \(1984, 1986a\)](#). These studies demonstrated the sensitivity of the method to both upper mantle and transition zone slab geometry and velocity heterogeneity, as well as to geometry of any steeply dipping slab extension into the lower mantle. Provocative results based on both P-wave modeling and S-wave modeling suggested that slab penetration to depths of at least 1000 km with little distortion other than steepening dip occurs in the Kuril, Marianas, and Japan arcs.

Additional applications of the residual sphere method were presented by [Fischer et al. \(1988, 1991\); Zhou and Anderson \(1989\); Zhou et al. \(1990\); Boyd and Creager \(1991\); Ding and Grand \(1994\); and Pankow and Lay \(1999\)](#). The method makes very explicit the limitations of arrival time data, as event location effects have a major effect on relative arrival time anomalies if the data coverage is limited (particularly true if

only teleseismic observations are used). As noted previously, tomographic methods are strongly biased by this unless the data coverage is such that residual patterns faithfully preserve the slab effects (which may be true when extensive upgoing and downgoing data are included, but not otherwise). Residual sphere modeling also makes clear the importance of deep mantle and receiver corrections, and early applications did not adequately address this issue. In fact, it has been shown that for S waves, much of what was initially attributed to near-source effects is eliminated when improved path corrections are applied (e.g., Deal and Nolet, 1999; Deal et al., 1999; Gaherty et al., 1991; Pankow and Lay, 1999; Schwartz et al., 1991). As global tomographic models improve further, this will become less of a problem. The analysis of differential residual spheres for events in the same slab, as first introduced by Toksöz et al. (1971), is one approach that has been pursued to suppress distant effects rather completely (e.g., Ding and Grand, 1994; Okano and Suetsugu, 1992; Pankow and Lay, 1999; Takei and Suetsugu, 1989). These studies indicate that in some cases, slabs may penetrate to depths of 800 km or more, but significant slab broadening may occur, as well as the reduction of velocity heterogeneity to on the order of 2%, much weaker than in early residual sphere studies and similar to the weak heterogeneity inferred when a priori slab structures are introduced into tomographic modeling. As regional and global tomography has advanced, there is a clear convergence with the results from the enhanced residual sphere modeling, with support for a few slabs directly penetrating into the lower mantle beneath Java and the Caribbean, but others such as the Izu and Japan slabs show strong deflections into large transition zone accumulations of slab material.

The analysis of upwelling regions is even more challenging, in that seismological imaging of low-velocity features is intrinsically difficult due to wave diffraction and wave front healing effects. Nonetheless, global tomography studies suggest that there are concentrated low-velocity regions beneath some of the major surface hot spots (e.g., Montelli et al., 2004; Schmerr et al., 2010; Sun et al., 2010; Takeuchi, 2009; Zhao, 2004), but the confidence in such features remains limited because the results appear to depend heavily on how inversions are parameterized and damped. While the evidence for lithospheric slab penetration into the upper portion of the lower mantle is relatively strong, the direct imaging of any plume upwellings remains in an early stage. Waveform healing effects and the intrinsic limitations of tomographic resolution for low-velocity regions require the evaluation of how tomography filters and smooths the images of specific deep mantle structures such as plumes (e.g., Boschi et al., 2007, 2008; Bull et al., 2009; Hwang et al., 2011; Ritsema et al., 2007; Styles et al., 2011). The complex structures near the base of the mantle that are described later include features attributed to plume-like instabilities from the thermochemical boundary layer above the CMB, but whether these features ascend to the surface or induce localized upwellings that do remains to be established.

## 1.22.4 D'' Region

The numerous efforts to image the detailed velocity structure below regions of subduction have been motivated as a test of

the hypothesis of stratified versus whole-mantle convection, a key issue in mantle dynamics. Similarly, studying the structure of the D'' region is largely motivated by the notion that this region may play a critical role in mantle convection, especially if there is significant heating from below (e.g., Garnero et al., 2007a; Lay and Garnero, 2004). While most estimates of Earth's heat flow budget suggest that only 10–30% of the mantle's heat fluxes upward through the CMB (Lay et al., 2008; Zhong, 2006), this is still substantial heating that will give rise to a thermal boundary layer. Internal heating, resulting from radiogenic materials distributed in the mantle, is expected to contribute to large-scale flow without producing concentrated structures. In contrast, boundary layer-driven flow is expected to yield both localized upwellings and downwellings, which provide specific targets for seismic imaging. D'' structure is thus of particular interest as this region serves as the lower boundary layer of the mantle convection system. It is now generally appreciated that the lowermost mantle is also of great importance to convection in the core and the resulting geodynamo (e.g., Glatzmaier et al., 1999; Takahashi et al., 2008; Willis et al., 2007). The structure of D'' appears to be very complex, and efforts to elucidate this complexity underlie many approaches to understanding core and mantle dynamics.

### 1.22.4.1 Large-Scale Seismic Velocity Attributes

There are several important seismological probes of the large-scale elastic velocity structure in the D'' region. The large seismic velocity reductions across the CMB cause seismic wave energy to diffract into the geometric shadow zone at distances >100°. Waves diffracted along the CMB are sensitive to the absolute velocities and the velocity gradients in the D'' region and have long been studied to constrain average and laterally varying structure (e.g., Alexander and Phinney, 1966; Bolt et al., 1970; Doornbos and Mondt, 1979; Mondt, 1977; Mula and Müller, 1980; Sacks, 1966; To and Romanowicz, 2009; To et al., 2011; Valenzuela and Wysession, 1998; Wysession, 1996; Wysession and Okal, 1989). These studies demonstrate that no single velocity structure sufficiently characterizes D'' everywhere and that in some cases, there are strong negative velocity gradients in D'', while in other places, there are near-zero or positive velocity gradients. There are also changes in the relative perturbation of P-wave and S-wave velocities that are likely due to mineralogical or textural origin (e.g., Wysession et al., 1999). Diffracted phases involve extensive lateral averaging of what appears to be a region rich in small-scale structure and therefore yield limited resolution, but they do provide important input into large-scale tomographic models for D'' because of their extensive spatial coverage (e.g., Bréger and Romanowicz, 1998; Castle et al., 2000; Kuo and Wu, 1997; Kuo et al., 2000).

The large-scale variations in D'' imaged by early global seismic wave travel time tomography studies were shown to have predominant degrees 2 and 3 spherical harmonic components (e.g., Dziewonski et al., 1996; Kuo and Wu, 1997; Kuo et al., 2000; Li and Romanowicz, 1996; Liu and Dziewonski, 1998; Masters et al., 1996; Su et al., 1994). These models established the presence of high shear velocities in D'' beneath the Pacific Ocean margins and low velocities beneath the central Pacific and the southeastern Atlantic and southern Africa

(Figure 4). This geometry results in a correlation between areas of slab subduction over the past several hundred million years (e.g., Lithgow-Bertelloni and Richards, 1998) and high-velocity regions of D'', which could result if slabs penetrate to the base of the mantle while retaining enough thermal anomaly to produce high seismic velocities. Similarly, the low-velocity regions of D'' are generally located below regions with hot spots at the surface, suggesting that D'' upwellings may penetrate all the way to Earth's surface.

#### 1.22.4.2 Thermal Boundary Layer Aspect

To first order, the lower mantle appears to be a relatively uniform layer with properties varying radially largely due to self-compression and having most lateral heterogeneity concentrated in the D'' region above the CMB. The latter is consistent with the presence of a thermal boundary layer, as expected to result from heat fluxing out of the core into the mantle. The existence of a thermal boundary layer is strongly supported by the calculations of energetics of the geodynamo, which suggest that there must be some net flux of heat out of the core to sustain the core convective regime. The precise amount of heat flux is uncertain, with estimates ranging from 0.5 to 10 TW, and this amount must be added to heat conducted down the core adiabat (at least 2–5 TW) (e.g., Buffett, 2003). Thus, at least several TWs, and possibly as much as 15 TW of heat, are fluxing into the base of the mantle (about 44 TW flux through Earth's surface) (e.g., Kellogg et al., 1999; Lay et al., 2008; Zhong, 2006).

The CMB is a major compositional boundary; therefore, the heat flux from the core must conduct into the base of D'' with a superadiabatic temperature gradient (e.g., Stacey and Loper, 1983). Such a thermal boundary layer is likely to thicken over time and to build up instabilities that give rise to thermal plumes that carry excess temperatures from the boundary layer upward (e.g., Leng and Zhong, 2008, 2009). Time-dependent flow and uncertainty in material properties make dynamic calculations of CMB heat flux carried by thermal plumes very uncertain, but these probably provide a lower-bound estimate of total heat flux across the CMB (e.g., Glisovic et al., 2012; Manthilake et al., 2011; Mittelstaedt and Tackley, 2006; Monnereau and Yuen, 2010; Nakagawa and Tackley, 2008).

The very low viscosity of the core-side alloy ensures that the CMB is maintained at nearly isothermal conditions, temperature estimates of the CMB being in the range 2700–4200 °C (e.g., Williams, 1998). If there is no thermal boundary layer in the transition zone or mid-mantle, the overall temperature drop across the CMB thermal boundary layer must be on the order of  $1000 \pm 500$  °C, comparable to that across the lithosphere. Lateral variations in temperature in the deep mantle will produce varying thermal gradients above the CMB resulting in a variable heat flux boundary condition on the core. In places where the mantle temperatures are relatively low, the heat flux will be higher than in places where the mantle temperature is relatively high. This heat flux variation is likely to exert a long-term influence of the mantle on the outer core convective regime (Buffett, 2003; Glatzmaier et al., 1999; Gubbins et al., 2007; Lay et al., 2004b; Sumita and Olson, 2000) and may influence the inner core as well (Sreenivasan and Gubbins, 2011).

The thickness of the boundary layer is quite uncertain due to significant pressure effects on material properties and questions about the existence of partial melting and chemical heterogeneity, but the general expectation is that the boundary layer may be as much as a few hundred kilometers thick (thicker than the lithospheric thermal boundary layer) mainly due to pressure effects suppressing the thermal expansion coefficient near the base of the mantle. In this case, the D'' region corresponds, at a minimum, to a thermal boundary layer with a rapid increase in temperature with depth. This is likely to be manifested as a reduction of seismic velocity gradients relative to the mid-mantle, given the inverse dependence of velocity on temperature. This may be a subtle effect in general due to the pressure effects on thermal expansion, but if the temperature increase approaches the eutectic melting point of the lower mantle or of some minor component in D'', very strong velocity reductions can occur for minor degrees of partial melting. The accurate determination of the velocity gradient above the CMB could thus potentially be used to constrain the thermal boundary layer properties (e.g., Doornbos et al., 1986; Lay and Helmberger, 1983a; Loper and Lay, 1995; Stacey and Loper, 1983), but this approach encounters the immediate challenge that the velocity gradient appears to vary laterally.

Like Earth's lithosphere, the thermal boundary layer at the base of the mantle is likely undergoing strong lateral and vertical flow, as upwellings produced by thermal boundary layer instabilities drain hot material from the boundary layer and downwellings replace it with cooler material. However, as a hot, low-viscosity boundary layer, there is probably much more small-scale structure in the D'' dynamic regime than is found in the cold, relatively stiff lithosphere. It is generally accepted that thermal heterogeneity within the boundary layer is partially responsible for the seismic inhomogeneity detected by Bullen (1949), and it likely contributes to the complexities described here, but it appears that more than just thermal heterogeneity is present.

As is true near Earth's surface, one cannot immediately attribute all variations in seismic velocities to the effects of temperature variations; chemistry may play an important or even the major part, especially given the inhibiting effects of great pressure on temperature derivatives for seismic velocities. The juxtaposition of the lowermost mantle boundary layer adjacent to the largest density contrast in Earth heightens the probability that there is also chemical heterogeneity in the D'' region. This may involve density-stratified residue from Earth's core formation process, ongoing chemical differentiation of the mantle, or even chemical reactions between the core and the mantle (e.g., Garnero and McNamara, 2008; Goarant et al., 1992; Hayden and Watson, 2007; Jeanloz, 1993; Knittle and Jeanloz, 1989; Lay, 1989; Manga and Jeanloz, 1996). The probability of both thermal and chemical heterogeneities existing within the lowermost mantle prompts the consideration of the region as a thermochemical boundary layer (e.g., Anderson, 1991; Lay, 1989; Lay et al., 2004b; Trønnes, 2009), much as Earth's lithosphere must be considered a thermochemical boundary layer due to large-scale chemical variations between oceanic and continental regions. The evidence for a thermochemical boundary layer is provided by several seismological attributes of the D'' region, as described in the next few sections.

### 1.22.5 D'' Discontinuities

Detailed studies of teleseismic waveforms indicate that P-wave and S-wave velocity structures both have a 0.5–3.0% velocity discontinuity at many locations near the top of the D'' region (the top of D'' is not precisely defined, and many researchers take it to correspond to either the depth at which there is a discontinuity or the onset of a change in velocity gradient, somewhere in the range from 50 to 350 km above the CMB). This feature is often called the D'' discontinuity (e.g., Wysession et al., 1998), and representative shear velocity structures obtained by waveform modeling are shown in Figure 6. These models, obtained for distinct regions of D'', involve a 2.5–3% shear velocity increase at depths from 130 to 300+ km above the CMB that is laterally extensive over intermediate-scale (500–1000 km) regions. Wysession et al. (1998) reviewed the many early studies of this structure, noting that there are substantial inferred variations in depth of the velocity discontinuity. Typically, S-wave velocity increases are larger than P-wave velocity increases, with the latter usually being 0.5–1.0%, though some

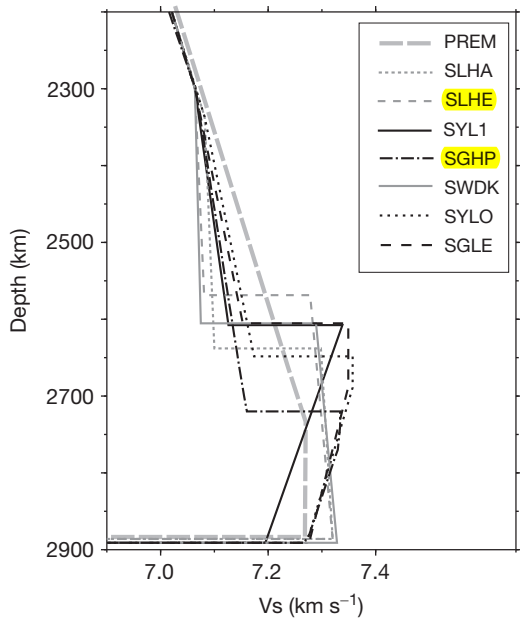


**Figure 6** Radial profiles of S-wave velocity in the lowermost mantle: PREM (Dziewonski and Anderson, 1981), SLHE, SLHA (Lay and Helmberger, 1983a), SYL1 (Young and Lay, 1987a), SGHP (Garnero et al., 1988), SWDK (Weber and Davis, 1990), SYLO (Young and Lay, 1990), and SGLE (Gaherty and Lay, 1992). The discontinuity models represent localized structures, determined for spatially limited regions of the D'' layer, the locations of which are indicated in Figure 6.8(a). Shear velocity increases of 2.5–3.0% are found in regions under Eurasia (SWDK and SGLE), Alaska (SYLO), Central America (SLHA), the Indian Ocean (SYL1), and the central Pacific (SGHP). The velocity increase is typically modeled as a sharp discontinuity, but it may be distributed over up to 50 km in depth. Decreased velocity gradients above the discontinuity may exist but are artifacts of the modeling in most cases. The reduction of velocity below the discontinuity in more recent models (orange) may be real but may be an artifact of modeling a heterogeneous region with a one-dimensional model. The variations in depth of the discontinuity are uncertain due to the lack of constraint on velocity above and below the discontinuity, but some variation appears to exist.

models do propose 3% discontinuities (e.g., Weber and Davis, 1990; Wright et al., 1985). The increase in velocity at the top of D'' may be distributed over up to 30–50 km in depth, or it may be very sharp (e.g., Lay, 2008; Lay and Helmberger, 1983a; Lay and Young, 1989; Young and Lay, 1987a).

#### 1.22.5.1 Seismic Wave Triplications

The velocity increases at the top of D'' are primarily detected by reflections and triplications, which arrive ahead of the core-reflected PcP and ScS phases (e.g., Avants et al., 2006b; Chaloner et al., 2009; Ding and Helmberger, 1997; Gaherty and Lay, 1992; Houard and Nataf, 1993; Hutko et al., 2008, 2009; Kendall and Nangini, 1996; Kendall and Shearer, 1994; Kito and Krüger, 2001; Kito et al., 2004, 2007a,b; Kohler et al., 1997; Lay and Helmberger, 1983a; Lay et al., 2004a, 2006; Reasoner and Revenaugh, 1999; Sun and Helmberger, 2008; Sun et al., 2006, 2009; Takeuchi and Obara, 2010; Thomas and Weber, 1997; Thomas et al., 2002, 2004a,b; Thorne et al., 2007; Weber, 1993; Weber and Davis, 1990; Wright and Lyons, 1975; Wright et al., 1985; Young and Lay, 1987a, 1990). The clearest observations of deep mantle triplications are from distances of 65° to 95°, where the critical angle interaction with the velocity increase greatly enhances the amplitudes of the reflected signals relative to precritical distance ranges. Examples of the triplication arrival are shown in Figure 7, with broadband shear-wave data having a strong arrival between S and ScS phases that would not be predicted by a smooth velocity model such as PREM. The reflector that produces this extra arrival varies in depth by several

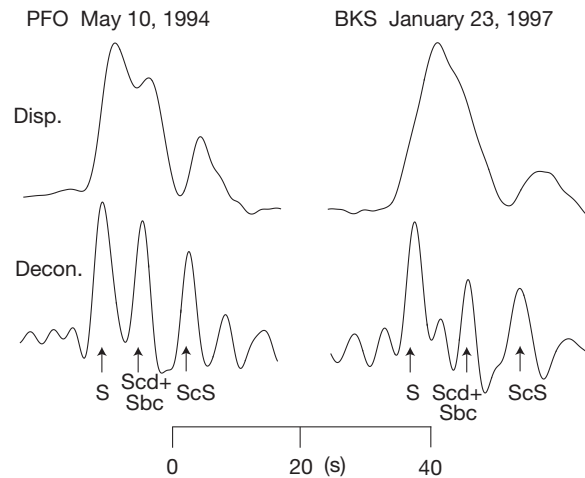


**Figure 7** Examples of broadband SH displacements at stations PFO ( $\Delta=79.8^\circ$ ) and BKS ( $\Delta=79.8^\circ$ ) for two deep South American events. Instrument-corrected ground displacements (disp.) are shown in the top row. The first arrival is S, and about 15–20 s later, ScS, the reflection from the core–mantle boundary, arrives. Deconvolution by the event-averaged source wavelets and low-pass filtering below 0.3 Hz yields the spike trains below for each record (decon.). The intermediate arrival, Scd + Sbc (SdS), which is produced by triplication from a deep mantle velocity increase, is clearly isolated in the deconvolutions. Reproduced from Lay T, Garnero EJ, and Russell S (2004a) Lateral variation of the D'' discontinuity beneath the Cocos Plate. *Geophysical Research Letters* 31: L15612, <http://dx.doi.org/10.1029/2004GL020300>.

hundred kilometers (e.g., Kendall and Shearer, 1994) and appears to have regional-scale lateral variations of on the order of a hundred kilometers that may produce scattering rather than simple reflections (e.g., Emery et al., 1999; Freybourger et al., 1999; Hutko et al., 2006; Krüger et al., 1995; Lay et al., 1997, 2004a; Scherbaum et al., 1997; Thomas et al., 2004a,b; van der Hilst et al., 2007; Weber, 1993; Yamada and Nakanishi, 1998).

It has been argued that the D'' discontinuities are actually globally extensive, with lateral variations in depth and strength being the result of lateral temperature variations and interactions with upwelling and downwelling flow (e.g., Nataf and Houard, 1993; Sidorin et al., 1998, 1999). Many studies suggest that no reflections from a discontinuity are observed for certain regions (e.g., Wysession et al., 1998), but most of these fail to establish whether the data truly preclude the presence of some velocity increase. Others studies have questioned whether there is a first-order discontinuity at all, preferring the notion that the extra seismic arrivals involve scattering from velocity gradients imaged in long-wavelength tomography models (e.g., Cormier, 1985; Haddon and Buchbinder, 1986; Liu et al., 1998; Schlittenhardt et al., 1985). The latter possibility requires large increases in the magnitude of the tomographic heterogeneities and/or sharpening of the velocity gradients, but there must be some relationship between the volumetric structure and the discontinuities (Ni et al., 2000). It has been demonstrated that scattering of SV energy into SH (Cormier, 1985) is not a likely explanation for the extra phases interpreted as triplication arrivals (Lay and Young, 1986). Young and Lay (1987b) showed that velocity decreases, as proposed by Haddon and Buchbinder (1986), cannot explain the data either. Thin high-velocity or low-velocity lamella models appear to fit some P-wave observations at least as well as first-order velocity discontinuity models (Freybourger et al., 1999; Thomas et al., 1998; Weber, 1994), but this has not been demonstrated convincingly for S-wave observations. An alternative is a transition in the heterogeneity spectrum with depth, possibly linking a gradient in anisotropy to the reflector (e.g., Cormier, 2000; Lay et al., 2004b).

One recent approach to determining the structure in the lowermost mantle with few assumptions about the nature of the structural complexity is waveform inversion, which uses large data sets and a complete calculation of waveform partial derivatives to structure for a set of basis functions. This approach has been applied to several areas where there had been previous forward modeling studies, allowing comparison of inferred structures. Applications have abounded (e.g., Fuji et al., 2010; He et al., 2010; Kawai and Geller, 2010b,c; Kawai et al., 2007a,b, 2009, 2010; Konishi et al., 2009, 2012). In general, there is fairly good agreement between forward modeling and waveform inversion studies for specific regions (Lay and Garnero, 2011), but it is clear that the resolution of velocity gradients and even depths of velocity increases and decreases is quite limited; details of all models, whether from forward modeling or inversion, must be interpreted with caution.

The regions with the strongest evidence for a shear-wave velocity discontinuity or strong velocity increase near the top of D'' are highlighted in Figure 8(a). Wysession et al. (1998) showed individual data sampling in greater detail. Some of

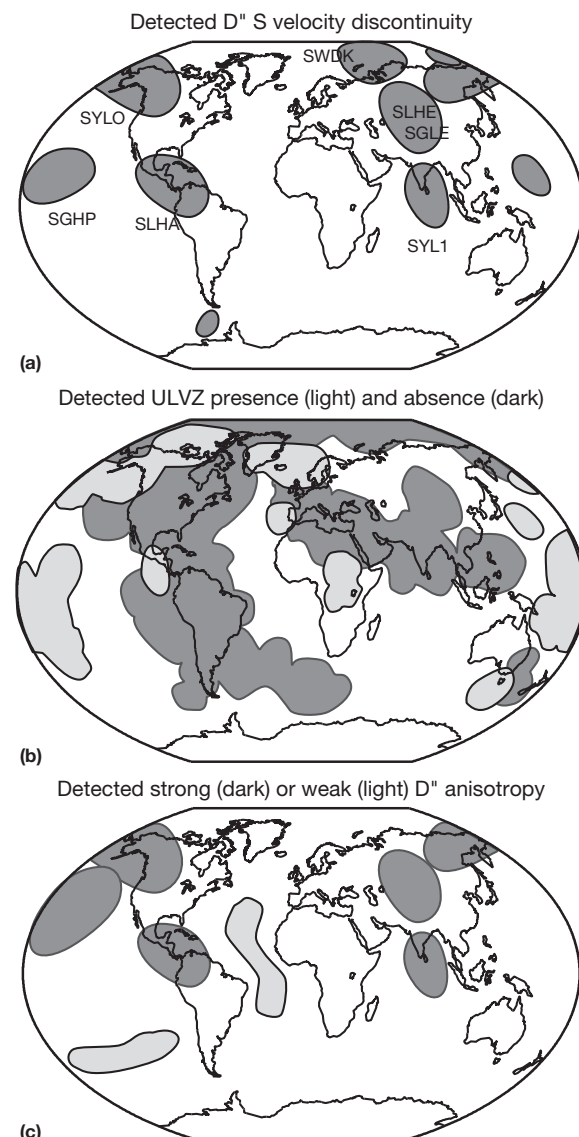


**Figure 8** Maps summarizing spatial variations of seismic wave characteristics of D''. (a) Regions where regional shear velocity discontinuities have been observed in large numbers of data, typically with 2–3% increase in velocity at depths from 200 to 300 km above the CMB (see labeled models in Figure 6). (b) Regions where ULVZ structures at the CMB have been detected or not, primarily based on SPdiffKS observations and assuming a Fresnel zone appropriate for a horizontal layer. (c) Regions where regional studies of D'' shear-wave splitting have been conducted. Most areas exhibiting splitting have waveforms compatible with vertical transverse isotropy, with decoupling (or only weak coupling) of the transverse and longitudinal components of the S-wavefield, with 1–2% faster transverse components. Modified from Lay T, Garnero EJ, and Williams Q (2004b) Partial melting in a thermo-chemical boundary layer at the base of the mantle. *Physics of the Earth and Planetary Interiors* 146: 441–467.

these areas also have evidence for a P-wave velocity discontinuity, but in some regions, such as under Alaska and Central America, any P-wave velocity discontinuity must be at or below the detection threshold of about 0.5% (Ding and Helmberger, 1997; Hutko et al., 2009; Reasoner and Revenaugh, 1999;

(Wright and Kuo, 2007; Young and Lay, 1989). Beneath Central America, there may be a small P-wave velocity reduction at the same depth as the S-wave velocity increase (Hutko et al., 2008). Stacking of array data is essential to detect such small discontinuities, and many ‘non-observations’ reported for individual seismograms must be viewed as inconclusive.

It is unlikely that long-period waveform inversion approaches will resolve the fine-scale structure reliably, so imaging methods will continue to play a major role in unveiling the structure. Several efforts have been made to apply industry-style migration methods to large data sets to image small-scale structures near the base of the mantle. Migrations of P-wave and S-wave data sets reveal both large-scale reflectors and localized, intermittent reflectors, with either velocity increases or decreases (e.g., Chambers and Woodhouse, 2006a,b; Hutko et al., 2006; Kito et al., 2007a,b; Ma et al., 2007; Rost and Thomas, 2010; van der Hilst et al., 2007; Wang et al., 2006, 2008). The complexity of structure in the deep mantle is approaching that of the lithosphere, and high-resolution imaging methods will be essential for making further progress.

The S-wave observations tend to be longer wavelength than the P-wave data used to look for the discontinuity, so it is viable that a transition zone several tens of kilometers thick may explain the absence of high-frequency precritical P-wave reflections. Most areas with strong evidence for an S-wave reflector are in the high-velocity regions beneath the circum-Pacific; the primary exception is under the central Pacific, where a variable S-wave velocity discontinuity is observed in a region having large-scale low D'' shear velocities (e.g., Avants et al., 2006b; Garnero et al., 1988; Kawai and Geller, 2010a; Lay et al., 2006; Russell et al., 2001). As the tomographic resolution of large-scale structure improves, the existence of strong lateral heterogeneities within both circum-Pacific and central Pacific regions is being recognized (Bréger and Romanowicz, 1998; Bréger et al., 2001; Fisher et al., 2003; Hung et al., 2005; Sun et al., 2007a, 2009; Wysession et al., 2001), so the bimodal characterization of the discontinuity structure is overly simplified.

It remains important to determine whether there is any density increase in D'' accompanying the seismic velocity increases, as this could help to resolve whether a chemical change or phase change is involved, either of which could strongly affect the dynamics of the boundary layer (e.g., Hansen and Yuen, 1988; Kellogg, 1997; Montague et al., 1998; Sleep, 1988; Tackley, 1998). Unfortunately, wide-angle triplication observations have very limited sensitivity to density contrasts, so this is an exceedingly difficult attribute to resolve, and normal modes have limited resolution of any small, laterally varying density increases in the relatively thin D'' region (e.g., Koelemeijer et al., 2012).

### 1.22.5.2 Phase Change in Perovskite

As noted in Section 1.22.1.2, the predominant lower mantle mineral, magnesium silicate ( $\text{Mg,FeSiO}_3$ ) perovskite, is stable over a huge domain of lower mantle conditions spanning a several thousand kilometer depth range. However, high-pressure experiments conducted in Japan (Murakami et al., 2004; Oganov and Ono, 2004) first demonstrated that for pressures

greater than about 120 GPa, corresponding to depths in the lowermost mantle within a few hundred kilometers of the CMB, magnesium silicate perovskite at a temperature near 2500 K undergoes a transition to a new mineral structure, called postperovskite. This phase transition is widely viewed as the probable explanation for the D'' discontinuity, as it can plausibly account for salient features of the seismic observations (Bower et al., 2013; Hirose, 2006, 2007; Lay and Garnero, 2007; Lay et al., 2005; Shim, 2008).

The phase transition from perovskite to postperovskite does not involve a change of mineral composition, but the postperovskite phase is about 1–1.2% denser and has higher shear modulus than perovskite. X-ray diffraction studies of experimental samples at high pressures established the existence and the change in volume of the postperovskite phase and provided constraints on the atomic lattice for theoretical modeling of the precise crystal structure of the mineral (Caracas and Cohen, 2006; Itaka et al., 2004; Komabayashi et al., 2008; Martin and Parise, 2008; Murakami et al., 2004, 2005; Oganov and Ono, 2004; Ono and Oganov, 2005; Stackhouse et al., 2005b; Tsuchiya et al., 2004a; Wentzcovitch et al., 2006). Molecular dynamics modeling is required to predict the crystal structure of the postperovskite phase, and the theoretical calculations provide many important physical characteristics of postperovskite. This includes the prediction of the slope of the phase boundary in pressure–temperature (P–T) space, called the Clapeyron slope. The computed Clapeyron slope for the pure Mg end-member composition,  $\text{MgSiO}_3$ , is about 7.5 MPa K<sup>−1</sup>, a rather large positive value typical of the postperovskite structure (Hirose and Fujita, 2005; Tsuchiya et al., 2004a). Experiments suggest the slope may be as large as 11.5 MPa K<sup>−1</sup> (Hirose et al., 2006; Tateno et al., 2009). The positive value indicates that the phase boundary should occur at lower pressure (shallower in the mantle) in regions that are relatively lower temperature. Large variations in the depth of the phase transition could thus result from the strong thermal heterogeneity expected to exist in the vicinity of the thermal boundary layer in the lowermost mantle (Lay et al., 2005). Experiments also indicate high electrical conductivity for postperovskite, which may enhance electromagnetic coupling across the CMB (Ohta et al., 2008b), and it has been explored whether this is detectable (Velimsky et al., 2012).

Numerical calculations (e.g., Stackhouse and Brodholt, 2007; Tsuchiya and Tsuchiya, 2006; Tsuchiya et al., 2004b) and recent laboratory experiments (e.g., Guignot et al., 2007; Murakami et al., 2007b) also predict the crystal elasticity of postperovskite for lower mantle P–T conditions, providing estimates of the seismic P-wave and S-wave velocities. The P-wave velocity changes little relative to that for perovskite as a result of competing effects of increasing shear modulus, increasing density, and decreasing bulk modulus (Wookey et al., 2005b); however, the S-wave velocity is about 0.5–2% faster than for perovskite. If the transition from perovskite to postperovskite is confirmed to occur over a small pressure (depth) range, the resulting rapid increase in S-wave velocity is expected to produce a velocity increase that can reflect shear-wave energy. This could account for the shear velocity discontinuities shown in Figure 6 (e.g., Kawai and Tsuchiya, 2009; Lay and Garnero, 2007; Tsuchiya et al., 2004b; Wookey et al., 2005b). The theoretical models of elasticity also predict

anisotropic properties of the postperovskite crystals. These differ significantly from those for perovskite in low-temperature calculations, with increasing temperature reducing the differences but still allowing a contrast in anisotropic properties under deep mantle conditions (e.g., [Merkel et al., 2006](#); [Oganov et al., 2005](#); [Stackhouse et al., 2005b](#)).

Numerous studies have used stable low-pressure mineral forms such as  $\text{CaIrO}_3$ ,  $\text{MnGeO}_3$ ,  $\text{MgGeO}_3$ ,  $\text{CdGeO}_3$ , and  $\text{CaRuO}_3$  and  $\text{NaCoF}_3$ ,  $\text{NaMgF}_3$ , and  $\text{NaNiF}_3$  as analogs for characterizing the postperovskite transition and deformational properties under relatively accessible (for both laboratory and computations)  $P$ - $T$  conditions (e.g., [Boffa Ballaran et al., 2007](#); [Cheng et al., 2010, 2011](#); [Dobson et al., 2011](#); [Hirose et al., 2005b, 2010](#); [Hunt et al., 2009](#); [Hustoft et al., 2008a,b](#); [Ito et al., 2010](#); [Kojitani et al., 2007a,b](#); [Kubo et al., 2006, 2008](#); [Martin et al., 2006a,b, 2007a,b](#); [Metsue et al., 2009](#); [Miyagi et al., 2008](#); [Miyajima et al., 2006, 2010](#); [Niwa et al., 2007, 2011, 2012](#); [Runge et al., 2006](#); [Shim et al., 2007](#); [Stolen and Tronnes, 2007](#); [Tateno et al., 2006, 2010](#); [Tsuchiya and Tsuchiya, 2007](#); [Umemoto et al., 2006](#); [Usui et al., 2010; Walte et al., 2007](#); [Wu et al., 2011](#)).

The pioneering experimental and theoretical work on postperovskite was performed for the pure magnesium ( $\text{MgSiO}_3$ ) end-member and its analogs, but effects of the presence of iron (Fe) and aluminum (Al) have now been extensively explored experimentally and theoretically ([Akber-Knutson et al., 2005](#); [Andrault et al., 2010](#); [Caracas, 2010a](#); [Caracas and Cohen, 2007, 2008](#); [Catalli et al., 2010a](#); [Grocholski et al., 2012](#); [Hirose et al., 2008](#); [Jackson et al., 2009](#); [Lee et al., 2009](#); [Mao et al., 2004, 2005, 2006a,b, 2007](#); [Metsue and Tsuchiya, 2011](#); [Nishio-Hamane and Yagi, 2009](#); [Nishio-Hamane et al., 2007](#); [Sakai et al., 2009b](#); [Shieh et al., 2011](#); [Shim et al., 2008, 2009](#); [Sinmyo et al., 2006, 2008a,b, 2011](#); [Spera et al., 2006](#); [Stackhouse et al., 2005a, 2006a](#); [Tateno et al., 2005, 2007](#); [Tschauner et al., 2008](#); [Tsuchiya and Tsuchiya, 2008](#); [Yamanaka et al., 2012](#); [Zhang and Ogonov, 2007](#); [Zhang et al., 2012](#)). It is believed that lower mantle silicates probably contain at least 10–15% iron substitution for magnesium. Initial work suggested that having iron in the postperovskite mineral should reduce the pressure of the phase transition, such that it may occur hundreds of kilometers shallower in the mantle than for an iron-free mineral ([Mao et al., 2004](#)). These results have been contested in experiments that find less pressure effect due to the inclusion of Fe ([Hirose et al., 2006](#)). Theoretical predictions of the effects of Al substitution for both Mg and Si in the crystal lattice suggest that there may be a significant depth range (a few hundred kilometers) over which perovskite and postperovskite can coexist, which would reduce any velocity discontinuity, weakening seismic wave reflections from the transition (e.g., [Akber-Knutson et al., 2005](#); [Andrault et al., 2010](#); [Catalli et al., 2009](#); [Tateno et al., 2005](#)). The compositional variations complicate any connection between seismic models and specific phase change properties, and there may be kinetic effects on the deep mantle phase change that have to be accounted for as well.

Lower mantle rocks, like all rocks in the Earth, will involve an assemblage of mineral phases, with variations in crystal size and rock fabric as a result of solid-state convection. While there has been some experimental work done on real rock samples at lower mantle pressures and temperatures with the

postperovskite phase being observed ([Murakami et al., 2005](#); [Shieh et al., 2006](#)), full assessment of coexisting multiphases is still in an early stage. For example, the properties of ferropericlase ( $\text{Mg,FeO}$ ) are important, especially the partitioning coefficient of iron between perovskite and ferropericlase (e.g., [Kobayashi et al., 2005](#); [Nakajima et al., 2012](#)). The Fe spin transitions may also influence the postperovskite phase boundary, with iron partitioning affecting the postperovskite composition ([Caracas, 2010b](#); [Hsu et al., 2012](#); [Li, 2007](#); [Lin et al., 2008](#); [Mao et al., 2010](#); [Sturhahn et al., 2005](#); [Yamanaka et al., 2010](#); [Yu et al., 2012](#)).

Subducted oceanic slab material could be relatively low temperature compared to surrounding ambient mantle, and if it penetrates to the base of the mantle, it may thus preferentially undergo transition to postperovskite, resulting in a reflecting surface at the phase change within slab material, even if the boundaries of the slab are not strong reflectors. Postperovskite may exist in large patches of lower mantle material cooled by recently subducted slab material, and as this heats up over time, the material may change back to perovskite. If the pattern of heterogeneity in [Figure 4](#) indicates relative temperatures (rather than a compositional change), low-velocity regions should be hotter, and therefore, any postperovskite phase transition may occur at greater depth or not at all in the low-shear-velocity regions ([Helmberger et al., 2005](#)). Seismologists are seeking to establish whether the low-shear-velocity regions have any S-wave velocity discontinuity, but there is so far limited evidence for this other than under the central Pacific (e.g., [Avants et al., 2006b](#); [Lay et al., 2006](#); [Russell et al., 2001](#)), and that may be for a region near the margin of the low-shear-velocity province. It is interesting to note that while the volumetric shear velocity in the central Pacific is relatively low, the discontinuity, while highly variable, is not located much deeper than in circum-Pacific regions, contrary to the predicted thermal effect. Compositional effects may compete with thermal effects on the phase transition in this region ([Ohta et al., 2008a](#)).

The CMB is likely to be at a temperature too high for postperovskite to be stable, so there may be a thin basal layer with rapidly increasing temperature below regions cooled by slab material, in which the minerals transform back to perovskite ([Hernlund et al., 2005](#); [Lay et al., 2006](#); [van der Hilst et al., 2007](#)). A deeper velocity discontinuity with a velocity decrease should be present if this is the case, but this is seismically much more difficult to observe than a velocity increase because there is no critical angle amplification ([Flores and Lay, 2005](#)). Waveform stacking and detailed modeling are essential for the confident identification of any small velocity decreases in  $D''$ . Stacking of ScS data traversing the high-velocity region under the Cocos plate does not reveal any negative velocity discontinuity below the positive velocity increase at the top of  $D''$ , but similar stacking for data traversing the central Pacific does show a sharp decrease about 60 km above the CMB ([Avants et al., 2006a,b](#); [Lay et al., 2006](#)). If paired velocity increases and decreases can be confidently identified, they present the opportunity to directly estimate the temperature gradient, under the assumption that the structure does involve double intersection of the phase boundary. Coupled with an assumption of thermal conductivity, one can then estimate heat flux directly ([Lay et al., 2006](#); [van der Hilst et al., 2007](#)), although the detailed

nature of the phase boundary in the thermal gradient is important to consider (Buffett, 2007; Hernlund, 2010; Hernlund and Labrosse, 2007). The importance of thermal conductivity in D'' has prompted a substantial experimental and theoretical research effort, complicated by the difficulty of reliably measuring thermal conductivity at extreme P-T conditions, the uncertain mineralogy Fe spin state, and uncertain relative contribution from phonon and radiative conductivity (e.g., Chen et al., 2012b; Goncharov et al., 2006, 2008, 2009, 2010; Haiges et al., 2012; Hofmeister, 2008; Keppler et al., 2007, 2008; Ohta et al., 2012; Stackhouse et al., 2010).

The large positive Clapeyron slope of the postperovskite phase boundary in the presence of lateral temperature differences at the base of the convecting mantle may influence the generation of boundary layer instabilities. Warmer regions of the boundary layer will have a thinner layer of dense postperovskite mineralogy, while colder regions of the boundary layer will have a thicker layer of the denser material. This thermally induced topography on the phase boundary is like that near the 410 km olivine/wadsleyite phase transition, and in both cases, the pattern promotes flow of material across the boundary layer (as the elevated dense material sinks, it pulls down overlying material that transforms to the denser phase). Because the Clapeyron slope for the deep mantle transition is about twice that of the upper mantle transition, the effect is enhanced, and convection models that include the postperovskite transition have quite unstable lower thermal boundary layers that tend to generate vigorous deep mantle flow (e.g., Cizkova et al., 2010; Kameyama and Yuen, 2006; Matyska and Yuen, 2004, 2006; Monnereau and Yuen, 2007; Nakagawa and Tackley, 2004, 2005, 2006; Tackley et al., 2007; Tosi et al., 2010; van den Berg et al., 2010; Yuen et al., 2007). Seismological mapping of the phase boundary can thus provide a probe of the thermal and dynamic processes in the lowermost mantle.

There are indications that D'' material may be very weak and have low viscosity (e.g., Ammann et al., 2010; Nakada and Karato, 2012; Nakada et al., 2012) due to both the high-temperature boundary layer effect on viscosity and efficient diffusion within the minerals. Such a low-viscosity layer has significant effect on boundary layer deformation and instabilities that may even influence the geoid (e.g., Cadek and Fleitout, 2006; Nakagawa and Tackley, 2011; Samuel and Tosi, 2012; Tosi et al., 2009).

## 1.22.6 Large Low-Shear-Velocity Provinces

The two large regions of low shear velocity in the lowermost mantle located beneath the south-central Pacific and southern Africa/southern Atlantic/southern Indian Ocean regions (Figure 4) are particularly unusual structures. Their lateral extent is far greater than might be expected for a hot upwelling plume from a thermal boundary layer, giving rise to the label 'superplumes.' However, attaching dynamic attributes to these regions based on the sign of their velocity anomaly may be misleading. For example, the continents have comparably large-scale regions of relatively high-shear-velocity material in the lithosphere, and one could thus infer that they are cold, sinking regions, whereas the reality is that they are chemically

buoyant. The deep mantle anomalies have much stronger S-wave velocity reductions than P-wave velocity reductions, which suggests that some chemical change may be involved. The uncertain thermochemical nature of these LLSVPs warrants a dynamically neutral name.

There are also smaller-scale regions with low seismic velocities in the lower mantle that may be consistent with plumes rising from the thermal boundary layer (e.g., Montelli et al., 2004; Zhao, 2004), and it remains to be determined whether these are distinct from the LLSVPs. For example, while the tomographic model of Ritsema et al. (1999) does not have a low-shear-velocity zone in the lower mantle beneath Iceland, Bijwaard and Spakman (1999) presented a P-wave velocity image with low velocity under Iceland all the way to the CMB, and Helmberger et al. (1998) found very low S-wave velocities in D'' beneath Iceland. Goes et al. (1999) found a low P-wave velocity structure beneath Europe from 660 to 2000 km depth, which they invoke as the source of small plumes in the upper mantle associated with volcanism in Europe. Smaller-scale plume or slab features that are below the current resolution of global seismic tomography, but can be resolved in regional-scale inversions (e.g., Hung et al., 2005; Wysession et al., 2001), exist in the D'' region as well. Innovative scattering analysis or array imaging may prove to be the only means by which to constrain even smaller-scale structures (e.g., Ji and Nataf, 1998; Tibuleac and Herrin, 1999; Tilman et al., 1998). The characterization of LLSVPs is rapidly improving and more detailed than for any of the smaller-scale structures, so this section will focus on them.

### 1.22.6.1 Seismic Velocity Properties

The existence of the LLSVPs was first indicated by mantle shear-wave velocity tomography models (e.g., Dziewonski et al., 1993), and as discussed earlier, there is fairly good consistency among recent global models for the large-scale structure (e.g., Lekic et al., 2012). The global distribution of sources and permanent seismic stations limits the resolution of velocity gradients and total extent of the LLSVPs under Africa (Figure 9) and the Pacific, so deployments of portable instruments have been important for detailed differential travel time analyses and waveform modeling used to improve the resolution of LLSVP structure.

Ritsema et al. (1998b) and Ni and Helmberger (2003a,b) found that low-shear-velocity structure under southern Africa involves 3% anomalies and strong lateral gradients, both of which are more pronounced than in tomographic models. The LLSVP model they advance extends upward about 800–1200 km from the CMB, so the anomalous material is not confined to D''. Even stronger anomalies are reported in the D'' region below the southeastern Atlantic and southern Indian Ocean, with 1–10% S-wave velocity reductions increasing with depth across a 300 km thick layer (Wang and Wen, 2004, 2007a; Wen, 2001, 2006; Wen et al., 2001). Intermediate estimates of shear velocity reductions (1–7%) under the south Pacific LLSVP have been reported (e.g., Ford et al., 2006; Tanaka, 2002; To et al., 2005), and the margins and internal structure of the Pacific LLSVP have been constrained by He et al. (2006), Takeuchi et al. (2008), Tanaka et al.

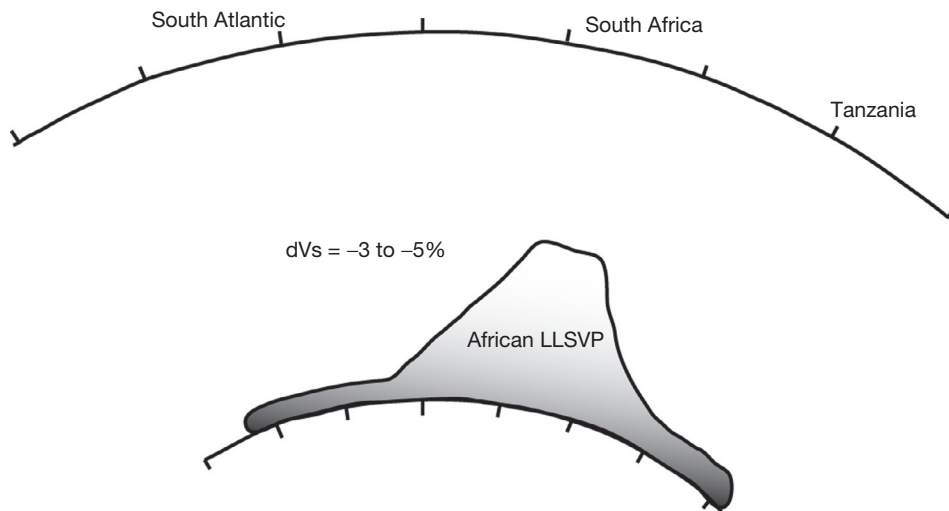


**Figure 9** A cross section through the LLSVP beneath Africa and the southern Atlantic, indicating the region of anomalously low shear velocities. The tick marks are  $10^\circ$  increments along a great-circle arc trending from southwest (left) to northeast (right). The velocity anomaly is about  $-3\%$  in the shallower part of the structure and may increase to about  $-5\%$  in the D'' region. The geometry of the structure is constrained by S, ScS, and SKS raypaths from various azimuths recorded at mainly African stations. The structure has the appearance of an upswept pile that is about 4000 km wide at the base and extends 1300 km upward from the CMB. Modified from Wang Y and Wen L (2007a) Geometry and P and S velocity structures of the "African Anomaly." *Journal of Geophysical Research* 112: B05313, <http://dx.doi.org/10.1029/2006JB004483>.

(2009), To and Romanowicz (2009), He and Wen (2009, 2011, 2012), Koki et al. (2012), and Takeuchi (2012).

There are very strong lateral gradients in seismic velocity structure in D'' on the margins of the LLSVPs that seem incompatible with thermal variations alone, unless there is a superimposed chemical or melting effect (e.g., He and Wen, 2012; Ni et al., 2002, 2005; To et al., 2005; Wen et al., 2001). Even in the mid-mantle, the lateral gradients remain strong, which is difficult, if not impossible, to explain by simple thermal gradients (e.g., Ni et al., 2002). Given the reduction of the sensitivity of shear velocity to temperature at deep mantle pressures, lateral thermal changes of 500–1000° over  $\sim 100$  km are needed to account for the observed velocity anomalies, which could lead to the onset of partial melting that can strongly reduce velocities (Lay et al., 2004b). But chemical variations appear to be important in LLSVPs, so the temperature contrasts may be far lower.

One of the key indications that LLSVPs involve chemical heterogeneity comes from comparisons of P-wave and S-wave velocities. Generally, global tomography models find good correlation between P-wave velocity and S-wave velocity structures in the lowermost mantle (e.g., Antolik et al., 2003; Houser et al., 2008; Masters et al., 2000); however, this correlation appears to break down in certain regions, such as beneath the northern Pacific, where P-wave velocity anomalies tend to be positive and S-wave velocity anomalies tend to be negative. A south-to-north decrease in the P-wave/S-wave velocity ratio has also been found using diffracted waves traversing D'' below the northern Pacific (Wysession et al., 1999). While the sampling of the lowermost mantle remains relatively poor for P waves (S-wave phases such as ScS and SKS greatly augment the deep mantle S-wave sampling), the LLSVPs do tend to have low-velocity expressions in global P-wave models. However, the relative strength of the anomalies is important to consider.

Shear velocity models show markedly stronger increases in RMS velocity heterogeneity in the lowermost 300 km of the mantle than do compressional velocity models, although the various models do differ in the extent to which shear velocity heterogeneity is concentrated toward the CMB (Figure 5). Even for well-correlated P-wave and S-wave velocity models (e.g., Houser et al., 2008; Masters et al., 2000), this raises the possibility of distinct behavior for P waves and S waves due to competing thermal and chemical variations, coupled with the possible presence of low degrees of partial melting (Lay et al., 2004b; Simmons and Grand, 2002). Indeed, the variability in velocity ratios and the occasional decorrelation of P-wave and S-wave anomalies provide strong evidence that thermal effects alone cannot explain all D'' seismic observations.

Simultaneous inversions of P-wave and S-wave data have been performed in attempts to isolate bulk sound velocity variations from shear velocity variations (e.g., Antolik et al., 2003; Houser et al., 2008; Kennett et al., 1998; Masters et al., 2000; Resovsky and Trampert, 2003; Robertson and Woodhouse, 1996; Su and Dziewonski, 1997; Trampert et al., 2004), but there are significant discrepancies between these models, perhaps as a consequence of incompatible resolution of P-wave and S-wave structures on a global basis. Della Mora et al. (2011) and Hernlund and Houser (2008) argued that resolution differences cannot account for the decorrelation overall. Direct comparisons of P-wave and S-wave travel time anomalies on specific paths support the possible decorrelation of these elastic velocities for localized regions within D'' (e.g., Lay et al., 2004b; Saltzer et al., 2001), as well as reaffirming the greater variations for S-wave velocities than P-wave velocities in LLSVPs (Figure 10; e.g., Simmons and Grand, 2002; Tkalcic and Romanowicz, 2002). The overall result is that LLSVPs have a bulk sound velocity anomaly that is anticorrelated with the S-wave velocity anomalies, and this dominates the pattern of

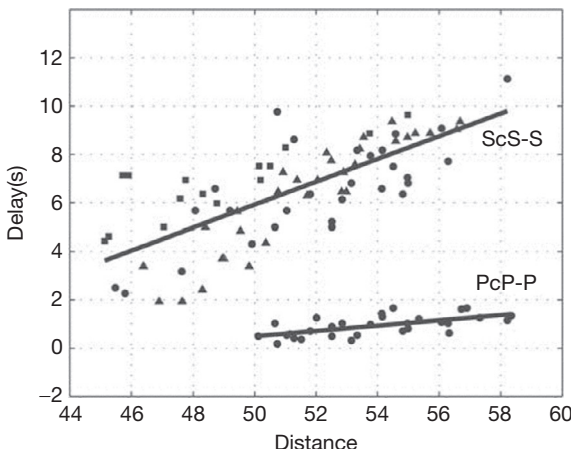


**Figure 10** Differential travel times for ScS-S and Pcp-P for paths sampling the southern margin of the African LLSVP. The S waves have much larger relative times, requiring shear velocity decreases 2–2.8 times stronger than the compressional velocity reductions depending on the depth extent of the anomalous region. This relative behavior is stronger than expected for a thermal variation in uniform lower mantle chemistry and requires either a compositional effect or a contribution from partial melting. Reproduced from Simmons NA and Grand SP (2002) Partial melting in the deepest mantle. *Geophysical Research Letters* 29, <http://dx.doi.org/10.1029/2001GL013716>.

the large-scale inversions for bulk sound velocity anomalies. This behavior requires an increase in incompressibility that contrasts with a decrease in rigidity in the LLSVPs. While this type of behavior is not necessarily unique to LLSVPs, it is generally accepted that at least part of (and possibly all of) their shear velocity anomaly is due to chemical anomaly, possibly involving enrichment in iron (Deschamps et al., 2011, 2012; Trampert et al., 2004). Some researchers have been reevaluating whether thermal effects alone dominate, using updated estimates of bulk chemistry and predicted elasticity, or whether the evidence for chemical heterogeneity in LLSVPs is truly compelling (e.g., Brodholz et al., 2007; Davies et al., 2012; Schubert et al., 2009). This is clearly important to resolve.

There is also some indication that density heterogeneity exists at the base of the mantle based on the analysis of normal modes and that on a large scale, dominated by the two LLSVPs, it is anticorrelated with shear velocity (and, hence, positively correlated with bulk velocity models), favoring chemical heterogeneity (Ishii and Tromp, 1999; Trampert et al., 2004). Thus, LLSVPs may be denser than surrounding mantle and hence dynamically stabilized even if they are hotter than their surroundings, a situation inverse to that for continents. This remains a topic of much uncertainty (e.g., Kuo and Romanowicz, 2002; Romanowicz, 2001), and resolving the density structure is critical for assessing whether LLSVPs are buoyant or not.

#### 1.22.6.2 Thermal-Chemical Interpretations

The very presence of the LLSVPs in the deep mantle at this stage of Earth evolution suggests that unless they are being replenished by some process, such as segregation of former oceanic crustal components, they are likely to be very long-lived and not

particularly buoyant (e.g., Ni and Helberger, 2003a). Their large vertical extent certainly could reflect some thermal buoyancy, perhaps in competition with chemical negative buoyancy, but the LLSVPs may also represent mounds of low-velocity chemical heterogeneities piled up under large-scale mantle upwellings (Garnero and McNamara, 2008; Garnero et al., 2007a; Maruyama et al., 2007; McNamara and Zhong, 2004, 2005). If the chemical anomaly in the LLSVP is primarily responsible for the sharp edges of these structures, which can be nearly vertical in the deep mantle, there are many ensuing implications. One is that it seems likely that LLSVPs will have thermal boundary layers developed along their discrete boundaries, with these boundary layers conducting heat out of (or into) the pile. If the LLSVPs are enriched in radiogenic materials, they may be relatively hot, and the enveloping thermal boundary layers might themselves become detached to rise as thermal plumes, perhaps entraining trace materials of the distinct chemistry of the LLSVP (Deschamps et al., 2012). The distinct material properties of LLSVPs associated with their chemistry (e.g., the relatively high incompressibility suggested by the Vp/Vs anomaly) have implications for the internal dynamics of the LLSVPs. High incompressibility can lead to a metastable condition for thermal upwellings that causes them to stall in the mid-mantle, producing the large mound of the LLSVP primarily by internal dynamics rather than external flow conditions (e.g., Sun et al., 2007b; Tan and Gurnis, 2005, 2007; Tan et al., 2011). Long-term oscillations of metastable plume may account for Pacific geoid anomalies (Cadio et al., 2011).

The general correlation of low-velocity regions in D'' with the surface distribution of hot spot volcanoes (e.g., Williams et al., 1998) has long been noted, but even stronger correlation is found between the margins of LLSVPs and hot spot volcanoes (Thorne et al., 2004), supporting the notion that boundary layer instabilities may shed from the edges of LLSVPs (Davaille, 1999; Jellinek and Manga, 2002), rather than the entire structure being a superplume. The present-day location of LLSVPs places their margins below many reconstructed locations of large igneous provinces produced over several hundred million years (e.g., Burke and Torsvik, 2004; Burke et al., 2008; Torsvik et al., 2006, 2008). This suggests the possibility of very long time stability of the thermochemical piles (Nebel et al., 2007) and their importance for generating boundary layer instabilities (e.g., Garnero et al., 2007a; Steinberger and Torsvik, 2012) that have affected Earth's surface profoundly throughout at least Cenozoic and Mesozoic time (Dziewonski et al., 2010). The notion that deep mantle heterogeneity, which displaces sluggishly relative to the upper mantle, may play a long-term role in surface geologic processes emphasizes the importance of resolving lower mantle structure and processes.

#### 1.22.7 Ultralow-Velocity Zones

Another important aspect of D'' that has been inferred from seismic waveform investigations is the widespread existence of a layer from 5 to 40 km thick overlying the CMB with very strong P-wave and S-wave velocity reductions of up to –10% and –30%, respectively (see Figure 8(b)). Early observations of these ULVZs are summarized by Garnero et al. (1998) and Thorne and Garnero (2004). Extensive regions of ULVZ appear

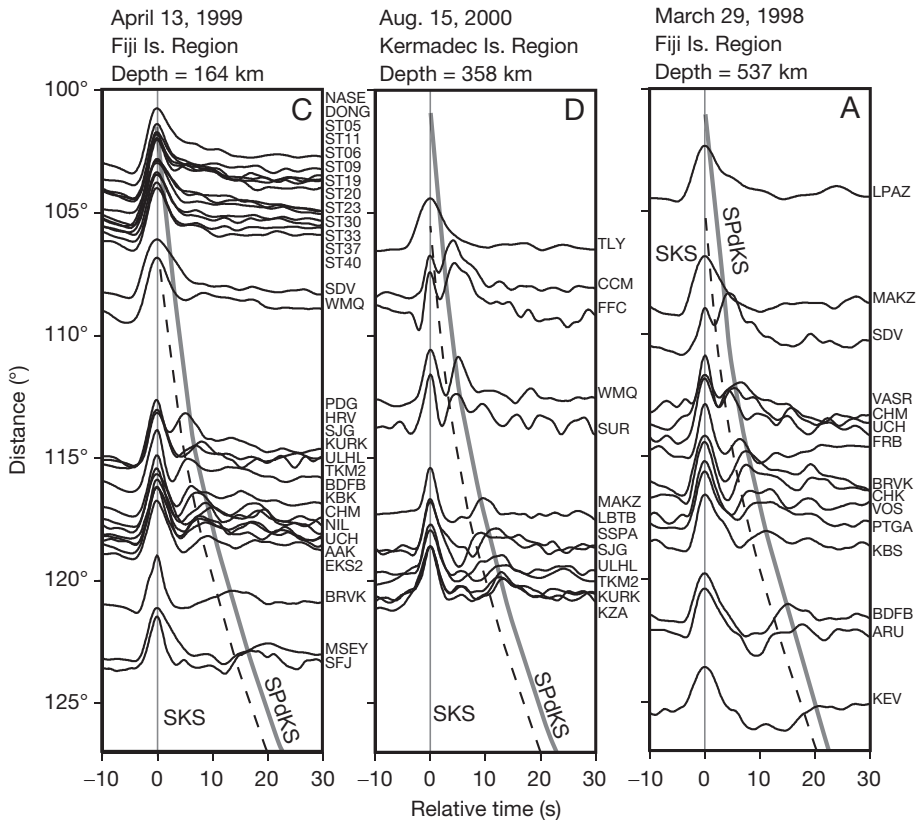


**Figure 11** Waveforms with anomalously late SPdKS arrivals. The signals are aligned on SKS, with the dashed curves indicating the expected time for the peak of SPdKS based on the PREM structure. The observed arrivals are 2–3 s later than expected, which must be due to anomalously low P velocity right at the CMB where SPdKS diffracts along the boundary. Modeling indicates that about 5–10% low P velocity in a layer 5–10 km thick can match the data. This strong P velocity reduction defines the ULVZ. Courtesy of Ed Garnero.

to exist, although the actual lateral extent is uncertain because either broad horizontally stratified regions or localized three-dimensional domes and blobs may explain the data (Helmberger et al., 1998, 2000). In some cases, the ULVZ region appears to be enhanced to scales of 600–900 km lateral extent and several tens of kilometers of thickness, as under the central Pacific (Cottaar and Romanowicz, 2012) and below the region northeast of Tonga (Thorne et al., 2013). Similarly, the absence of seismically detectable ULVZ does not preclude the presence of a very thin (<5 km) layer that is not resolved by seismic probes of the CMB, and only upper bounds on thickness and velocity drop can be determined (Stutzmann et al., 2000). Nonetheless, there are regions where there is no evidence of complexity in structure right at the CMB in high-quality short-period data (e.g., Castle and van der Hilst, 2000; Persch et al., 2001) and other regions with evidence for rapid small-scale variations in ULVZ structure (e.g., Havens and Revenaugh, 2001; Rost and Revenaugh, 2003). Thus, there are certainly variations in ULVZ structure, so these structures are not globally represented by any one-dimensional model.

#### 1.22.7.1 Seismic Phases Used for Detection

Evidence for a ULVZ at the base of the mantle was first presented by Garnero et al. (1993) and Silver and Bina (1993) based on the behavior of SKS phases that interact with the

CMB. The primary evidence for the ULVZ involves delayed SP<sub>diff</sub>KS phases (Figure 11; e.g., Garnero and Helmberger, 1995, 1998; Helmberger et al., 1998; Rondenay and Fischer, 2003; Rondenay et al., 2010; Thorne et al., 2013), precursors to Pcp reflections (e.g., Mori and Helmberger, 1995; Revenaugh and Meyer, 1997; Ross et al., 2004; Rost et al., 2006, 2010b), precursors to Scs reflections (Figure 12; Avants et al., 2006a), S-wave diffractions (Cottaar and Romanowicz, 2012; To et al., 2011), precursors/postcurors to ScP reflections (Garnero and Vidale, 1999; Idehara, 2011; Idehara et al., 2007; Reasoner and Revenaugh, 2000; Rost and Revenaugh, 2001, 2003; Rost et al., 2005, 2006, 2010a), and SKKS/SKS ratios (Zhang et al., 2009). Strong scattering of PKP and PKKP precursors has also been used to constrain ULVZ structure at the CMB (Rost and Garnero, 2006; Vidale and Hedlin, 1998; Wen, 2000; Wen and Helmberger, 1998; Xu and Koper, 2009; Zou et al., 2007). A variety of seismic wave probes of ULVZ structure are needed in order to characterize the P-wave, S-wave, and density structures, as each phase has sensitivity to more than one parameter. For some phases, there are strong trade-offs with structure on the core side of the CMB as well, with a thin layer of finite rigidity in the outermost core being an alternate possibility (e.g., Buffett et al., 2000; Garnero and Jeanloz, 2000; Rost and Revenaugh, 2001). This yields significant non-uniqueness in the models, but it does appear that the S-wave velocity reductions tend to be larger than the P-wave velocity

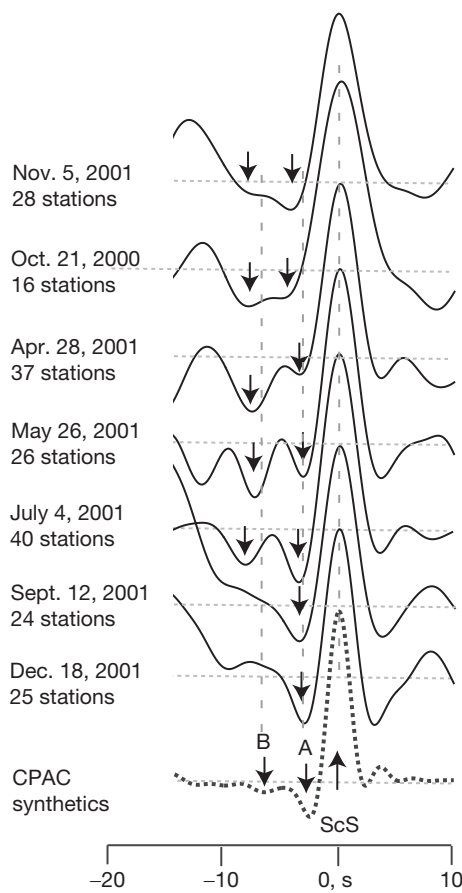


**Figure 12** Stacks of the indicated number of deconvolved seismograms for several deep-focus events in the Tonga subduction zone, aligned on ScS, ordered by increasing event distance from California from top to bottom. Two stable negative amplitude peaks in the 10 s window before ScS are observed in the five closer events, with only one precursor being observed for the two more distant events. A stack of synthetics for a model CPAC with  $-1.1\%$  and  $-3.8\%$  discontinuities 70 and 30 km above the CMB, respectively. Direct S energy arrives 10–25 s before the windows shown. These data indicate that structure above the CMB is more complex than a single ULVZ. Reproduced from Avants M, Lay T, and Garnero EJ (2006a) A new probe of ULVZ S-wave velocity structure: Array stacking of ScS waveforms. *Geophysical Research Letters* 33: L07314, <http://dx.doi.org/10.1029/2005GL024989>.

reductions, and the density may increase by several to tens of percent.

#### 1.22.7.2 Partial Melting and Chemical Anomalies

The strong velocity reductions in ULVZs are most easily explained by the presence of a melt component (Williams and Garnero, 1996), suggesting that either the mantle eutectic is exceeded at the hottest temperatures in the thermal boundary layer or there is infiltration of core material into the lowermost mantle. There is some correlation between locations of ULVZ patches and surface hot spots, which may further suggest a relationship between partial melting in D'' and large-scale upwellings (e.g., Garnero et al., 2007b; Lay et al., 2004b; Williams et al., 1998). Thermally induced rigidity variations

can produce large shear velocity fluctuations relative to compressional velocities ( $R = d(\ln V_s)/d(\ln V_p) = 2.7$ ), whereas chemical variations tend to produce smaller values of  $R \sim 1–2$ . Partial melting can produce  $R$ -values of  $\sim 2.7–3.0$  (e.g., Berryman, 2000; Williams and Garnero, 1996). The ratio of S-wave velocity anomaly to P-wave velocity anomaly in ULVZs has thus been of importance to assessing whether there is a significant chemical anomaly involved, even while partial melting appears to be the only way to approach the magnitude of the velocity decrements in ULVZs. Unfortunately, the ratio is very difficult to resolve given the many trade-offs in model parameters. Available results do favor a ratio closer to three than to one, but further analysis of P-wave velocity and S-wave velocity structure in the same spot using multiple seismic probes is needed to robustly resolve this issue. The observed  $\sim 10\%$  P-wave velocity decrement associated with the ULVZ and the more poorly constrained  $\sim 30\%$  S-wave velocity decrease imply melt fractions of between  $\sim 6\%$  for 1:100 aspect ratio films of melt and  $\sim 30\%$  for spherical melt inclusions (Berryman, 2000; Williams and Garnero, 1996).

The presence of a melt component in the ULVZ has important dynamic and chemical implications. Somehow the melt (if denser than the coexisting solids) does not simply percolate deeper to form a pure melt layer overlying the core. Alternatively, if the melt is buoyant, it would be expected either to rise to its depth of neutral buoyancy or to resolidify during adiabatic ascent (Hernlund and Jellinek, 2010; Hernlund and Tackley, 2007). This juxtaposition of solids and liquids thus implies that one of several possible effects occurs within the ULVZ: (1) the melt is not interconnected and thus is physically unable to efficiently drain from the surrounding solids; (2) the melt density closely matches that of the surrounding solids, so the buoyancy forces on the melt are insufficient to allow the melt to efficiently percolate; or (3) the average vertical convective velocity within the ULVZ is substantially greater than the velocity of melt percolation. Lay et al. (2004b) considered these scenarios, tending to favor the second or third as a means of developing a volumetrically extensive region with a melt component. Many ULVZ locations are on or within the margins of LLSVPs, suggesting some relationship to the thermal and dynamic processes in the LLSVPs. If the LLSVPs are dynamically configured by surrounding mantle flow and the ULVZs are configured by internal LLSVP dynamics, mapping of the structures provides first-order information on the location of deep mantle reservoirs (McNamara et al., 2010).

The presence of a melt component within the basal layer of the mantle is likely to have enhanced chemical interactions with the core through time and may be indicative of an enrichment of this zone in elements that are incompatible in mantle minerals near CMB pressures and temperatures. Thus, iron enrichment of D'' may have occurred through melt descent from above (e.g., Knittle, 1998), through subduction of iron-rich ancient oceanic crust (Dobson and Brodholt, 2005), or possibly through core interactions from below (e.g., Sakai et al., 2006). Recent work indicates that the core is undersaturated in Si and O, so the likelihood of significant diffusion of Fe into the mantle now appears low, and the lowermost mantle may instead be depleted in Fe (Ozawa et al., 2008). Mechanical mechanisms of core infiltration might still be plausible (e.g., Kanda and Stevenson, 2006; Otsuka and Karato, 2012). Labrosse et al. (2007) considered a model of ULVZ being

remnant of a much more extensive dense magma ocean above the CMB, which has cooled and solidified over time, concentrating partial melt into the ULVZ. Silicate melts in the deep mantle appear likely to be denser than surround material, allowing them to accumulate over time (e.g., Mosenfelder et al., 2009; Murakami and Bass, 2011; Thomas et al., 2012). The enrichment of radiogenic elements in D'' within the solidified basal magma ocean is generally consistent with a magmatic evolution for this boundary layer (Lay et al., 2004a,b): radiogenic element enrichment within the boundary layer has been suggested as a mechanism to reduce the required heat flux out of the outer core (Buffett, 2003).

A subsolidus mechanism to account for ULVZs involving postperovskite has been proposed by Mao et al. (2006a,b). Experiments indicate that postperovskite is tolerant of quite large amounts of Fe, up to 40% or higher, and that such large iron content has a dramatic effect on both S-wave and P-wave velocities. If postperovskite is stable at the hottest temperatures in the mantle at CMB pressures, this idea offers an alternative to having a dense melt component present. As noted earlier, there is large uncertainty in the absolute temperature in D'', and there is substantial uncertainty in the Clapeyron slope of the phase transition, so this possibility remains highly conjectural. Experimental measurements of sound velocities in  $(\text{Mg}_{.16}\text{Fe}_{.84})\text{O}$  by Wicks et al. (2010) indicate that large uptake of Fe in magnesiowüstite results in pronounced seismic velocity reductions as well. Bower et al. (2011) proposed that iron-rich  $(\text{Mg},\text{Fe})\text{O}$  concentrations in localized patches account for the ULVZ. Further testing of these alternatives to partial melt fractions as an explanation for ULVZs is of high priority.

### 1.22.8 Lower Mantle Anisotropy

While the bulk of the lower mantle does not appear to have large-scale organized anisotropy, the D'' region has been shown to have extensive regions where shear-wave splitting occurs (see reviews by Kendall, 2000; Lay et al., 1998a,b; Moore et al., 2003; Nowacki et al., 2011). These observations have prompted increased consideration of the anisotropic crystallography of high-pressure phases likely to be present in the lower mantle along with what deformation mechanisms are likely to control the formation of fabrics (e.g., Karato, 1998; Stixrude, 1998). There remain substantial uncertainties in the nature of the anisotropy and its cause. Strong shear flows in the boundary layer may induce lattice-preferred orientation (LPO) of the anisotropic lower mantle minerals, but it is not immediately clear why this would not also hold for the overlying lower mantle. Sheared inclusions of chemical heterogeneities and pockets of partial melt may also play a role in generating the seismic anisotropy. The postperovskite phase transition may also be important. As observational and laboratory constraints improve, it is likely that modeling anisotropy in D'' will provide important constraints on the thermal and dynamic processes in the boundary layer, and impressive efforts in this direction have commenced (Walker et al., 2011).

#### 1.22.8.1 Shear-Wave Splitting Observations

Observations of splitting for ScS phases have been made for several decades (e.g., Lay and Helmberger, 1983b; Mitchell and

Helmberger, 1973; Rokosky et al., 2004), but observations of diffracted waves and wide-angle grazing S waves convincingly demonstrate that anisotropy is present in D'' (e.g., Ford et al., 2006; Garnero and Lay, 1997, 1999; Garnero et al., 2004a,b; Kendall and Silver, 1996; Lay and Young, 1991; Matzel et al., 1996; Maupin et al., 2005; Panning and Romanowicz, 2004; Ritsema, 2000; Ritsema et al., 1998a; Russell et al., 1998; Thomas and Kendall, 2002; Vinnik et al., 1989, 1995, 1998b). Figure 8(c) indicates the regions that have been studied in detail. All observations of D'' anisotropy are subject to uncertainties because of the limitations of the corrections for upper mantle anisotropy and the possibility of significant near-source anisotropy even for deep-focus earthquakes. Komatitsch et al. (2010) demonstrated that isotropic structure can produce apparent splitting for diffracted waves, so caution is required for diffracted data interpretations.

The large majority of observations involve horizontally polarized shear-wave components (SH) traveling faster through D'' than vertically polarized shear waves (SV) for grazing incidence or wide-angle reflections, with relatively large-scale regions of D'' displaying 0.5–1.5% anisotropy (e.g., Fouch et al., 2001; Garnero and Lay, 2003; Kendall and Silver, 1996; Ritsema, 2000; Rokosky et al., 2004; Thomas and Kendall, 2002; Thomas et al., 2007, 2011; Usui et al., 2005, 2008; Vinnik et al., 1998b; Walker et al., 2011; Wang and Wen, 2007b; Wookey and Kendall, 2008). While almost none of the studies have significant azimuthal raypath sampling, the observations are at least compatible with extensive vertical transverse isotropy, as may be caused by hexagonally symmetrical material with a vertical symmetry axis or fine-scale horizontal layering. The onset of shear-wave splitting appears to be linked to the S-wave velocity increase at the top of D'' in high-velocity regions (e.g., Garnero and Lay, 1997; Matzel et al., 1996), but the resolution of the depth extent of the anisotropy in the boundary layer remains very limited (Moore et al., 2003).

Localized observations of shear-wave splitting in D'' with SV velocities being higher than SH velocities have been reported, with localized upwellings in the boundary layer being invoked as one possible way to modify the symmetry axis for shape-preferred orientation (SPO) or LPO (e.g., Pulliam and Sen, 1998; Rokosky et al., 2004; Russell et al., 1998, 1999). Garnero et al. (2004a), Niu and Perez (2004), Maupin et al. (2005), Wookey et al. (2005a), Rokosky et al. (2006), Long (2009), and Nowacki et al. (2010) presented clear observations of azimuthal anisotropy from the analysis of S, SKS, and SKKS phases (Figure 13), with fast and slow waves mixed on the SH and SV components. Restivo and Helffrich (2006) did find that on the large scale, differential splitting of SKS and SKKS is relatively minor, with azimuthal anisotropy <2% for extended regions.

#### 1.22.8.2 Mineralogical/Dynamic Implications

Anisotropy compatible with the primary seismic observations of shear-wave splitting in D'' could be the result of LPO for a D'' mineral component or the result of SPO of chemical or partial melt components in a sheared boundary layer. A candidate major component of the lower mantle that may develop anisotropy with SH velocity faster than SV velocity in a horizontally sheared boundary layer is MgO or ferropericlase (e.g., Karato, 1998; Karki et al., 1999; Kendall, 2000; Long et al.,

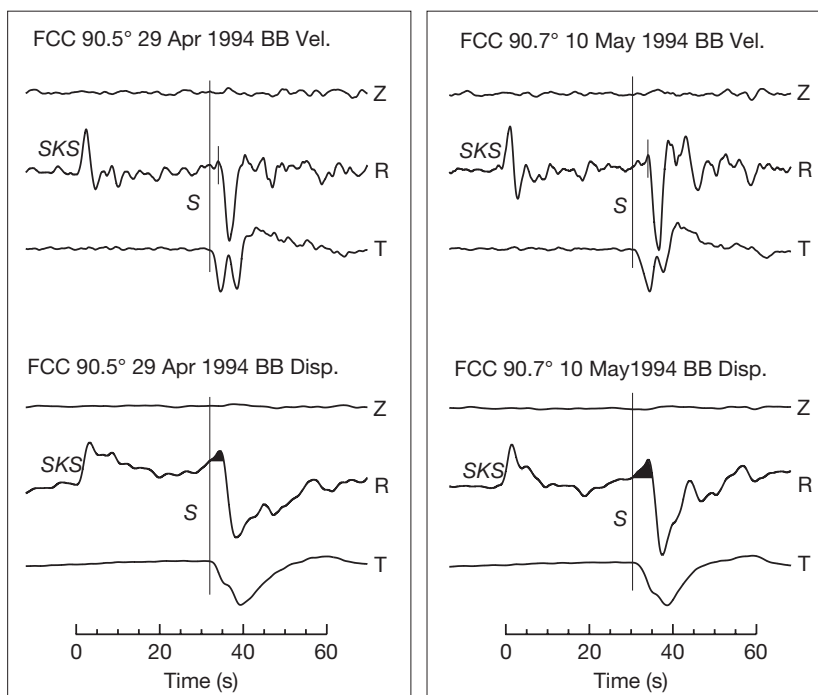


**Figure 13** Three-component records from station FCC (Fort Churchill, Canada) for two deep South American earthquakes, showing ground velocity (upper plots) and ground displacement (lower plots) spanning the SKS and S arrivals. Corrections for receiver lithospheric anisotropy have been applied (note that no SKS energy is seen on the transverse component), and the Z and R rotations are to the wave front normal and wave front parallel directions for the SKS arrival, respectively. The arrival time of S is indicated by the vertical lines. The small reverse-polarity upswing at the beginning of the S wave on the radial components of the displacement seismograms is colored in black. This feature is easily missed in the velocity records, and one is tempted to pick a sharp correct-polarity negative arrival as the first SV arrival (small ticks). The reverse-polarity energy is produced by azimuthal anisotropy, either in D'' or possibly near the source, which couples the fast arrival to the R and T components. Reproduced from Maupin V, Garnero EJ, Lay T, and Fouch MJ (2005) Azimuthal anisotropy in the D'' layer beneath the Caribbean. *Journal of Geophysical Research* 110: B08301, <http://dx.doi.org/10.1029/2004JB003506>.

2006; Mainprice et al., 2000; Marquardt et al., 2009a; Stixrude, 1998; Yamazaki and Karato, 2002), whereas low-velocity lamellae composed of partially melted crust or other chemical heterogeneities are also possible causes of such anisotropy (e.g., Fouch et al., 2001; Kendall and Silver, 1998; Moore et al., 2003; Wyssession et al., 1999). Anisotropy of perovskite has also been quantified (e.g., Mainprice et al., 2008). McNamara et al. (2001, 2002, 2003) used thermal convection models to compute variations in temperature and stress regime that might result in the localization of dislocation creep that favor LPO in some areas and diffusion-dominated deformation in others that would require SPO to account for any anisotropy. These dynamic calculations indicate that conditions favorable for mid-mantle anisotropy may exist in down-wellings, but as yet, there is no clear evidence for anisotropy in the bulk of the mid-mantle (e.g., Kaneshima and Silver, 1995; Meade et al., 1995).

The anisotropic properties of postperovskite may further explain the strong association between regions with a lower mantle S-wave velocity discontinuity and regions with S-wave splitting that is stronger than observed in lower-velocity regions. Stackhouse et al. (2005b) computed the anisotropic properties of postperovskite and considered the propensity for developing LPO compatible with seismic observations. It appears that postperovskite has more favorable properties

than perovskite for acquiring LPO in D'' (Nowacki et al., 2010, 2012; Wookey and Kendall, 2007). The deformation of postperovskite and analog materials also supports the notion that postperovskite may acquire anisotropic fabrics in the lowermost mantle (Carrez et al., 2007b; Merkel et al., 2006, 2007; Miyagi et al., 2010, 2011; Niwa et al., 2007, 2012; Okada et al., 2010; Walte et al., 2009; Wenk et al., 2011; Yamazaki and Karato, 2007; Yamazaki et al., 2006; Yoshino and Yamazaki, 2007; Zhan, 2011). The size of the D'' discontinuity may exceed the velocity increase for the postperovskite phase change on average, and anisotropic properties may be required to match the observations (Murakami et al., 2007b).

### 1.22.9 Small-Scale Heterogeneities

The emphasis in the foregoing sections has been on intermediate and large-scale structure, as this is most readily resolved by tomographic and waveform modeling procedures. However, as is true of the lithosphere, key dynamic and chemical structures exist in D'' on scales below the limit of deterministic resolution using seismic waves with wavelengths longer than 10 km or so. Very fine structure will scatter seismic energy, and statistical attributes of the structure can be constrained using various approaches.

### 1.22.9.1 Scattering in D''

Small-scale variations in D'', with about 1% heterogeneities on scale lengths of about 10 km, are revealed by scattered P-wave signals. This has been demonstrated by the analysis of short-period precursors to PKP phases (e.g., Bataille and Flatté, 1988; Bataille et al., 1990; Brana and Helffrich, 2004; Cao and Romanowicz, 2007; Cleary and Haddon, 1972; Cormier, 1999; Doornbos, 1976; Garcia et al., 2009; Haddon and Cleary, 1974; Hedlin and Shearer, 2000; Hedlin et al., 1997; Miller and Niu, 2008; Thomas et al., 2009) and P'P' (Wu et al., 2012). The small-scale structure is also analyzed using diffracted coda waves (e.g., Bataille and Lund, 1996), PKKP reflections (e.g., Earle and Shearer, 1997; Rost and Earle, 2010), triplications (e.g., Kohler et al., 1997), and scatterer migrations (e.g., Thomas et al., 1999). Some studies purport to show evidence for thin layers of anomalous properties or lamellae in the boundary layer (e.g., Lay and Helmberger, 1983b; Thomas et al., 1998; Weber, 1994). The structural heterogeneities involve scale lengths of a few to tens of kilometers, with various estimates of velocity fluctuations of a few to 10%. It has generally been believed that the levels of heterogeneity increase in D'' relative to the overlying mantle, but there is evidence that small-scale structure in D'' is not distinctive from that throughout the mantle (e.g., Hedlin et al., 1997). Nonetheless, it is clear that some of the strongest scattering, involving much larger velocity heterogeneities, does arise within D'' (Vidale and Hedlin, 1998; Wen and Helmberger, 1998), and this is likely associated with the patchy ULVZ just above the CMB. The bandwidth of the signals used in scattering analyses controls the sensitivity to scatterers of different dimensions, and the analysis of broadband data indicates a rich spectrum of scattering scale lengths in D''.

Cormier (2000) had developed the perspective of D'' being a transition in the heterogeneity spectrum of the lowermost mantle, with a relatively 'red' spectrum, having substantial power at long wavelengths but still significant strength at short wavelengths. It is plausible that small-scale structure also exists on the core side of the CMB, concentrated in topographic highs (e.g., Buffett et al., 2000; Garnero and Jeanloz, 2000; Rost and Revenaugh, 2003).

### 1.22.9.2 Core–Mantle Boundary Topography

Given the complexity of structure at all scales in D'', it is not surprising that large uncertainty remains as to whether there is much topography on the CMB itself. Long-wavelength topography of the CMB was proposed by Creager and Jordan (1986b) and Morelli and Dziewonski (1987) based on studies of bulletin PcP and PKP arrival times, but it has been demonstrated that allowing for strong heterogeneity in D'' and the limited resolution of the available data make CMB topography models very uncertain (e.g., Doornbos and Hilton, 1989; Garcia and Souriau, 2000; Obayashi and Fukao, 1997; Pulliam and Stark, 1993; Rodgers and Wahr, 1993; Sze and van der Hilst, 2003). As models for the entire mantle improve, this may prove to be a solvable problem, and it is a critical one, for CMB topography plays a major role in estimating the extent of mechanical coupling between the core and the mantle. For imaging shorter-wavelength topography of the CMB, the primary approach has

involved travel time fluctuations and precursors to underside reflections of internal core reverberations (PKKP). These phases provide an upper bound of about 100 m topography on 10 km scale lengths (e.g., Bataille and Flatté, 1988; Chang and Cleary, 1978; Doornbos, 1974, 1980; Earle and Shearer, 1997, 1998; Tanaka, 2010). Nutation data bounds very long-wavelength topography on the CMB to a few hundred meters (Defraigne et al., 1996). The calculations of topography induced by flow (e.g., Lassak et al., 2007; Yoshida, 2008; Youngs and Houseman, 2007) provide testable predictions that can be evaluated by using seismic observations (Lassak et al., 2010).

## 1.22.10 Conclusions

Any attempt to characterize the knowledge of the lower mantle and D'' region can only provide a snapshot of a rapidly evolving, even exploding topic. Interdisciplinary progress in mineral physics theory and experimentation, geodynamics, and geochemistry resonates with advances in seismological imaging, redefining conceptual models with remarkable rapidity. One decade's 'superplumes' become the next decade's 'superpiles,' with major shifts in perception of the roles played by seismically detected heterogeneities. This is both stimulating and unsettling, with our understanding of the mantle system acquiring more and more levels of complexity. The extensive citations provided here are intended to help the reader penetrate into the deluge of findings from multiple disciplines addressing lower mantle and D'' topics. This is an increasingly daunting task with a very distributed literature, and there is no slowing down of activity as yet.

So, what lies ahead? There continues to be great potential to make major advances in our understanding of the thermal regime in the lowermost mantle if the postperovskite phase transition is shown to be the correct explanation for the D'' discontinuity. This is because a phase transition can be calibrated in actual  $P$ - $T$  space, greatly reducing the uncertainty in temperature estimates currently obtained by extrapolation over thousands of kilometers in depth. Parallel efforts in mineral physics and seismology can advance this topic much as they have advanced our understanding of transition zone conditions; however, it has become clear just how important the role of precise chemistry of each mineral phase is, compounded by the effects of iron spin transitions.

Increasing densification and accumulation of seismological data sets is enabling new approaches such as migration to be applied to deep mantle targets. While coverage is, and will remain, embarrassingly limited compared to exploration industry data sets, the advantage of generally parameterized migrations for rough structure has already been established and promises to reveal important structural characteristics in the lower mantle. Large data sets are also critical to one of the persistent challenges in deep Earth imaging, separating source, deep, and receiver contributions to the signals. Studies of lower mantle scattering, lower mantle anisotropy, and lower mantle stratification are all plagued by near-source and near-receiver signal-generated noise. Improved suppression of these effects by combining empirical filters and stacking approaches holds much promise for improving seismological resolution of deep structure. The large data sets enable full waveform inversion

approaches to some extent, although the problem in deep mantle applications is the severe limitation of azimuthal path sampling, so it is not clear yet whether there is any true gain to be had by waveform inversions over imaging methods. It is clear that expanding global coverage of seismic observations, particularly by increased long-term operation of ocean floor recording systems, is essential for better characterizing deep Earth structure globally. With new procedures such as noise correlation allowing deep structure to be probed between all pairs of stations (e.g., Lin et al., 2013), each new observation point provides extensive new probing of deep mantle structure below each station.

Seismological structures in the deep mantle LLSVPs have been shown to have lateral gradients as strong as radial gradients, and the search for steeply dipping interfaces using azimuthal data gathers has proved fruitful. Approaches to quantifying three-dimensional structures for poorly sampled wave fields require both efficient 3D computational tools and new strategies for modeling, and significant progress is being made in this arena. Approaches based on iterating from initial tomographic models have shown some success, but the wave field complexity often involves smaller scales than constrained by tomography. One cannot help but feel that we have still only scratched the surface of the complex regime that likely exists in the deep mantle. Much work remains.

## Acknowledgment

T. Lay's research on lower mantle structure is supported by NSF Grant EAR1245717.

## References

- Adams DJ and Oganov AR (2006) Ab initio molecular dynamics study of CaSiO<sub>3</sub> perovskite at P-T conditions of Earth's lower mantle. *Physical Review B* 73: 184106.
- Adams LH and Williamson ED (1923) The composition of the Earth's interior. Smithsonian Institute Annual Reports, 241–260.
- Aizawa Y and Yoneda A (2006) P-V-T equation of state of MgSiO<sub>3</sub> perovskite and MgO periclase: Implications for lower mantle composition. *Physics of the Earth and Planetary Interiors* 155: 87–95. <http://dx.doi.org/10.1016/j.pepi.2005.10.002>.
- Akber-Knutson S, Steinle-Neumann G, and Asimow PD (2005) Effect of Al on the sharpness of the MgSiO<sub>3</sub> perovskite to post-perovskite phase transition. *Geophysical Research Letters* 32: L14303. <http://dx.doi.org/10.1029/2005GL023192>.
- Alexander SS and Phinney RA (1966) A study of the core–mantle boundary using P-waves diffracted by the Earth's core. *Journal of Geophysical Research* 71: 5943–5958.
- Ammann MW, Brodholt JP, and Dobson DP (2011) Ferrous iron diffusion in ferro-periclase across the spin transition. *Earth and Planetary Science Letters* 302: 393–402.
- Ammann MW, Brodholt JP, Wookey J, and Dobson DP (2010) First-principles constraints on diffusion in lower-mantle minerals and a weak D'' layer. *Nature* 465: 462–465. <http://dx.doi.org/10.1038/nature09052>.
- Anderson DL (1967) The anelasticity of the mantle. *Geophysical Journal of the Royal Astronomical Society* 14: 135–164.
- Anderson DL (1991) Chemical boundaries in the mantle. In: Sabadini R, Lambeck K, and Boschi E (eds.) *Glacial Isostasy, Sea-Level and Mantle Rheology*, pp. 379–401. The Netherlands: Kluwer.
- Anderson DL (1998) The EDGES of the mantle. In: Gurnis M, Wysession ME, Knittle E, and Buffett BA (eds.) *The Core–Mantle Boundary Region*, pp. 255–271. Washington, DC: American Geophysical Union.
- Anderson DL and Hart RS (1978) Q of the Earth. *Journal of Geophysical Research* 83: 5869–5882.
- Anderson DL, Kanamori H, Hart RS, and Liu H-P (1977) The Earth as a seismic absorption band. *Science* 196: 1104–1106.
- Andrault D, Boltan-Casanova N, Bouhifd MA, Guignot N, and Kawamoto T (2007) The role of Al-defects on the equation of state of Al-(Mg,Fe)SiO<sub>3</sub> perovskite. *Earth and Planetary Science Letters* 263: 167–179.
- Andrault D, Muñoz M, Boltan-Casanova N, et al. (2010) Experimental evidence for perovskite and post-perovskite coexistence throughout the whole D'' region. *Earth and Planetary Science Letters* 293: 90–96.
- Antolik M, Gu YJ, and Ekström G (2003) J362D28: A new joint model of compressional and shear velocity in the Earth's mantle. *Geophysical Journal International* 153: 443–466.
- Antonangeli D, Siebert J, Aracne CM, et al. (2011) Spin crossover in ferropericlase at high pressure: A seismologically transparent transition? *Science* 331(6013): 64–67.
- Auzende A-L, Badro J, Reyerson FJ, et al. (2008) Element partitioning between magnesium silicate perovskite and ferropericlase: New insights into bulk lower-mantle geochemistry. *Earth and Planetary Science Letters* 269: 164–174. <http://dx.doi.org/10.1016/j.epsl.2008.02.001>.
- Avants M, Lay T, and Garnero EJ (2006) A new probe of ULVZ S-wave velocity structure: Array stacking of ScS waveforms. *Geophysical Research Letters* 33: L07314. <http://dx.doi.org/10.1029/2005GL024989>.
- Avants M, Lay T, Russell SA, and Garnero EJ (2006) Shear velocity variation within the D'' region beneath the Central Pacific. *Journal of Geophysical Research* 111: B05305. <http://dx.doi.org/10.1029/2004JB003270>.
- Badro J, Fiquet G, Guyot F, et al. (2003) Iron partitioning in Earth's mantle: Toward a deep lower mantle discontinuity. *Science* 300: 789–791.
- Badro J, Rueff J-P, Vankó G, Monaco G, Fiquet G, and Guyot F (2004) Electronic transitions in perovskite: Possible nonconvecting layers in the lower mantle. *Science* 305: 383–386.
- Bataille K and Flatté SM (1988) Inhomogeneities near the core–mantle boundary inferred from short-period scattered PKP-waves recorded at the global digital seismograph network. *Journal of Geophysical Research* 93: 15057–15064.
- Bataille K and Lund F (1996) Strong scattering of short-period seismic waves by the core–mantle boundary and the P-diffracted wave. *Geophysical Research Letters* 18: 2413–2416.
- Bataille K, Wu RS, and Flatté SM (1990) Inhomogeneities near the core–mantle boundary evidenced from scattered waves: A review. *Pure and Applied Geophysics* 132: 151–173.
- Bengtson A, Li J, and Morgan D (2009) Mossbauer modeling to interpret the spin state of iron in (Mg,Fe)SiO<sub>3</sub> perovskite. *Geophysical Research Letters* 36: L15301. <http://dx.doi.org/10.1029/2009GL038340>.
- Bengtson A, Persson K, and Morgan D (2008) Ab initio study of the composition dependence of the pressure-induced spin crossover in perovskite (Mg<sub>1-x</sub>, Fe<sub>x</sub>)SiO<sub>3</sub>. *Earth and Planetary Science Letters* 265: 535–545.
- Berryman JG (2000) Seismic velocity decrement ratios for regions of partial melt in the lower mantle. *Geophysical Research Letters* 27: 421–424.
- Bijwaard H and Spakman W (1999) Tomographic evidence for a narrow whole mantle plume below Iceland. *Earth and Planetary Science Letters* 166: 121–126.
- Bijwaard H, Spakman W, and Engdahl ER (1998) Closing the gap between regional and global travel time tomography. *Journal of Geophysical Research* 103: 30055–30078.
- Boffa Ballaran T, Kurnosov A, Konstantin G, et al. (2012) Effect of chemistry on the compressibility of silicate perovskite in the lower mantle. *Earth and Planetary Science Letters* 333–334: 181–190.
- Boffa Ballaran T, Trønnes RG, and Frost DJ (2007) Equations of state of CaIrO<sub>3</sub> perovskite and post-perovskite phases. *American Mineralogist* 92: 1760–1763.
- Boltan-Casanova N, Andrault D, Amiguet E, and Guignot N (2009) Equation of state and post-stishovite transformation of Al-bearing silica up to 100 GPa and 3000 K. *Physics of the Earth and Planetary Interiors* 174: 70–77.
- Bolt BA, Niazi M, and Somerville MR (1970) Diffracted ScS and the shear velocity at the core boundary. *Geophysical Journal of the Royal Astronomical Society* 19: 299–305.
- Bolton H (1996) Long Period Travel Times and the Structure of the Mantle. Ph.D. Thesis, University of California, San Diego, 204 pp.
- Boschi L, Becker TW, and Steinberger B (2007) Mantle plumes: Dynamic models and seismic images. *Geochemistry, Geophysics, Geosystems* 8: Q10006. <http://dx.doi.org/10.1029/2007GC001733>.
- Boschi L, Becker TW, and Steinberger B (2008) On the statistical significance of correlations between synthetic mantle plumes and tomographic models. *Physics of the Earth and Planetary Interiors* 167: 230–238.
- Boschi L and Dziewonski AM (1999) High-and low-resolution images of the Earth's mantle: Implications of different approaches to tomographic modeling. *Journal of Geophysical Research* 104: 25567–25594.

- Boschi L and Dziewonski AM (2000) Whole Earth tomography from delay times of P, P<sub>c</sub>P, and PKP phases: Lateral heterogeneities in the outer core or radial anisotropy in the mantle? *Journal of Geophysical Research* 105: 13675–13696.
- Bouillard E, Menguy N, Auzende AL, et al. (2012) Experimental investigation of the stability of Fe-rich carbonates in the lower mantle. *Journal of Geophysical Research* 117: B02208. <http://dx.doi.org/10.1029/2011JB008733>.
- Bower DJ, Gurnis M, Jackson JM, and Sturhahn W (2009) Enhanced convection and fast plumes in the lower mantle induced by the spin transition in ferropericlase. *Geophysical Research Letters* 36: L10306. <http://dx.doi.org/10.1029/2009GL037706>.
- Bower DJ, Gurnis M, and Sun D (2013) Dynamic origins of seismic wavespeed variation in D''. *Physics of the Earth and Planetary Interiors* 214: 74–86.
- Bower DJ, Wicks JK, Gurnis M, and Jackson JM (2011) A geodynamic and mineral physics model of a solid-state ultralow-velocity zone. *Earth and Planetary Science Letters* 303: 193–202.
- Boyd TM and Creager KC (1991) The geometry of Aleutian subduction: Three-dimensional seismic imaging. *Journal of Geophysical Research* 96: 2267–2291.
- Brana L and Helffrich G (2004) A scattering region near the core–mantle boundary under the North Atlantic. *Geophysical Journal International* 153: 625–636. <http://dx.doi.org/10.1111/j.1365-246X.2004.02306.x>.
- Bréger L and Romanowicz B (1998) Three-dimensional structure at the base of the mantle beneath the central Pacific. *Science* 282: 718–720.
- Bréger L, Romanowicz B, and Ng C (2001) The Pacific plume as seen by S, ScS, and SKS. *Geophysical Research Letters* 28: 1859–1862.
- Brodholt JP, Helffrich G, and Trampert J (2007) Chemical versus thermal heterogeneity in the lower mantle: The most likely role of anelasticity. *Earth and Planetary Science Letters* 262: 429–437. <http://dx.doi.org/10.1016/j.epsl.2007.07.054>.
- Buffett BA (2003) The thermal state of Earth's core. *Science* 299: 1675–1677.
- Buffett BA (2007) A bound on heat flow below a double crossing of the perovskite–postperovskite phase transition. *Geophysical Research Letters* 34: L17302. <http://dx.doi.org/10.1029/2007GL030930>.
- Buffett BA, Garnero EJ, and Jeanloz R (2000) Sediments at the top of Earth's core. *Science* 290: 1338–1342.
- Bull AL, McNamara AK, and Ritsema J (2009) Synthetic tomography of plume clusters and thermochemical piles. *Earth and Planetary Science Letters* 278: 152–162.
- Bullen KE (1949) Compressibility-pressure hypothesis and the Earth's interior. *Monthly Notes of the Royal Astronomical Society. Geophysical Supplement* 5: 355–368.
- Burdick LJ and Powell C (1980) Apparent velocity measurements for the lower mantle from a wide aperture array. *Journal of Geophysical Research* 85: 3845–3856.
- Burke K, Steinberger B, Torsvik TH, and Smethurst MA (2008) Plume generation zones at the margins of large low shear velocity provinces on the core–mantle boundary. *Earth and Planetary Science Letters* 265: 49–60.
- Burke K and Torsvik TH (2004) Derivation of large igneous provinces of the past 200 million years from long-term heterogeneities in the deep mantle. *Earth and Planetary Science Letters* 227: 531–538.
- Cadek O and Fleitout L (2006) Effect of lateral viscosity variations in the core–mantle boundary region on predictions of the long-wavelength geoid. *Studia Geophysica et Geodaetica* 50: 217–232.
- Cadio C, Panet I, Davaille A, Diamant M, Métivier L, and de Viron O (2011) Pacific geoid anomalies revisited in light of thermochemical oscillating domes in the lower mantle. *Earth and Planetary Science Letters* 306: 123–135.
- Cammarano F, Marquardt H, Speziale S, and Tackley PJ (2010) Role of iron–spin transition in ferropericlase on seismic interpretation: A broad thermochemical transition in the mid mantle? *Geophysical Research Letters* 37: L03308. <http://dx.doi.org/10.1029/2009GL041583>.
- Cao A and Romanowicz B (2007) Locating scatterers in the mantle using array analysis of PKP precursors from an earthquake doublet. *Earth and Planetary Science Letters* 255: 22–31.
- Caracas R (2010a) Elasticity of AlFeO<sub>3</sub> and FeAlO<sub>3</sub> perovskite and post-perovskite from first-principles calculations. *Geophysical Research Letters* 37: L20306. <http://dx.doi.org/10.1029/2010GL044404>.
- Caracas R (2010b) Spin and structural transitions in AlFeO<sub>3</sub> and FeAlO<sub>3</sub> perovskite and post-perovskite. *Physics of the Earth and Planetary Interiors* 182: 10–17.
- Caracas R and Cohen RE (2006) Theoretical determination of the Raman spectra of MgSiO<sub>3</sub> perovskite and post-perovskite at high pressure. *Geophysical Research Letters* 33: L12S05. <http://dx.doi.org/10.1029/2006GL025736>.
- Caracas R and Cohen RE (2007) Effect of chemistry on the physical properties of perovskite and post-perovskite. In: Hirose K, et al. (eds.) *Post-Perovskite: The Last Mantle Phase Transition. Geophysical Monograph Series*, vol. 174, pp. 115–128. Washington, DC: AGU.
- Caracas R and Cohen RE (2008) Ferrous iron in post-perovskite from first-principles calculations. *Physics of the Earth and Planetary Interiors* 168: 147–152.
- Caracas R, Mainprice D, and Thomas C (2010) Is the spin transition in Fe<sup>2+</sup>-bearing perovskite visible in seismology? *Geophysical Research Letters* 37: L13309. <http://dx.doi.org/10.1029/2010GL043320>.
- Carrez P, Ferré D, and Cordier P (2007a) Implications for plastic flow in the deep mantle from modeling dislocations in MgSiO<sub>3</sub> minerals. *Nature* 446: 68–70.
- Carrez P, Ferré D, and Cordier P (2007b) Peierls-Nabarro model for dislocations in MgSiO<sub>3</sub> post-perovskite calculated at 120 GPa from first principles. *Philosophical Magazine* 1–19. <http://dx.doi.org/10.1080/14786430701268914>.
- Castle JC and Creager KC (1999) A steeply dipping discontinuity in the lower mantle beneath Izu-Bonin. *Journal of Geophysical Research* 104: 7279–7292.
- Castle JC, Creager KC, Winchester JP, and van der Hilst RD (2000) Shear wave speeds at the base of the mantle. *Journal of Geophysical Research* 105: 21543–21557.
- Castle JC and van der Hilst RD (2000) The core–mantle boundary under the Gulf of Alaska: No ULVZ for shear waves. *Earth and Planetary Science Letters* 176: 311–321.
- Catalli K, Shim S-H, Dera P, et al. (2011) Effects of Fe<sup>3+</sup> spin transition on the properties of aluminous perovskite—New insights for lower-mantle seismic heterogeneities. *Earth and Planetary Science Letters* 310: 293–302.
- Catalli K, Shim S-H, Prakapenka V (2009) Thickness and Clapeyron slope of the post-perovskite boundary. *Nature* 462: 782–785.
- Catalli K, Shim S-H, Prakapenka V, Zhao J, and Sturhahn W (2010) x-Ray diffraction and Mossbauer spectroscopy of Fe<sup>3+</sup>-bearing Mg-silicate post-perovskite at 128–138 GPa. *American Mineralogist* 95: 418–421.
- Catalli K, Shim S-H, Prakapenka VB, et al. (2010) Spin state of ferric iron in MgSiO<sub>3</sub> perovskite and its effect on elastic properties. *Earth and Planetary Science Letters* 289: 68–75.
- Chaloner J, Thomas C, and Rietbrock A (2009) P-and S-wave reflectors in D'' beneath southeast Asia. *Geophysical Journal International* 179: 1080–1092.
- Chambers K and Woodhouse JH (2006a) Transient D'' discontinuity revealed by seismic migration. *Geophysical Research Letters* 33: L17312. <http://dx.doi.org/10.1029/2006GL027043>.
- Chambers K and Woodhouse JH (2006b) Investigating the lowermost mantle using migrations of long-period S-ScS data. *Geophysical Journal International* 166: 667–678.
- Chang AC and Cleary JR (1978) Precursors to PKKP. *Bulletin of the Seismological Society of America* 68: 1059–1079.
- Chen Y, Chernatynskiy A, Brown D, Schelling PK, Artacho E, and Phillipot SR (2012a) Critical assessment of classical potentials for MgSiO<sub>3</sub> perovskite with application to thermal conductivity calculations. *Physics of the Earth and Planetary Interiors* 210–211: 75–89.
- Chen B, Jackson JM, Sturhahn W, et al. (2012b) Spin crossover equation of state and sound velocities of (Mg<sub>0.65</sub>Fe<sub>0.35</sub>)O ferropericlase to 140 GPa. *Journal of Geophysical Research* 117: B08208.
- Cheng J-G, Zhou JS, and Goodenough JB (2010) Stress-induced perovskite to postperovskite transition in CaIrO<sub>3</sub> at room temperature. *Physical Review B* 82: 132103.
- Cheng J-G, Zhou JS, Goodenough JB, Sui Y, Ren Y, and Suchomel MR (2011) High-pressure synthesis and physical properties of perovskite and post-perovskite Ca<sub>1-x</sub>Sr<sub>x</sub>IrO<sub>3</sub>. *Physical Review B* 83: 064401.
- Chinnery MA and Toksöz MN (1967) P-wave velocities in the mantle below 700 km. *Bulletin of the Seismological Society of America* 57: 199–226.
- Cizkova H, Cadek O, Matyska C, and Yuen DA (2010) Implications of post-perovskite transport properties for core–mantle dynamics. *Physics of the Earth and Planetary Interiors* 180: 235–243.
- Clayton R and Comer R (1983) A tomographic analysis of mantle heterogeneities from body wave travel time data (abstract). *Eos, Transactions of the American Geophysical Union* 64: 776.
- Cleary JR and Haddon RAW (1972) Seismic wave scattering near the core–mantle boundary: A new interpretation of precursors to PKP. *Nature* 240: 549–551.
- Cobden L, Goes S, Ravenna M, et al. (2009) Thermochemical interpretation of 1-D seismic data for the lower mantle: The significance of nonadiabatic thermal gradients and compositional heterogeneity. *Journal of Geophysical Research* 114: B11309. <http://dx.doi.org/10.1029/2008JB006262>.
- Cobden L, Mosca I, Trampert J, and Ritsema J (2012) On the likelihood of post-perovskite near the core–mantle boundary: A statistical interpretation of seismic observations. *Physics of the Earth and Planetary Interiors* 201–211: 21–35.
- Cordier P, Ungár T, Zsoldos L, and Tichý G (2004) Dislocation creep in MgSiO<sub>3</sub> perovskites at conditions of Earth's uppermost lower mantle. *Nature* 428: 837–840. <http://dx.doi.org/10.1038/nature02472>.
- Cormier VF (1985) Some problems with S, SKS, and ScS observations and implications for the structure of the base of the mantle and the outer core. *Journal of Geophysics* 57: 14–22.

- Cormier VF (1999) Anisotropy of heterogeneity scale lengths in the lower mantle from PKIP precursors. *Geophysical Journal International* 136: 373–384.
- Cormier VF (2000) D'' as a transition in the heterogeneity spectrum of the lowermost mantle. *Journal of Geophysical Research* 105: 16193–16205.
- Cottaar S and Romanowicz B (2012) An unusually large ULVZ at the base of the mantle near Hawaii. *Earth and Planetary Science Letters* 355–356: 213–222.
- Courtier AM, Bagley B, and Revenaugh J (2007) Whole mantle discontinuity structure beneath Hawaii. *Geophysical Research Letters* 34: L17304. <http://dx.doi.org/10.1029/2007GL031006>.
- Courtier AM and Revenaugh J (2008) Slabs and shear wave reflectors in the midmantle. *Journal of Geophysical Research* 113: B08312. <http://dx.doi.org/10.1029/2007JB005261>.
- Creager KC and Jordan TH (1984) Slab penetration into the lower mantle. *Journal of Geophysical Research* 89: 3031–3049.
- Creager KC and Jordan TH (1986a) Slab penetration into the lower mantle beneath the Mariana and other island arcs of the northwest Pacific. *Journal of Geophysical Research* 91: 3573–3589.
- Creager KC and Jordan TH (1986b) Aspherical structure of the core–mantle boundary from PKP traveltimes. *Geophysical Research Letters* 13: 1497–1500.
- Crowhurst J, Brown J, Goncharov A, and Jacobsen S (2008) Elasticity of (Mg,Fe)O through the spin transition of iron in the lower mantle. *Science* 319: 451–453. <http://dx.doi.org/10.1126/science.1149606>.
- Datt R and Muirhead KJ (1976) Evidence for a sharp velocity increase near 770 km depth. *Physics of the Earth and Planetary Interiors* 13: 37–46.
- Davaille A (1999) Simultaneous generation of hotspots and superswells by convection in a heterogeneous planetary mantle. *Nature* 402: 756–760.
- Davies G (1984) Geophysical and isotopic constraints on mantle convection: An interim synthesis. *Journal of Geophysical Research* 89: 6017–6040.
- Davies DR, Goes S, Davies JH, Schubert BSA, Bunge H-P, and Ritsema J (2012) Reconciling dynamic and seismic models of Earth's lower mantle: The dominant role of thermal heterogeneity. *Earth and Planetary Science Letters* 353–354: 253–269.
- Davies G and Gurnis M (1986) Interaction of mantle dregs with convection: Lateral heterogeneity at the core–mantle boundary. *Geophysical Research Letters* 13: 1517–1520.
- de Koker N (2010) Thermal conductivity of MgO periclase at high pressure: Implications for the D'' region. *Earth and Planetary Science Letters* 292: 392–398.
- de Koker N, Karki BB, and Stixrude L (2013) Thermodynamics of the MgO–SiO<sub>2</sub> liquid system in Earth's lowermost mantle from first principles. *Earth and Planetary Science Letters* 361: 58–63.
- de Koker N and Stixrude L (2009) Self-consistent thermodynamic description of silicate liquids with application to shock melting of MgO periclase and MgSiO<sub>3</sub> perovskite. *Geophysical Journal International* 178: 162–179.
- Deal MM and Nolet G (1999) Slab temperature and thickness from seismic tomography 2. Izu-Bonin, Japan, and Kuril subduction zones. *Journal of Geophysical Research* 104: 28803–28812.
- Deal MM, Nolet G, and van der Hilst RD (1999) Slab temperature and thickness from seismic tomography. 1. Method and application to Tonga. *Journal of Geophysical Research* 104: 28789–28802.
- Defraigne P, Dehant V, and Wahr J (1996) Internal loading of an inhomogeneous compressible earth with phase boundaries. *Geophysical Journal International* 125: 173–192.
- Della Mora S, Boschi L, Tackley PJ, Nakagawa T, and Giardini D (2011) Low seismic resolution cannot explain S/P decorrelation in the lower mantle. *Geophysical Research Letters* 38: L12303. <http://dx.doi.org/10.1029/2011GL047559>.
- Deng L, Gong Z, and Fei Y (2008) Direct shock wave loading of MgSiO<sub>3</sub> perovskite to lower mantle conditions and its equation of state. *Physics of the Earth and Planetary Interiors* 170: 210–214.
- Deschamps F, Cobden L, and Tackley PJ (2012) The primitive nature of large low shear-wave velocity provinces. *Earth and Planetary Science Letters* 349–350: 198–208.
- Deschamps F, Kaminski E, and Tackley PJ (2011) A deep mantle origin for the primitive signature of ocean island basalt. *Nature Geoscience* 4: 879–882.
- Deschamps F and Tackley PJ (2008) Searching for models of thermo-chemical convection that explain probabilistic tomography. I. Principles and influence of rheological parameters. *Physics of the Earth and Planetary Interiors* 171: 357–373.
- Deschamps F and Trampert J (2003) Mantle tomography and its relation to temperature and composition. *Physics of the Earth and Planetary Interiors* 140: 272–291.
- Ding X-Y and Grand SP (1994) Seismic structure of the deep Kurile subduction zone. *Journal of Geophysical Research* 99: 23767–23786.
- Ding X and Helmberger DV (1997) Modeling D'' structure beneath Central America with broadband seismic data. *Physics of the Earth and Planetary Interiors* 101: 245–270.
- Dobson DP and Brodholt JP (2005) Subducted banded iron formations as a source of ultralow-velocity zones at the core–mantle boundary. *Nature* 434: 371–374.
- Dobson DP, Hunt SA, Lindsay-Scott A, and Wood IG (2011) Towards better analogues for MgSiO<sub>3</sub> post-perovskite: NaCoF<sub>3</sub> and NaNiF<sub>3</sub>, two new recoverable fluoride post-perovskites. *Physics of the Earth and Planetary Interiors* 189: 171–175.
- Doornbos DJ (1974) Seismic wave scattering near caustics: Observations of PKKP precursors. *Nature* 247: 352–353.
- Doornbos DJ (1976) Characteristics of lower mantle inhomogeneities from scattered waves. *Geophysical Journal of the Royal Astronomical Society* 44: 447–470.
- Doornbos DJ (1980) The effect of a rough core–mantle boundary on PKKP. *Physics of the Earth and Planetary Interiors* 21: 351–358.
- Doornbos DJ and Hilton T (1989) Models of the core–mantle boundary and the travel times of internally reflected core phases. *Journal of Geophysical Research* 94: 15741–15751.
- Doornbos DJ and Mondt JC (1979) P and S-waves diffracted around the core and the velocity structure at the base of the mantle. *Geophysical Journal of the Royal Astronomical Society* 57: 381–395.
- Doornbos DJ, Spiliopoulos S, and Stacey FD (1986) Seismological properties of D'' and the structure of a thermal boundary layer. *Physics of the Earth and Planetary Interiors* 41: 225–239.
- Dorfman SM, Shieh SR, Meng Y, Prakapenka VB, and Duffy TS (2012) Synthesis and equation of state of perovskites in the (Mg,Fe)<sub>3</sub>Al<sub>2</sub>Si<sub>3</sub>O<sub>12</sub> system to 177 GPa. *Earth and Planetary Science Letters* 357–358: 194–202.
- Dziewonski AM (1984) Mapping the lower mantle: Determination of lateral heterogeneity in P velocity up to degree and order 6. *Journal of Geophysical Research* 89: 5929–5942.
- Dziewonski AM and Anderson DL (1981) Preliminary reference Earth model. *Physics of the Earth and Planetary Interiors* 25: 297–356.
- Dziewonski AM, Ekström G, and Liu X-F (1996) Structure at the top and bottom of the mantle. In: Husebye ES and Dainty AM (eds.) *Monitoring a Comprehensive Test Ban Treaty*, pp. 521–550. The Netherlands: Kluwer.
- Dziewonski AM, Forte AM, Su W-J, and Woodward RL (1993) Seismic tomography and geodynamics. In: Aki K and Dmowska R (eds.) *Relating Geophysical Structures and Processes: The Jeffreys Volume*, pp. 67–105. Washington, DC: American Geophysical Union.
- Dziewonski AM, Hager BH, and O'Connell RJ (1977) Large scale heterogeneity in the lower mantle. *Journal of Geophysical Research* 82: 239–255.
- Dziewonski AM, Hales AL, and Lapwood ER (1975) Parametrically simple Earth models consistent with geophysical data. *Physics of the Earth and Planetary Interiors* 10: 12–48.
- Dziewonski AM, Lekic V, and Romanowicz BA (2010) Mantle anchor structure: An argument for bottom up tectonics. *Earth and Planetary Science Letters* 299: 69–79. <http://dx.doi.org/10.1016/j.epsl.2010.08.013>.
- Earle PS and Shearer PM (1997) Observations of PKKP precursors used to estimate small-scale topography on the core–mantle boundary. *Science* 277: 677–680.
- Earle PS and Shearer PM (1998) Observations of high-frequency scattered energy associated with the core phase PKKP. *Geophysical Research Letters* 25: 405–408.
- Emery V, Maupin V, and Nataf H-C (1999) Scattering of S-waves diffracted at the core–mantle boundary; forward modeling. *Geophysical Journal International* 139: 325–344.
- Fang C and Ahuja R (2008) Local structure and electronic-spin transition of Fe-bearing MgSiO<sub>3</sub> perovskite under conditions of the Earth's lower mantle. *Physics of the Earth and Planetary Interiors* 16: 77–82.
- Fei Y, Zhang L, Corgne A, et al. (2007) Spin transition and equations of state of (Mg,Fe)O solid solutions. *Geophysical Research Letters* 34: L17307. <http://dx.doi.org/10.1029/2007GL030712>.
- Ferré D, Carrez P, and Cordier P (2007) First principles determination of dislocations properties of MgSiO<sub>3</sub> perovskite at 30 GPa based on the Peierls-Nabarro model. *Physics of the Earth and Planetary Interiors* 163: 283–291.
- Fiquet G, Auzende AL, Siebert J, et al. (2010) Melting of peridotite to 140 Gigapascals. *Science* 329: 1516–1518.
- Fiquet G, Dewaele A, Andraud D, Kunz M, and Le Bihan T (2000) Thermoelastic properties and crystal structure of MgSiO<sub>3</sub> perovskite at lower mantle pressure and temperature conditions. *Geophysical Research Letters* 27: 21–24.
- Fischer KM, Creager KC, and Jordan TH (1991) Mapping the Tonga slab. *Journal of Geophysical Research* 96: 14403–14427.
- Fischer KM, Jordan TH, and Creager KC (1988) Seismic constraints on the morphology of deep slabs. *Journal of Geophysical Research* 93: 4773–4783.
- Fisher JL, Wyession ME, and Fischer KM (2003) Small-scale lateral variations in D'' attenuation and velocity structure. *Geophysical Research Letters* 30. <http://dx.doi.org/10.1029/2002GL016179>.
- Flores C and Lay T (2005) The trouble with seeing double. *Geophysical Research Letters* 32: L24305. <http://dx.doi.org/10.1029/2005GL024366>.
- Ford SR, Garnero EJ, and McNamara AK (2006) A strong lateral shear velocity gradient and anisotropy heterogeneity in the lowermost mantle beneath the southern Pacific.

- Journal of Geophysical Research* 111: B03306. <http://dx.doi.org/10.1029/2004JB003574>.
- Ford SR, Garnero EJ, and Thorne MS (2012) Differential t\* measurements via instantaneous frequency matching: Observations of lower mantle shear attenuation heterogeneity beneath western Central America. *Geophysical Journal International* 189: 513–523. <http://dx.doi.org/10.1111/j.1365-246X.2011.05348.x>.
- Forte AM and Mitrovica JX (2001) Deep-mantle high-viscosity flow and thermochemical structure inferred from seismic and geodynamic data. *Nature* 410: 1049–1056.
- Forte AM, Peltier WR, Dziewonski AM, and Woodward RL (1993) Dynamic surface topography: A new interpretation based upon mantle flow models derived from seismic tomography. *Geophysical Research Letters* 20: 225–228.
- Forte AM, Woodward RL, and Dziewonski AM (1994) Joint inversions of seismic and geodynamic data for models of three-dimensional mantle heterogeneity. *Journal of Geophysical Research* 99: 21857–21877.
- Fouch MJ, Fischer KM, and Wysession ME (2001) Lowermost mantle anisotropy beneath the Pacific: Imaging the source of the Hawaiian plume. *Earth and Planetary Science Letters* 190: 167–180.
- Freybourger M, Krüger F, and Achauer U (1999) A 22° long seismic profile for the study of the top of D''. *Geophysical Research Letters* 26: 3409–3412.
- Frost DJ, Liebske C, Langenhorst F, McCammon CA, Trannes RG, and Rubie DC (2004) Experimental evidence for the existence of iron-rich metal in the Earth's lower mantle. *Nature* 428: 409–412.
- Fuji N, Kawai K, and Geller RJ (2010) A methodology for inversion of broadband seismic waveforms for elastic and anelastic structure and its application to the mantle transition zone beneath the Northwestern Pacific. *Physics of the Earth and Planetary Interiors* 180: 118–137.
- Fujino K, Nishio-Hamane D, Seto Y, et al. (2012) Spin transition of ferric iron in Al-bearing Mg-perovskite up to 200 GPa and its implication for the lower mantle. *Earth and Planetary Science Letters* 317–318: 407–412.
- Fukao Y, Obayashi M, Inoue H, and Nenba M (1992) Subducting slabs stagnant in the mantle transition zone. *Journal of Geophysical Research* 97: 4809–4822.
- Fukao Y, Widjiantoro S, and Obayashi M (2001) Stagnant slabs in the upper and lower mantle transition region. *Reviews of Geophysics* 39: 291–323.
- Fukui H, Tsuchiya T, and Baron AQR (2012) Lattice dynamics calculations for ferropericlase with internally consistent LDA+U method. *Journal of Geophysical Research* 117: B12202. <http://dx.doi.org/10.1029/2012JB009591>.
- Gaherty JB and Lay T (1992) Investigation of laterally heterogeneous shear velocity structure in D'' beneath Eurasia. *Journal of Geophysical Research* 97: 417–435.
- Gaherty JB, Lay T, and Vidale JE (1991) Investigation of deep slab structure using long period S-waves. *Journal of Geophysical Research* 96: 16349–16367.
- Garcia RF, Chevrot S, and Calvet M (2009) Statistical study of seismic heterogeneities at the base of the mantle from PKP differential traveltimes. *Geophysical Journal International* 179: 1607–1616.
- Garcia R and Souriau A (2000) Amplitude of the core–mantle boundary topography estimated by stochastic analysis of core phases. *Physics of the Earth and Planetary Interiors* 117: 345–359.
- Garnero EJ (2000) Heterogeneity of the lowermost mantle. *Annual Reviews of the Earth and Planetary Sciences* 28: 509–537.
- Garnero EJ, Grand SP, and Helmberger DV (1993) Low P-wave velocity at the base of the mantle. *Geophysical Research Letters* 20: 1843–1846.
- Garnero EJ and Helmberger DV (1995) A very slow basal layer underlying large-scale low velocity anomalies in the lower mantle beneath the Pacific: Evidence from core phases. *Physics of the Earth and Planetary Interiors* 91: 161–176.
- Garnero EJ and Helmberger DV (1998) Further structural constraints and uncertainties of a thin laterally varying ultralow-velocity layer at the base of the mantle. *Journal of Geophysical Research* 103: 12495–12509.
- Garnero EJ, Helmberger DV, and Engen G (1988) Lateral variation near the core–mantle boundary. *Geophysical Research Letters* 20: 1843–1846.
- Garnero EJ and Jeanloz R (2000) Fuzzy patches on the Earth's core–mantle boundary. *Geophysical Research Letters* 27: 2777–2780.
- Garnero EJ and Lay T (1997) Lateral variations in the lowermost mantle shear wave anisotropy beneath the north Pacific and Alaska. *Journal of Geophysical Research* 102: 8121–8135.
- Garnero EJ and Lay T (1999) Effects of D'' anisotropy on seismic velocity models of the outermost core. *Geophysical Research Letters* 25: 2341–2344.
- Garnero EJ and Lay T (2003) D'' shear velocity heterogeneity, anisotropy and discontinuity structure beneath the Caribbean and Central America. *Physics of the Earth and Planetary Interiors* 140: 219–242.
- Garnero EJ, Lay T, and McNamara AK (2007) Implications of lower-mantle structural heterogeneity for existence and nature of whole-mantle plumes. In: Foulger GR and Jurdy DM (eds.) *Plates, Plumes, and Planetary Processes*, pp. 79–109. Geological Society of America, Geological Society of America Special Paper 430, 2007.
- Garnero EJ, Maupin V, Lay T, and Fouch MJ (2004) Variable azimuthal anisotropy in Earth's lowermost mantle. *Science* 306: 259–261.
- Garnero EJ and McNamara AK (2008) Structure and dynamics of Earth's lower mantle. *Science* 320: 626–628.
- Garnero EJ, McNamara A, Thorne M, and Rost S (2007) Fine-scale ultra-low velocity zone layering at the core–mantle boundary and superplumes. In: Yuen DA, et al. (eds.) *Superplumes: Beyond Plate Tectonics*, pp. 139–158. New York: Springer.
- Garnero EJ, Moore MM, Lay T, and Fouch MJ (2004) Isotropy or weak vertical transverse isotropy in D'' beneath the Atlantic Ocean. *Journal of Geophysical Research* 109: B08308. <http://dx.doi.org/10.1029/2004JB003004>.
- Garnero EJ, Revenaugh JS, Williams Q, Lay T, and Kellogg LH (1998) Ultralow velocity zone at the core–mantle boundary. In: Gurnis M, Wysession ME, Knittle E, and Buffett BA (eds.) *The Core–Mantle Boundary Region*, pp. 319–334. Washington, DC: American Geophysical Union.
- Garnero EJ and Vidale JE (1999) ScP: A probe of ultralow velocity zones at the base of the mantle. *Geophysical Research Letters* 26: 377–380.
- Gilbert F and Dziewonski AM (1975) An application of normal mode theory to the retrieval of structural parameters and source mechanisms from seismic spectra. *Philosophical Transactions of the Royal Society of London, Series A* 278: 187–269.
- Glatzmaier GA, Coe RS, Hongre L, and Roberts PH (1999) The role of the Earth's mantle in controlling the frequency of geomagnetic reversals. *Nature* 401: 885–890.
- Gleason AE, Marquardt H, Chen B, Speziale S, Wu J, and Jeanloz R (2011) Anomalous sound velocities in polycrystalline MgO under non-hydrostatic compression. *Geophysical Research Letters* 38: L03304. <http://dx.doi.org/10.1029/2010GL045860>.
- Glisovic P, Forte AM, and Moucha R (2012) Time-dependent convection models of mantle thermal structure constrained by seismic tomography and geodynamics: Implications for mantle plume dynamics and CMB heat flux. *Geophysical Journal International* 190: 785–815.
- Goarant F, Guyot F, Peyronneau J, and Poirier J-P (1992) High pressure and high temperature reactions between silicates and liquid iron alloys in the diamond anvil cell, studied by analytical electron microscopy. *Journal of Geophysical Research* 97: 4477–4487.
- Goes S, Spakman W, and Bijwaard H (1999) A lower mantle source for Central European volcanism. *Science* 286: 1928–1931.
- Goncharov AF, Beck P, Struzhkin VV, Haugen BD, and Jacobsen SD (2009) Thermal conductivity of lower-mantle minerals. *Physics of the Earth and Planetary Interiors* 174: 24–32.
- Goncharov AF, Haugen BD, Struzhkin VV, Beck P, and Jacobsen SD (2008) Radiative conductivity in the Earth's lower mantle. *Nature* 456: 231–234. <http://dx.doi.org/10.1038/nature07412>.
- Goncharov AF, Struzhkin VV, and Jacobsen SD (2006) Reduced radiative conductivity of low-spin (Mg,Fe)O in the lower mantle. *Science* 312(5777): 1205–1208.
- Goncharov AF, Struzhkin VV, Montoya JA, et al. (2010) Effect of composition, structure and spin state on the thermal conductivity of the Earth's lower mantle. *Physics of the Earth and Planetary Interiors* 180: 148–153.
- Gong Z, Fei Y, Dai F, Zhang L, and Jing F (2004) Equation of state and phase stability of mantle perovskite up to 140 GPa shock pressure and its geophysical implications. *Geophysical Research Letters* 31: L04614. <http://dx.doi.org/10.1029/2003GL019132>.
- Grand SP (2002) Mantle shear-wave tomography and the fate of subducted slabs. *Philosophical Transactions of the Royal Society of London, Series A* 360: 2475–2491.
- Grand SP, van der Hilst RD, and Widjiantoro S (1997) Global seismic tomography: A snapshot of convection in the Earth. *Geological Society of America Today* 7: 1–7.
- Green DH and Falloon TJ (1998) Pyrolite: A Ringwood concept and its current expression. In: Jackson I (ed.) *The Earth's Mantle*, pp. 311–378. Cambridge: Cambridge University Press.
- Grocholski B, Catalli K, Shim S-H, and Prakapenka V (2012) Mineralogical effects on the detectability of the postperovskite boundary. *Proceedings of the National Academy of Sciences of the United States of America* 109: 2275–2279.
- Grocholski B, Shim S-H, Sturhahn W, Zhao J, Xiao Y, and Chow PC (2009) Spin and valence states of iron in  $(\text{Mg}_{0.8}\text{Fe}_{0.2})\text{SiO}_3$  perovskite. *Geophysical Research Letters* 36: L24303.
- Gu YJ, Dziewonski AM, Su W, and Ekström G (2001) Models of the mantle shear velocity and discontinuities in the pattern of lateral heterogeneities. *Journal of Geophysical Research* 106: 11169–11199.
- Gubbins D, Willis AP, and Sreenivasan B (2007) Correlation of Earth's magnetic field with lower mantle thermal and seismic structure. *Physics of the Earth and Planetary Interiors* 162: 256–260.
- Guignot N, Andrault D, Morard G, Bolfan-Casanova N, and Mezouar M (2007) Thermoelastic properties of post-perovskite phase  $\text{MgSiO}_3$  determined

- experimentally at core–mantle boundary  $P$ – $T$  conditions. *Earth and Planetary Science Letters* 256: 162–168.
- Haddon RA and Buchbinder GGR (1986) Wave propagation effects and the Earth's structure in the lower mantle. *Geophysical Research Letters* 13: 1489–1492.
- Haddon RA and Cleary JR (1974) Evidence for scattering of seismic PKP-waves near the core–mantle boundary. *Physics of the Earth and Planetary Interiors* 8: 211–234.
- Hager B (1984) Subducted slabs and the geoid: Constraints on mantle rheology and flow. *Journal of Geophysical Research* 89: 6003–6015.
- Hager B and Clayton RW (1989) Constraints on the structure of mantle convection using seismic observations, flow models, and the geoid. In: Peltier WR (ed.) *Mantle Convection: Plate Tectonics and Global Dynamics*, pp. 657–763. Newark, NJ: Gordon and Breach.
- Hager B, Clayton RW, Richards MA, Comer RP, and Dziewonski AM (1985) Lower mantle heterogeneity, dynamic topography and the geoid. *Nature* 313: 541–545.
- Hager B and Richards MA (1989) Long-wavelength variations in the Earth's geoid: Physical models and dynamical implications. *Philosophical Transactions of the Royal Society of London, Series A* 328: 309–327.
- Haigis V, Salanne M, and Jahn S (2012) Thermal conductivity of  $\text{MgO}$ ,  $\text{MgSiO}_3$  perovskite and post-perovskite in the Earth's deep mantle. *Earth and Planetary Science Letters* 355–356: 102–108.
- Hales AL, Cleary JR, and Roberts JL (1968) Velocity distribution in the lower mantle. *Bulletin of the Seismological Society of America* 58: 1975–1989.
- Hales AL and Roberts JL (1970) Shear velocities in the lower mantle and the radius of the core. *Bulletin of the Seismological Society of America* 60: 1427–1436.
- Hansen U and Yuen DA (1988) Numerical simulations of thermal-chemical instabilities at the core–mantle boundary. *Nature* 334: 237–240.
- Havens E and Revenaugh J (2001) A broadband study of the lowermost mantle beneath Mexico: Constraints on ultralow velocity zone elasticity and density. *Journal of Geophysical Research* 106: 30809–30820.
- Hayden LA and Watson EB (2007) A diffusion mechanism for core–mantle interaction. *Nature* 450: 709–711.
- He Y, Levander A, and Niu F (2010) A localized waveform inversion at teleseismic distances: An application to the D'' region beneath the Cocos plate. *Geophysical Journal International* 180: 1344–1352. <http://dx.doi.org/10.1111/j.1365-246X.2009.04489.x>.
- He Y and Wen L (2009) Structural features and shear-velocity structure of the “Pacific Anomaly.” *Journal of Geophysical Research* 114: B02309. <http://dx.doi.org/10.1029/2008JB005814>.
- He Y and Wen L (2011) Seismic velocity structure and detailed features of the D'' discontinuity near the core–mantle boundary beneath eastern Eurasia. *Physics of the Earth and Planetary Interiors* 189: 176–184.
- He Y and Wen L (2012) Geographic boundary of the “Pacific Anomaly” and its geometry and transitional structure in the north. *Journal of Geophysical Research* 117: B09308. <http://dx.doi.org/10.1029/2012JB009436>.
- He Y, Wen L, and Zheng T (2006) Geographic boundary and shear wave velocity structure of the “Pacific anomaly” near the core–mantle boundary beneath western Pacific. *Earth and Planetary Science Letters* 244: 302–314.
- Hedlin MAH and Shearer PM (2000) An analysis of large-scale variations in small-scale mantle heterogeneity using Global Seismographic Network recordings of precursors to PKP. *Journal of Geophysical Research* 105: 13655–13673.
- Hedlin MAH, Shearer PM, and Earle PS (1997) Seismic evidence for small-scale heterogeneity throughout the Earth's mantle. *Nature* 387: 145–150.
- Helmburger DV, Lay T, Ni S, and Gurnis M (2005) Deep mantle structure and the postperovskite phase transition. *Proceedings of the National Academy of Sciences of the United States of America* 102: 17257–17263. <http://dx.doi.org/10.1073/pnas.0502504102>.
- Helmburger DV, Ni S, Wen L, and Ritsema J (2000) Seismic evidence for ultra-low velocity zones beneath Africa and eastern Atlantic. *Journal of Geophysical Research* 105: 23865–23878.
- Helmburger DV, Wen L, and Ding X (1998) Seismic evidence that the source of the Iceland hotspot lies at the core–mantle boundary. *Nature* 396: 251–255.
- Hernlund JW (2010) On the interaction of the geotherm with a post-perovskite phase transition in the deep mantle. *Physics of the Earth and Planetary Interiors* 180: 222–234.
- Hernlund JW and Houser C (2008) On the statistical distribution of seismic velocities in Earth's deep mantle. *Earth and Planetary Science Letters* 265: 423–437.
- Hernlund JW and Jellinek AM (2010) Dynamics and structure of a stirred partially molten ultralow-velocity zone. *Earth and Planetary Science Letters* 296: 1–8.
- Hernlund JW and Labrosse S (2007) Geophysically consistent values of the perovskite to post-perovskite transition Clapeyron slope. *Geophysical Research Letters* 34: L05309. <http://dx.doi.org/10.1029/2006GL028961>.
- Hernlund JW and Tackley PJ (2007) Some dynamical consequences of partial melting in Earth's deep mantle. *Physics of the Earth and Planetary Interiors* 162: 149–163.
- Hernlund JW, Thomas C, and Tackley PJ (2005) A doubling of the post-perovskite phase boundary and structure of the Earth's lowermost mantle. *Nature* 434: 882–886.
- Herrin E (1968) Introduction to “1968 Seismological Tables for P-phases”. *Bulletin of the Seismological Society of America* 58: 1193–1195.
- Hirose K (2006) Postperovskite phase transition and its geophysical implications. *Reviews of Geophysics* 44: RG3001. <http://dx.doi.org/10.1029/2005RG000186>.
- Hirose K (2007) Discovery of post-perovskite phase transition and the nature of D'' layer. In: Hirose K, Brodholt J, Lay T, and Yuen DA (eds.) *Post-perovskite: The Last Mantle Phase Transition*, pp. 19–35. Washington, DC: American Geophysical Union.
- Hirose K and Fujita Y (2005) Clapeyron slope of the post-perovskite phase transition in  $\text{CaIrO}_3$ . *Geophysical Research Letters* 32: L13313. <http://dx.doi.org/10.1029/2005GL023219>.
- Hirose K, Kawamura K, Ohishi Y, Tateno S, and Sata N (2005) Stability and equation of state of  $\text{MgGeO}_3$  post-perovskite phase. *American Mineralogist* 90: 262–265.
- Hirose K, Nagaya Y, Merkel S, and Ohishi Y (2010) Deformation of  $\text{MnGeO}_3$  post-perovskite at lower mantle pressure and temperature. *Geophysical Research Letters* 37: L20302. <http://dx.doi.org/10.1029/2010GL044977>.
- Hirose K, Simmyo R, Sata N, and Ohishi Y (2006) Determination of post-perovskite phase transition boundary in  $\text{MgSiO}_3$  using  $\text{Au}$  and  $\text{MgO}$  pressure standards. *Geophysical Research Letters* 33: L01310. <http://dx.doi.org/10.1029/2005GL024468>.
- Hirose K, Takafuji N, Fujino K, Shieh SR, and Duffy TS (2008) Iron partitioning between perovskite and post-perovskite: A transmission electron microscope study. *American Mineralogist* 93: 1678–1681. <http://dx.doi.org/10.2138/am.2008.3001>.
- Hirose K, Takafuji N, Sata N, and Ohishi Y (2005) Phase transition and density of subducted MORB crust in the lower mantle. *Earth and Planetary Science Letters* 237: 239–251.
- Hofmeister AM (2006) Is low-spin  $\text{Fe}^{2+}$  present in Earth's mantle? *Earth and Planetary Science Letters* 243: 44–52.
- Hofmeister AM (2008) Inference of high thermal transport in the lower mantle from laser-flash experiments and the damped harmonic oscillator model. *Physics of the Earth and Planetary Interiors* 170: 201–206.
- Houard S and Nataf HC (1993) Laterally varying reflector at the top of D'' beneath northern Siberia. *Geophysical Journal International* 115: 168–182.
- Houser C, Masters G, Shearer P, and Laske G (2008) Shear and compressional velocity models of the mantle from cluster analysis of long-period waveforms. *Geophysical Journal International* 174: 195–212.
- Hsu H, Blaha P, Cococcioni M, and Wentzcovitch RM (2011) Spin-state crossover and hyperfine interactions of ferric iron in  $\text{MgSiO}_3$  perovskite. *Physical Review Letters* 106: 118501.
- Hsu H, Umehoto K, Blaha P, and Wentzcovitch RM (2010) Spin states and hyperfine interactions of iron in  $(\text{Mg}, \text{Fe})\text{SiO}_3$  perovskite under pressure. *Earth and Planetary Science Letters* 294: 19–26.
- Hsu H, Yu YG, and Wentzcovitch RM (2012) Spin crossover of iron in aluminous  $\text{MgSiO}_3$  perovskite and post-perovskite. *Earth and Planetary Science Letters* 359–360: 34–39.
- Hung S-H, Garnero EJ, Chiao L-Y, Kuo B-Y, and Lay T (2005) Finite-frequency tomography of D'' shear velocity heterogeneity beneath the Caribbean. *Journal of Geophysical Research* 110: B07305. <http://dx.doi.org/10.1029/2004JB003373>.
- Hunt SA, Weidner DJ, Li L, et al. (2009) Weakening of calcium iridate during its transformation from perovskite to post-perovskite. *Nature Geosciences* 2: 794–797.
- Hustoft J, Cataldi K, Shim S-H, Kubo A, Prakapenka VB, and Kunz M (2008) Equation of state of  $\text{NaMgF}_3$  postperovskite: Implication for the seismic velocity changes in the D'' region. *Geophysical Research Letters* 35: L10309. <http://dx.doi.org/10.1029/2008GL034042>.
- Hustoft J, Shim S-H, Kubo A, and Nishiyama N (2008) Raman spectroscopy of  $\text{CaIrO}_3$  postperovskite up to 30 GPa. *American Mineralogist* 93: 1654–1658.
- Hutko A, Lay T, Garnero EJ, and Revenaugh JS (2006) Seismic detection of folded, subducted lithosphere at the core–mantle boundary. *Nature* 441: 333–336.
- Hutko AR, Lay T, and Revenaugh J (2009) Localized double-array stacking analysis of PcP, D'', and ULVZ structure beneath the Cocos Plate, Mexico, central Pacific and north Pacific. *Physics of the Earth and Planetary Interiors* 173: 60–74.
- Hutko A, Lay T, Revenaugh J, and Garnero EJ (2008) Anticorrelated seismic velocity anomalies from post-perovskite in the lowermost mantle. *Science* 320: 1070–1074.
- Hwang YK and Ritsema J (2011) Radial structure of the lower mantle from teleseismic body-wave spectra. *Earth and Planetary Science Letters* 303: 369–375.
- Hwang YK, Ritsema J, van Keeken PE, Goes S, and Styles E (2011) Wavefront healing renders deep plumes seismically invisible. *Geophysical Journal International* 187: 273–277. <http://dx.doi.org/10.1111/j.1365-246X.2011.05173.x>.
- Idehara K (2011) Structural heterogeneity of an ultra-low-velocity zone beneath the Philippine Islands: Implications for core–mantle chemical interactions induced by

- massive partial melting at the bottom of the mantle. *Physics of the Earth and Planetary Interiors* 184: 80–90.
- Idehara K, Yamada A, and Zhao D (2007) Seismological constraints on the ultralow velocity zones in the lowermost mantle from core-reflected waves. *Physics of the Earth and Planetary Interiors* 165: 25–46.
- Itaya T, Hirose K, Kawamura K, and Murakami M (2004) The elasticity of the  $\text{MgSiO}_3$  post-perovskite phase in the Earth's lowermost mantle. *Nature* 430: 442–444.
- Irfune T, Shirmei T, McCammon CA, Miyajima N, Rubie DC, and Frost DJ (2010) Iron partitioning and density changes of pyrolyte in Earth's lower mantle. *Science* 327: 193–195.
- Ishii M and Tromp J (1999) Normal-mode and free-air gravity constraints on lateral variations in velocity and density of Earth's mantle. *Science* 285: 1231–1236.
- Ito E, Akaogi M, Topor L, and Navrotsky A (1990) Negative pressure–temperature slopes for reactions forming  $\text{MgSiO}_3$  perovskite from calorimetry. *Science* 249: 1275–1278.
- Ito E and Takahashi E (1989) Postspinel transforms in the system  $\text{Mg}_2\text{SiO}_4$ – $\text{Fe}_2\text{SiO}_4$  and some geophysical implications. *Journal of Geophysical Research* 94: 10637–10646.
- Ito Y and Toriumi M (2010) Silicon self-diffusion of  $\text{MgSiO}_3$  perovskite by molecular dynamics and its implication for lower mantle rheology. *Journal of Geophysical Research* 115: B12205. <http://dx.doi.org/10.1029/2010JB000843>.
- Ito E, Yamazaki D, Yoshino T, et al. (2010) Pressure generation and investigation of the post-perovskite transformation in  $\text{MgGeO}_3$  by squeezing the Kawai-cell equipped with sintered diamond anvils. *Earth and Planetary Science Letters* 293: 84–89.
- Jackson I and Kung J (2008) Thermoelastic behavior of silicate perovskites: Insights from new high-temperature ultrasonic data for  $\text{ScAlO}_3$ . *Physics of the Earth and Planetary Interiors* 167: 195–204.
- Jackson JM, Sinogeikin SV, Jacobsen SD, Reichmann HJ, Mackwell SJ, and Bass JD (2006) Single-crystal elasticity and sound velocities of  $(\text{Mg}_{0.94}\text{Fe}_{0.06})\text{O}$  ferropericlase to 20 GPa. *Journal of Geophysical Research* 111: B09203. <http://dx.doi.org/10.1029/2005JB004052>.
- Jackson JM, Sturhahn W, Shen G, et al. (2005) A synchrotron Mossbauer spectroscopy study of  $(\text{Mg},\text{Fe})\text{SiO}_3$  perovskite up to 120 GPa. *American Mineralogist* 90: 199–205.
- Jackson JM, Sturhahn W, Tschauner O, Lerche M, and Fei Y (2009) Behavior of iron in  $(\text{Mg},\text{Fe})\text{SiO}_3$  post-perovskite assemblages at Mbarr pressures. *Geophysical Research Letters* 36: L10301. <http://dx.doi.org/10.1029/2009GL037815>.
- Jeanloz R (1993) Chemical reactions at Earth's core–mantle boundary: Summary of evidence and geomagnetic implications. In: Aki K and Dmowska R (eds.) *Relating Geophysical Structures and Processes: The Jeffreys Volume*. *Geophysical Monograph Series*, vol. 76, pp. 121–127. Washington, DC: American Geophysical Union.
- Jellinek AM and Manga M (2002) The influence of a chemical boundary layer on the fixity, spacing and lifetime of mantle plumes. *Nature* 418: 760–763.
- Ji Y and Nataf H-C (1998) Detection of mantle plumes in the lower mantle by diffraction tomography: Theory. *Earth and Planetary Science Letters* 159: 87–98.
- Johnson LR (1969) Array measurements of P velocities in the lower mantle. *Bulletin of the Seismological Society of America* 59: 973–1008.
- Jordan TH (1977) Lithospheric slab penetration into the lower mantle beneath the Sea of Okhotsk. *Journal of Geophysics* 43: 473–496.
- Jordan TH and Anderson DL (1974) Earth structure from free oscillations and travel times. *Geophysical Journal of the Royal Astronomical Society* 36: 411–459.
- Jordan TH and Lynn WS (1974) A velocity anomaly in the lower mantle. *Journal of Geophysical Research* 79: 2679–2685.
- Jung DY and Oganov AR (2005) Ab initio study of the high-pressure behavior of  $\text{CaSiO}_3$  perovskite. *Physics and Chemistry of Minerals* 32: 146–153.
- Jung DY, Vinograd VL, Fabrichnaya OB, Oganov AR, Schmidt MW, and Winkler B (2010) Thermodynamics of mixing in the  $\text{MgSiO}_3$ – $\text{Al}_2\text{O}_3$  perovskite and ilmenite from ab initio calculations. *Earth and Planetary Science Letters* 295: 477–486.
- Kameyama M and Yuen DA (2006) 3-D convection studies on the thermal state in the lower mantle with post-perovskite phase transition. *Geophysical Research Letters* 33: L12S10. <http://dx.doi.org/10.1029/2006GL025744>.
- Kanamori H and Anderson DL (1977) Importance of physical dispersion in surface-wave and free oscillation problems, Review. *Reviews of Geophysics and Space Physics* 15: 105–112.
- Kanda RVS and Stevenson DJ (2006) Suction mechanism for iron entrainment into the lower mantle. *Geophysical Research Letters* 33: L02310. <http://dx.doi.org/10.1029/2005GL025009>.
- Kaneshima S (2009) Seismic scatterers at the shallowest lower mantle beneath subducted slabs. *Earth and Planetary Science Letters* 286: 304–315.
- Kaneshima S and Helffrich G (1998) Detection of lower mantle scatterers northeast of the Mariana subduction zone using short-period array data. *Journal of Geophysical Research* 103: 4825–4838.
- Kaneshima S and Helffrich G (2009) Lower mantle scattering profiles and fabric below Pacific subduction zones. *Earth and Planetary Science Letters* 282: 234–239.
- Kaneshima S and Silver PG (1995) Anisotropic loci in the mantle beneath central Peru. *Physics of the Earth and Planetary Interiors* 88: 257–272.
- Kantor I, Dubrovinsky LS, and McCammon CA (2006) Spin crossover in  $(\text{Mg},\text{Fe})\text{O}$ : A Mossbauer effect study with an alternative interpretation of x-ray emission spectroscopy data. *Physical Review B* 73: 100101.
- Karason H and van der Hilst RD (2001) Tomographic imaging of the lowermost mantle with differential times of refracted and diffracted core phases (PKP, Pdiff). *Journal of Geophysical Research* 106: 6569–6587.
- Karato S-I (1998) Some remarks on the origin of seismic anisotropy in the D'' layer. *Earth, Planets and Space* 50: 1019–1028.
- Karki BB, Wentzcovitch RM, de Gironcoli S, and Baroni S (1999) First-principles determination of elastic anisotropy and wave velocities of  $\text{MgO}$  at lower mantle conditions. *Science* 286: 1705–1709.
- Katsura T, Yokoshi S, Kawabe K, et al. (2009)  $P$ – $V$ – $T$  relations of  $\text{MgSiO}_3$  perovskite determined by in situ x-ray diffraction using a large-volume high-pressure apparatus. *Geophysical Research Letters* 36: L01305. <http://dx.doi.org/10.1029/2008GL035658>.
- Kawai K and Geller RJ (2010a) Waveform inversion for localized seismic structure and an application to D'' structure beneath the Pacific. *Journal of Geophysical Research* 115: B01305. <http://dx.doi.org/10.1029/2009JB006503>.
- Kawai K and Geller RJ (2010b) Inversion of seismic waveforms for shear wave velocity structure in the lowermost mantle beneath the Hawaiian hotspot. *Physics of the Earth and Planetary Interiors* 183: 136–142.
- Kawai K and Geller RJ (2010c) The vertical flow in the lowermost mantle beneath the Pacific from inversion of seismic waveforms for anisotropic structure. *Earth and Planetary Science Letters* 297: 190–198.
- Kawai K, Geller RJ, and Fuji N (2007) D'' beneath the Arctic from inversion of shear waveforms. *Geophysical Research Letters* 34: L21305. <http://dx.doi.org/10.1029/2007GL031517>.
- Kawai K, Geller RJ, and Fuji N (2010) Waveform inversion for S-wave structure in the lowermost mantle beneath the Arctic: Implications for mineralogy and chemical composition. *Geophysical Research Letters* 37: L16301. <http://dx.doi.org/10.1029/2010GL043654>.
- Kawai K, Sekine S, Fuji N, and Geller RJ (2009) Waveform inversion for D'' structure beneath northern Asia using Hi-net tiltmeter data. *Geophysical Research Letters* 36: L20314. <http://dx.doi.org/10.1029/2009GL039651>.
- Kawai K, Takeuchi N, Geller RJ, and Fuji N (2007) Possible evidence for a double crossing phase transition in D'' beneath Central America from inversion of seismic waveforms. *Geophysical Research Letters* 34: L09314. <http://dx.doi.org/10.1029/2007GL029642>.
- Kawai K and Tsuchiya T (2009) Temperature profile in the lowermost mantle from seismological and mineral physics joint modeling. *Proceedings of the National Academy of Sciences of the United States of America* 106: 22119–22123.
- Kawakatsu H and Niu FL (1994) Seismic evidence for a 920-km discontinuity in the mantle. *Nature* 371: 301–305.
- Kellogg LH (1997) Growing the Earth's D'' layer: Effect of density variations at the core–mantle boundary. *Geophysical Research Letters* 22: 2749–2752.
- Kellogg LH, Hager BH, and van der Hilst RD (1999) Compositional stratification in the deep mantle. *Science* 283: 1881–1884.
- Kendall JM (2000) Seismic anisotropy in the boundary layers of the mantle. In: Karato SI, Forte AM, Liebermann RC, Masters G, and Stixrude L (eds.) *Earth's Deep Interior: Mineral Physics and Tomography From the Atomic to the Global Scale*, pp. 133–159. Washington, DC: American Geophysical Union.
- Kendall JM and Nangnai C (1996) Lateral variations in D'' below the Caribbean. *Geophysical Research Letters* 23: 399–402.
- Kendall JM and Shearer PM (1994) Lateral variations in D'' thickness from long-period shear wave data. *Journal of Geophysical Research* 99: 11575–11590.
- Kendall JM and Silver PG (1996) Constraints from seismic anisotropy on the nature of the lowermost mantle. *Nature* 381: 409–412.
- Kendall JM and Silver PG (1998) Investigating causes of D'' anisotropy. In: Gurnis M, Wyession ME, Knittle E, and Buffett BA (eds.) *The Core–Mantle Boundary Region*, pp. 97–118. Washington, DC: American Geophysical Union.
- Kennett BLN and Engdahl ER (1991) Travel times for global earthquake location and phase identification. *Geophysical Journal International* 105: 429–465.
- Kennett BLN, Engdahl ER, and Buland R (1995) Constraints on seismic velocities in the Earth from travel times. *Geophysical Journal International* 122: 108–124.
- Kennett BLN, Widjiantoro S, and van der Hilst RD (1998) Joint seismic tomography for bulk sound and shear wave speed in the Earth's mantle. *Journal of Geophysical Research* 103: 12469–12493.

- Keppler H, Dubrovinsky LS, Narygina O, and Kantor I (2008) Optical absorption and radiative thermal conductivity of silicate perovskite to 125 gigapascals. *Science* 322: 1529–1532. <http://dx.doi.org/10.1126/science.1164609>.
- Keppler H, Kantor I, and Dubrovinsky L (2007) Optical absorption of ferropericlase to 84 GPa. *American Mineralogist* 92: 433–436.
- Kito T and Krüger F (2001) Heterogeneities in D'' beneath the southwestern Pacific inferred from scattered and reflected P-waves. *Geophysical Research Letters* 28: 2545–2548.
- Kito T, Krüger F, and Negishi H (2004) Seismic heterogeneous structure in the lowermost mantle beneath the southwestern Pacific. *Journal of Geophysical Research* 109: B09304. <http://dx.doi.org/10.1029/2002JB002677>.
- Kito T, Rietbrock A, and Thomas C (2007) Slowness-backazimuth weighted migration: A new array approach to a high-resolution image. *Geophysical Journal International* 169: 1201–1209.
- Kito T, Rost S, Thomas C, and Garnero EJ (2007) New insights into the P- and S-wave velocity structure of the D'' discontinuity beneath the Cocos plate. *Geophysical Journal International* 169: 631–645.
- Kito T, Thomas C, Rietbrock A, Garnero EJ, Nippes SEJ, and Heath AE (2008) Seismic evidence for a sharp lithospheric base persisting to the lowermost mantle beneath the Caribbean. *Geophysical Journal International* 174: 1019–1028. <http://dx.doi.org/10.1111/j.1365-246X.2008.03880.x>.
- Knittle E (1998) The solid/liquid partitioning of major and radiogenic elements at lower mantle pressures: Implications for the core–mantle boundary region. In: Gurnis M, Wyession ME, Knittle E, and Buffett BA (eds.) *The Core–Mantle Boundary Region*, pp. 119–130. Washington, DC: American Geophysical Union.
- Knittle E and Jeanloz R (1987) Synthesis and equation of state of  $(\text{Mg}, \text{Fe})\text{SiO}_3$  perovskite to over 100 gigapascals. *Science* 235: 668–670.
- Knittle E and Jeanloz R (1989) Simulating the core–mantle boundary: An experimental study of high pressure reactions between silicates and liquid iron. *Geophysical Research Letters* 16: 609–612.
- Kobayashi Y, Kondo T, Ohtani E, et al. (2005) Fe–Mg partitioning between  $(\text{Mg}, \text{Fe})\text{SiO}_3$  post-perovskite, perovskite, and magnesiowüstite in the Earth's lower mantle. *Geophysical Research Letters* 32: L19301. <http://dx.doi.org/10.1029/2005GL023257>.
- Koelemeijer PJ, Deuss A, and Trampert J (2012) Normal mode sensitivity to Earth's D'' layer and topography on the core–mantle boundary: What we can and cannot see. *Geophysical Journal International* 190: 553–568. <http://dx.doi.org/10.1111/j.1365-246X.2012.05499.x>.
- Kohler MD, Vidale JE, and Davis PM (1997) Complex scattering within D'' observed on the very dense Los Angeles Region Seismic Experiment passive array. *Geophysical Research Letters* 24: 1855–1858.
- Kojitani H, Furukawa A, and Akaogi M (2007) Thermochemistry and high-pressure equilibria of the post-perovskite phase transition in  $\text{Ca}\text{Al}_2\text{O}_4$ . *American Mineralogist* 92: 229–232.
- Kojitani H, Shirako Y, and Akaogi M (2007) Post-perovskite phase transition in  $\text{CaRuO}_3$ . *Physics of the Earth and Planetary Interiors* 165: 127–134.
- Kojitani H, Wakabayashi Y, Tejima Y, Kato C, Haraguchi M, and Akaogi M (2009) High-pressure phase relations in  $\text{Ca}_2\text{AlSiO}_{55}$  and energetics of perovskite-related compounds with oxygen defects in the  $\text{Ca}_2\text{Si}_2\text{O}_6-\text{Ca}_2\text{Al}_2\text{O}_5$  join. *Physics of the Earth and Planetary Interiors* 173: 349–353.
- Koki I, Tanaka S, and Takeuchi N (2012) High velocity anomaly adjacent to the western edge of the Pacific low-velocity province. *Geophysical Journal International*. <http://dx.doi.org/10.1093/gji/gjs002>.
- Komabayashi T, Hirose K, Nagaya Y, Sugimura E, and Ohishi Y (2010) High temperature compression of ferropericlase and the effect of temperature on iron spin transition. *Earth and Planetary Science Letters* 297: 691–699. <http://dx.doi.org/10.1016/j.epsl.2010.07.025>.
- Komabayashi T, Hirose K, Sata N, Ohishi Y, and Dubrovinsky LS (2007) Phase transition in  $\text{CaSiO}_3$  perovskite. *Earth and Planetary Science Letters* 260: 564–569.
- Komabayashi T, Hirose K, Sugimura E, Sata N, Ohishi Y, and Dubrovinsky LS (2008) Simultaneous volume measurements of post-perovskite and perovskite in  $\text{MgSiO}_3$  and their thermal equations of state. *Earth and Planetary Science Letters* 265: 515–524. <http://dx.doi.org/10.1016/j.epsl.2007.10.036>.
- Komatsch D, Vinnik LP, and Chevrot S (2010) Shdiff–SVdiff splitting in an isotropic Earth. *Journal of Geophysical Research* 115: B07312. <http://dx.doi.org/10.1029/2009JB006795>.
- Konishi K, Kawai K, Geller RJ, and Fuji N (2009) MORB in the lowermost mantle beneath the western Pacific: Evidence from waveform inversion. *Earth and Planetary Science Letters* 278: 219–225.
- Konishi K, Kawai K, Geller RJ, and Fuji N (2012) Waveform inversion of broad-band body wave data for the S-velocity structure in the lowermost mantle beneath the Indian subcontinent and Tibetan Plateau. *Geophysical Journal International* 191: 305–316. <http://dx.doi.org/10.1111/j.1365-246X.2012.05614.x>.
- Kono Y, Higo Y, Ohfuji H, Inoue T, and Irfune T (2007) Elastic wave velocities of garnetite with a MORB composition up to 14 GPa. *Geophysical Research Letters* 34: L14308. <http://dx.doi.org/10.1029/2007GL030312>.
- Krüger F, Weber M, Scherbaum F, and Schlüterhardt J (1995) Normal and inhomogeneous lowermost mantle and core–mantle boundary under the Arctic and Northern Canada. *Geophysical Journal International* 122: 637–658.
- Kubo A, Kiefer B, Shen G, Prakapenka VB, Cava RJ, and Duffy TS (2006) Stability and equation of state of the post-perovskite phase in  $\text{MgGeO}_3$  to 2 Mbar. *Geophysical Research Letters* 33: L12S12. <http://dx.doi.org/10.1029/2006GL025686>.
- Kubo A, Kiefer B, Shim S-H, Shen GY, Prakapenka VB, and Duffy TS (2008) Rietveld structure refinement of  $\text{MgGeO}_3$  post-perovskite phase to 1 Mbar. *American Mineralogist* 93: 965–976.
- Kudo Y, Hirose K, Murakami M, et al. (2012) Sound velocity measurements of  $\text{CaSiO}_3$  perovskite to 133 GPa and implications for lowermost mantle seismic anomalies. *Earth and Planetary Science Letters* 345–350: 1–7.
- Kuo BY, Garnero EJ, and Lay T (2000) Tomographic inversion of S-SKS times for shear velocity heterogeneity in D''. Degree 12 and hybrid models. *Journal of Geophysical Research* 105: 28139–28157.
- Kuo C and Romanowicz B (2002) On the resolution of density anomalies in the Earth's mantle using spectral fitting of normal-mode data. *Geophysical Journal International* 150: 162–179.
- Kuo BY and Wu KY (1997) Global shear velocity heterogeneities in the D'' layer: Inversion from Sd-SKS differential travel times. *Journal of Geophysical Research* 102: 1177511788.
- Kustowski B, Ekstrom G, and Dziewonski AM (2008) Anisotropic shear-wave velocity structure of the Earth's mantle: A global model. *Journal of Geophysical Research* 113: B06306. <http://dx.doi.org/10.1029/2007JB005169>.
- Labrosse S, Hernlund JW, and Coltice N (2007) A crystallizing dense magma ocean at the base of the Earth's mantle. *Nature* 450: 866–869.
- Lakshtanov DL, Sinogeikin SV, Litasov KD, et al. (2007) The post-stishovite phase transition in hydrous alumina-bearing  $\text{SiO}_2$  in the lower mantle of the Earth. *Proceedings of the National Academy of Sciences of the United States of America* 104: 13588–13590.
- Lassak TM, McNamara AK, Garnero EJ, and Zhong S (2010) Core–mantle boundary topography as a possible constraint on lower mantle chemistry and dynamics. *Earth and Planetary Science Letters* 289: 232–241.
- Lassak TM, McNamara AK, and Zhong S (2007) Influence of thermochemical piles on topography at Earth's core–mantle boundary. *Earth and Planetary Science Letters* 261: 443–455.
- Lavina B, Dera P, Downs RT, et al. (2009) Siderite at lower mantle conditions and the effects of the pressure-induced spin-pairing transition. *Geophysical Research Letters* 36: L23306. <http://dx.doi.org/10.1029/2009GL039652>.
- Lavina B, Dera P, Downs RT, et al. (2010) Structure of siderite  $\text{FeCO}_3$  to 56 GPa and hysteresis of its spin-pairing transition. *Physical Review B* 82: 064110. <http://dx.doi.org/10.1103/PhysRevB.82.064110>.
- Lawrence JG and Wyession ME (2006) QLM9: A new radial quality factor (Q') model for the lower mantle. *Earth and Planetary Science Letters* 241: 962–971.
- Lay T (1983) Localized velocity anomalies in the lower mantle. *Geophysical Journal of the Royal Astronomical Society* 72: 483–516.
- Lay T (1989) Structure of the core–mantle transition zone: A chemical and thermal boundary layer. *EoS, Transactions of the American Geophysical Union* 70: 49, 54–55, 58–59.
- Lay T (2008) Sharpness of the D'' discontinuity beneath the Cocos Plate: Implications for the perovskite to post-perovskite phase transition. *Geophysical Research Letters* 35: L03304. <http://dx.doi.org/10.1029/2007GL032465>.
- Lay T and Garnero EJ (2004) Core–mantle boundary structures and processes. In: Sparks RSJ and Hawkesworth CJ (eds.) *The State of the Planet: Frontiers and Challenges in Geophysics*, pp. 25–41. Washington, DC: American Geophysical Union.
- Lay T and Garnero EJ (2007) Reconciling the post-perovskite phase with seismological observations of lowermost mantle structure. In: Hirose K, et al. (ed.) *Post-Perovskite: The Last Mantle Phase Transition*, pp. 129–153. Washington, DC: American Geophysical Union.
- Lay T and Garnero EJ (2011) Deep mantle seismic modeling and imaging. *Annual Reviews of Earth and Planetary Sciences* 39: 91–123.
- Lay T, Garnero EJ, and Russell S (2004a) Lateral variation of the D'' discontinuity beneath the Cocos Plate. *Geophysical Research Letters* 31: L15612. <http://dx.doi.org/10.1029/2004GL020300>.
- Lay T, Garnero EJ, and Williams Q (2004b) Partial melting in a thermo-chemical boundary layer at the base of the mantle. *Physics of the Earth and Planetary Interiors* 146: 441–467.
- Lay T, Garnero EJ, Young CJ, and Gaherty JB (1997) Scale-lengths of shear velocity heterogeneity at the base of the mantle from S-wave differential travel times. *Journal of Geophysical Research* 102: 9887–9910.

- Lay T, Heinz D, Ishii M, et al. (2005) Multidisciplinary impact of the lower mantle perovskite phase transition. *EoS, Transactions of the American Geophysical Union* 86: 1–5.
- Lay T and Helmberger DV (1983a) A lower mantle S-wave triplication and the velocity structure of D''. *Geophysical Journal of the Royal Astronomical Society* 75: 799–837.
- Lay T and Helmberger DV (1983b) The shear wave velocity gradient at the base of the mantle. *Journal of Geophysical Research* 88: 8160–8170.
- Lay T, Hernlund J, and Buffett BA (2008) Core–mantle boundary heat flow. *Nature Geoscience* 1: 25–32.
- Lay T, Hernlund J, Garner EJ, and Thorne MS (2006) A post-perovskite lens and D'' heat flux beneath the central Pacific. *Science* 314: 1272–1276.
- Lay T and Wallace TC (1995) *Modern Global Seismology*. San Diego: Academic Press, 521 pp.
- Lay T, Williams Q, and Garnero EJ (1998) The core–mantle boundary layer and deep earth dynamics. *Nature* 392: 461–468.
- Lay T, Williams Q, Garnero EJ, Kellogg L, and Wyssession ME (1998) Seismic wave anisotropy in the D'' region and its implications. In: Gurnis M, Wyssession ME, Knittle E, and Buffett BA (eds.) *The Core–Mantle Boundary Region*, pp. 299–318. Washington, DC: American Geophysical Union.
- Lay T and Young CJ (1986) The effect of SKS scattering on models of the shear velocity-structure of the D'' region. *Journal of Geophysics* 59: 11–15.
- Lay T and Young CJ (1989) Waveform complexity in teleseismic broadband SH displacements: Slab diffractions or deep mantle reflections? *Geophysical Research Letters* 16: 605–608.
- Lay T and Young CJ (1991) Analysis of seismic SV waves in the core's penumbra. *Geophysical Research Letters* 18: 1373–1376.
- Lee RC and Johnson LR (1984) Extremal bounds on the seismic velocities in the Earth's mantle. *Geophysical Journal of the Royal Astronomical Society* 77: 667–681.
- Lee KKM, Steinle-Neumann G, and Akber-Knudson S (2009) Ab initio predictions of potassium partitioning between Fe and Al-bearing  $\text{MgSiO}_3$  perovskite and post-perovskite. *Physics of the Earth and Planetary Interiors* 174: 247–253.
- Lei J and Zhao D (2006) Global P-wave tomography: On the effect of various mantle and core phases. *Physics of the Earth and Planetary Interiors* 154: 44–69.
- Lekic V, Cottaar S, Dziewonski A, and Romanowicz B (2012) Cluster analysis of global lower mantle tomography: A new class of structure and implications for chemical heterogeneity. *Earth and Planetary Science Letters* 357–358: 68–77.
- Leng W and Zhong S (2008) Controls on plume heat flux and plume excess temperature. *Journal of Geophysical Research* 113: B04408. <http://dx.doi.org/10.1029/2007JB005155>.
- Leng W and Zhong S (2009) More constraints on internal heating rate of the Earth's mantle from plume observations. *Geophysical Research Letters* 36: L02306. <http://dx.doi.org/10.1029/2008GL036449>.
- Li J (2007) Electronic transitions and spin states in perovskite and post-perovskite. In: Hirose K, et al. (eds.) *Post-Perovskite: The Last Mantle Phase Transition. Geophysical Monograph Series*, vol. 174, pp. 47–69. Washington, DC: AGU.
- Li L, Brodholt JP, Stackhouse S, Weidner DJ, Alfredsson M, and Price GD (2005) Electronic spin state of ferric iron in Al-bearing perovskite in the lower mantle. *Geophysical Research Letters* 32: L17307. <http://dx.doi.org/10.1029/2005GL023045>.
- Li X-D and Romanowicz B (1996) Global mantle shear velocity model developed using nonlinear asymptotic coupling theory. *Journal of Geophysical Research* 101: 2224522272.
- Li J, Struzhkin VV, Mao HK, et al. (2004) Electronic spin state of iron in lower mantle perovskite. *Proceedings of the National Academy of Sciences of the United States of America* 101(39): 14027–14030. <http://dx.doi.org/10.1073/pnas.0405804101>.
- Li J, Sturhahn W, Jackson JM, et al. (2006) Pressure effect on the electronic structure of iron in  $(\text{Mg}, \text{Fe})_{(\text{Si}, \text{Al})\text{O}_3}$  perovskite: A combined synchrotron Mossbauer and x-ray emission spectroscopy study up to 100 GPa. *Physics and Chemistry of Minerals* 33(8–9): 575–585. <http://dx.doi.org/10.1007/s00269-006-0105-y>.
- Li C, van der Hilst RD, Engdahl ER, and Burdick W (2008) A new global model for P wave speed variations in Earth's mantle. *Geochemistry, Geophysics, Geosystems* 9: Q05018. <http://dx.doi.org/10.1029/2007GC001806>.
- Li L, Weidner DJ, Brodholt J, et al. (2006a) Elasticity of  $\text{CaSiO}_3$  perovskite at high pressure and high temperature. *Physics of the Earth and Planetary Interiors* 155: 249–259.
- Li L, Weidner DJ, Brodholt J, et al. (2006b) Phase stability of  $\text{CaSiO}_3$  perovskite at high pressure and temperature: Insights from ab initio molecular dynamics. *Physics of the Earth and Planetary Interiors* 155: 260–268.
- Liebske C and Frost DJ (2012) Melting phase relations in the  $\text{MgO}-\text{MgSiO}_3$  system between 16 and 26 GPa: Implications for melting in Earth's deep interior. *Earth and Planetary Science Letters* 345–348: 159–170.
- Lin J-F, Gavriliuk AG, Struzhkin VV, et al. (2006) Pressure-induced electronic spin transition of iron in magnesiowustite-( $\text{Mg}, \text{Fe}\text{O}$ ). *Physical Review B* 73: 113107.
- Lin J-F, Jacobsen SD, Sturhahn W, Jackson JM, Zhao J, and Yoo C-S (2006) Sound velocities of ferropericlase in the Earth's lower mantle. *Geophysical Research Letters* 33: L22304. <http://dx.doi.org/10.1029/2006GL028099>.
- Lin J-F, Struzhkin VV, Jacobsen SD, et al. (2005) Spin transition of iron in magnesiowustite in the Earth's lower mantle. *Nature* 436: 377–380.
- Lin F-C, Tsai VC, Schmandt B, Duputel Z, and Zhan Z (2013) Extracting seismic core phases with array interferometry. *Geophysical Research Letters* 40. <http://dx.doi.org/10.1002/grl.50237>.
- Lin J-F and Tsuchiya T (2008) Spin transition of iron in the Earth's lower mantle. *Physics of the Earth and Planetary Interiors* 170: 248–259.
- Lin J-F, Vankó G, Jacobsen SD, et al. (2007) Spin transition zone in Earth's lower mantle. *Science* 317: 1740–1743.
- Lin J-F, Watson H, Vankó G, et al. (2008) Intermediate-spin ferrous iron in lowermost mantle post-perovskite and perovskite. *Nature Geoscience* 1: 688–691.
- Lin J-F, Weir ST, Jackson DD, et al. (2007) Electrical conductivity of the lower-mantle ferropericlase across the electronic spin transition. *Geophysical Research Letters* 34: L16305. <http://dx.doi.org/10.1029/2007GL030523>.
- Litasov KD, Fei Y, Ohtani E, Kurabayashi T, and Funakoshi K (2008) Thermal equation of state of magnesite to 32 GPa and 2073 K. *Physics of the Earth and Planetary Interiors* 168: 191–203. <http://dx.doi.org/10.1016/j.pepi.2008.06.018>.
- Lithgow-Bertelli C and Richards MA (1998) The dynamics of Cenozoic and Mesozoic plate motions. *Reviews of Geophysics* 36: 27–78.
- Liu L-G (1974) Silicate perovskite from phase transformation of pyrope-garnet at high pressure and temperature. *Geophysical Research Letters* 1: 277–280.
- Liu H-P, Anderson DL, and Kanamori H (1976) Velocity dispersion due to anelasticity: Implications for seismology and mantle composition. *Geophysical Journal of the Royal Astronomical Society* 47: 41–58.
- Liu X-F and Dziewonski AM (1998) Global analysis of shear wave velocity anomalies in the lowermost mantle. In: Gurnis M, Wyssession ME, Knittle E, and Buffet BA (eds.) *The Core–Mantle Boundary Region*, pp. 21–36. Washington, DC: American Geophysical Union.
- Liu X-F, Tromp J, and Dziewonski AM (1998) Is there a first-order discontinuity in the lowermost mantle? *Earth and Planetary Science Letters* 160: 343–351.
- Long MD (2009) Complex anisotropy in D'' beneath the eastern Pacific from SKS-SKKS splitting discrepancies. *Earth and Planetary Science Letters* 283: 181–189.
- Long MD, Xiao X, Jiang Z, Evans B, and Karato S-I (2006) Lattice preferred orientation in deformed polycrystalline  $(\text{Mg}, \text{Fe})\text{O}$  and implications for seismic anisotropy in D''. *Physics of the Earth and Planetary Interiors* 156: 75–88.
- Loper DE and Lay T (1995) The core–mantle boundary region. *Journal of Geophysical Research* 100: 6397–6420.
- Lundin S, Catalli K, Santillán J, et al. (2008) Effect of Fe on the equation of state of mantle silicate perovskite over 1 Mbar. *Physics of the Earth and Planetary Interiors* 168: 97–102.
- Ma P, Wang P, Tenorio L, de Hoop MV, and van der Hilst RD (2007) Imaging of structure at and near the core–mantle boundary using a generalized radon transform: 2. Statistical inference of singularities. *Journal of Geophysical Research* 112: B08303. <http://dx.doi.org/10.1029/2006JB004513>.
- Mainprice D, Barruol G, and Ben Ismail W (2000) The seismic anisotropy of the Earth's mantle: From single crystal to polycrystal. In: Karato S-I, Forte AM, Liebermann RC, Masters G, and Sixrude L (eds.) *Earth's Deep Interior: Mineral Physics and Tomography From the Atomic to the Global Scale*, pp. 237–264. Washington, DC: American Geophysical Union.
- Mainprice D, Tommasi A, Ferré D, Carrez P, and Cordier P (2008) Predicted glide systems and crystal preferred orientations of polycrystalline silicate Mg-Perovskite at high pressure: Implications for the seismic anisotropy in the lower mantle. *Earth and Planetary Science Letters* 271: 135–144.
- Manga M and Jeanloz R (1996) Implications of a metal bearing chemical boundary layer in D'' for mantle dynamics. *Geophysical Research Letters* 23: 3091–3094.
- Manthilake GM, de Koker N, Frost DJ, and McCammon CA (2011) Lattice thermal conductivity of lower mantle minerals and heat flux from Earth's core. *Proceedings of the National Academy of Sciences of the United States of America* 108: 17901–17904.
- Mao Z, Armentrout M, Rainey E, et al. (2011a) Dolomite III: A new candidate lower mantle carbonate. *Geophysical Research Letters* 38: L22303. <http://dx.doi.org/10.1029/2011GL049519>.
- Mao Z, Lin J-F, Liu J, and Prakapenka VB (2011b) Thermal equation of state of lower-mantle ferropericlase across the spin crossover. *Geophysical Research Letters* 38: L22308. <http://dx.doi.org/10.1029/2011GL049915>.
- Mao WL, Campbell AJ, Prakapenka VB, Hemley RJ, and Mao H-K (2007) Effect of iron on the properties of post-perovskite silicate. In: Hirose K, et al. (eds.) *Post-Perovskite: The Last Mantle Phase Transition. Geophysical Monograph Series*, vol. 174, pp. 37–46. Washington, DC: AGU.

- Mao Z, Lin JF, Jacobs C, et al. (2010) Electronic spin and valence states of Fe in CaIrO<sub>3</sub>-type silicate post-perovskite in the Earth's lowermost mantle. *Geophysical Research Letters* 37: L22304. <http://dx.doi.org/10.1029/2010GL045021>.
- Mao WL, Mao H-K, Prakapenka VB, Shu J, and Hemley RJ (2006a) The effect of pressure on the structure and volume of ferromagnesian postperovskite. *Geophysical Research Letters* 33: L12S02. <http://dx.doi.org/10.1029/2006GL025770>.
- Mao WL, Mao H-K, Sturhahn W, et al. (2006b) Iron-rich post-perovskite and the origin of ultralow-velocity zones. *Science* 312: 564–565.
- Mao WL, Meng Y, Shen G, et al. (2005) Iron-rich silicates in the Earth's D'' layer. *Proceedings of the National Academy of Sciences of the United States of America* 102: 9751–9753.
- Mao WL, Shen G, Prakapenka VB, et al. (2004) Ferromagnesian postperovskite silicates in the D'' layer of the Earth. *Proceedings of the National Academy of Sciences of the United States of America* 101: 15867–15869.
- Marquardt H, Speziale S, Reichmann HJ, Frost DJ, and Schilling FR (2009) Single-crystal elasticity of (Mg<sub>0.9</sub>Fe<sub>0.1</sub>)O to 81 GPa. *Earth and Planetary Science Letters* 287: 345–352.
- Marquardt H, Speziale S, Reichmann HJ, Frost DJ, Schilling FR, and Garnero EJ (2009) Elastic shear anisotropy of ferropericlase in Earth's lower mantle. *Science* 324: 224–226.
- Martin CD, Chapman KW, Chupas PJ, et al. (2007) Compression, thermal expansion, structure, and instability of CaIrO<sub>3</sub>, the structure model of MgSiO<sub>3</sub> post-perovskite. *American Mineralogist* 92(7): 1048–1053.
- Martin CD, Crichton WA, Liu HZ, Prakapenka VB, Chen J, and Parise JB (2006a) In-situ Rietveld structure refinement of perovskite and post-perovskite phases of NaMgF<sub>3</sub> (Neighborite) at high pressures. *American Mineralogist* 91(10): 1703–1706.
- Martin CD, Crichton WA, Liu H, Prakapenka V, Chen J, and Parise JB (2006b) Phase transitions and compressibility of NaMgF<sub>3</sub> (Neighborite) in perovskite- and post-perovskite-related structures. *Geophysical Research Letters* 33: L11305. <http://dx.doi.org/10.1029/2006GL026150>.
- Martin CD and Parise JB (2008) Structure constraints and instability leading to the postperovskite phase transition of MgSiO<sub>3</sub>. *Earth and Planetary Science Letters* 265: 630–640.
- Martin CD, Smith RI, Marshall WG, and Parise JB (2007) High pressure structure and bonding in CaIrO<sub>3</sub>: the structure model of MgSiO<sub>3</sub> post-perovskite investigated with time-of-flight neutron powder diffraction. *American Mineralogist* 92(11–12): 1912–1918.
- Maruyama S, Santosh M, and Zhao D (2007) Superplume, supercontinent, and post-perovskite: Mantle dynamics and anti-plate tectonics on the core–mantle boundary. *Gondwana Research* 11: 7–37. <http://dx.doi.org/10.1016/j.gr.2006.06.003>.
- Masters G and Gilbert F (1983) Attenuation in the Earth at low frequencies. *Philosophical Transactions of the Royal Society of London, Series A* 308: 479–522.
- Masters G, Johnson S, Laske G, and Bolton H (1996) A shear-velocity model of the mantle. *Philosophical Transactions of the Royal Society of London, Series A* 354: 1385–1411.
- Masters G, Jordan TH, Silver PG, and Gilbert F (1982) Aspherical Earth structure from fundamental spheroidal mode data. *Nature* 298: 609–613.
- Masters G, Laske G, Bolton H, and Dziewonski AM (2000) The relative behavior of shear velocity, bulk sound speed, and compressional velocity in the mantle: Implications for chemical and thermal structure. In: Karato S-I, Forte AM, Liebermann RC, Masters G, and Stixrude L (eds.) *Earth's Deep Interior: Mineral Physics and Tomography From the Atomic to the Global Scale*, pp. 63–87. Washington, DC: American Geophysical Union.
- Masters G, Laske G, Dziewonski A, and Boschi L (1999) Towards a spherical reference Earth model. *EoS, Transactions of the American Geophysical Union* 80: F27.
- Matas J, Bass J, Ricard Y, Mattern E, and Bukowinski MST (2007) On the bulk composition of the lower mantle: Predictions and limitations from generalized inversion of radial seismic profiles. *Geophysical Journal International* 170: 764–780. <http://dx.doi.org/10.1111/j.1365-246X.2007.03454.x>.
- Matyska C and Yuen DA (2004) The importance of radiative heat transfer for superplumes with a deep mantle phase transition. *Earth and Planetary Science Letters* 225: 255–266.
- Matyska C and Yuen DA (2006) Lower mantle dynamics with the post-perovskite phase change, radiative thermal conductivity, temperature-and depth-dependent viscosity. *Physics of the Earth and Planetary Interiors* 154: 196–207.
- Matzel E, Sen MK, and Grand SP (1996) Evidence for anisotropy in the deep mantle beneath Alaska. *Geophysical Research Letters* 23: 2417–2420.
- Maupin V, Garnero EJ, Lay T, and Fouch MJ (2005) Azimuthal anisotropy in the D'' layer beneath the Caribbean. *Journal of Geophysical Research* 110: B08301. <http://dx.doi.org/10.1029/2004JB003506>.
- McCammon C, Dubrovinsky L, Narygina O, et al. (2010) Low-spin Fe<sup>2+</sup> in silicate perovskite and a possible layer at the base of the lower mantle. *Physics of the Earth and Planetary Interiors* 180: 215–221.
- McCammon C, Kantor I, Narygina O, et al. (2008) Stable intermediate-spin ferrous iron in lower-mantle perovskite. *Nature Geoscience* 1: 684–687.
- McNamara AK, Garnero EJ, and Rost S (2010) Tracking deep mantle reservoirs with ultra-low velocity zones. *Earth and Planetary Science Letters* 299: 1–9. <http://dx.doi.org/10.1016/j.epsl.2010.07.042>.
- McNamara AK, Karato S-I, and van Keken PE (2001) Localization of dislocation creep in the lower mantle: Implications for the origin of seismic anisotropy. *Earth and Planetary Science Letters* 191: 85–99.
- McNamara AK, van Keken PE, and Karato S-I (2002) Development of anisotropic structure in the Earth's lower mantle by solid-state convection. *Nature* 416: 310–314.
- McNamara AK, van Keken PE, and Karato S-I (2003) Development of finite strain in the convecting lower mantle and its implications for seismic anisotropy. *Journal of Geophysical Research* 108(B5): 2230. <http://dx.doi.org/10.1029/2002JB001970>.
- McNamara AK and Zhong S (2004) Thermochemical structures within a spherical mantle: Superplumes or piles? *Journal of Geophysical Research* 109: B07402. <http://dx.doi.org/10.1029/2003JB02847>.
- McNamara AK and Zhong S (2005) Thermochemical structures beneath Africa and the Pacific Ocean. *Nature* 437: 1136–1139. <http://dx.doi.org/10.1038/nature04066>.
- Meade C, Silver PG, and Kaneshima S (1995) Laboratory and seismological observations of lower mantle isotropy. *Geophysical Research Letters* 22: 1293–1296.
- Mégnin C and Romanowicz B (2000) The three-dimensional shear velocity structure of the mantle from the inversion of body, surface, and higher-mode waveform. *Geophysical Journal International* 143: 709–728.
- Merkel S, Kubo A, Miyagi L, et al. (2006) Plastic deformation of MgGeO<sub>3</sub> post-perovskite at lower mantle pressures. *Science* 311: 644–646.
- Merkel S, McNamara AK, Kubo A, et al. (2007) Deformation of (Mg,Fe)SiO<sub>3</sub> post-perovskite and D'' anisotropy. *Science* 316: 1729–1732. <http://dx.doi.org/10.1126/science.1140609>.
- Metsue A, Carrez P, Mainprice D, and Cordier P (2009) Numerical modeling of dislocations and deformation mechanisms in CaIrO<sub>3</sub> and MgGeO<sub>3</sub> post-perovskites—Comparison with MgSiO<sub>3</sub> post-perovskite. *Physics of the Earth and Planetary Interiors* 174: 165–173. <http://dx.doi.org/10.1016/j.pepi.2008.04.003>.
- Metsue A and Tsuchiya T (2011) Lattice dynamics and thermodynamic properties of (Mg,Fe<sup>2+</sup>)SiO<sub>3</sub> postperovskite. *Journal of Geophysical Research* 116: B08207. <http://dx.doi.org/10.1029/2010JB008018>.
- Miller MS and Niu F (2008) Bulldozing the core–mantle boundary: Localized seismic scatterers beneath the Caribbean Sea. *Physics of the Earth and Planetary Interiors* 170: 89–94.
- Minster JB (1980) Anelasticity and attenuation. In: Dziewonski AM and Boschi E (eds.) *Physics of the Earth's Interior*, pp. 152–212. Amsterdam: North-Holland.
- Minster JB and Anderson DL (1981) A model of dislocation controlled rheology for the mantle. *Philosophical Transactions of the Royal Society of London* 299: 319–356.
- Mitchell BJ and Helmlberger DV (1973) Shear velocities at the base of the mantle from observations of S and ScS. *Journal of Geophysical Research* 78: 6009–6020.
- Mitrovica JX and Forte AM (1997) Radial profile of mantle viscosity: Results from the joint inversion of convection and postglacial rebound observables. *Journal of Geophysical Research* 102: 2751–2769.
- Mitrovica JX and Forte AM (2004) A new inference of mantle viscosity based upon joint inversion of convection and glacial isostatic adjustment data. *Earth and Planetary Science Letters* 225: 177–189.
- Mittelstaedt E and Tackley PJ (2006) Plume heat flow is much lower than CMB heat flow. *Earth and Planetary Science Letters* 241: 202–210.
- Miyagi L, Kanitpanyacharoen W, Kærcher P, Lee KKM, and Wenk H-R (2010) Slip systems in MgSiO<sub>3</sub> post-perovskite: Implications for D'' anisotropy. *Science* 329: 1639–1642.
- Miyagi L, Kanitpanyacharoen W, Stackhouse S, Militzer B, and Wenk H-R (2011) The enigma of post-perovskite anisotropy: Deformation versus transformation textures. *Physical Chemistry of Minerals* 38: 665–678.
- Miyagi L, Merkel S, Yagi T, Sata N, Ohishi Y, and Wenk HR (2006) Quantitative Rietveld texture analysis of CaSiO<sub>3</sub> perovskite deformed in a diamond anvil cell. *Journal of Physics: Condensed Matter* 18: S995–S1005.
- Miyagi L, Merkel S, Yagi T, Sata N, Ohishi Y, and Wenk H-R (2009) Diamond anvil cell deformation of CaSiO<sub>3</sub> perovskite up to 49 GPa. *Physics of the Earth and Planetary Interiors* 174: 159–164.
- Miyagi L, Nishiyama N, Wang Y, et al. (2008) Deformation and texture development in CaIrO<sub>3</sub> post-perovskite phase up to 6 GPa and 1300 K. *Earth and Planetary Science Letters* 268: 515–525. <http://dx.doi.org/10.1016/j.epsl.2008.02.005>.
- Miyajima N, Niwa K, Heidelbach F, Yagi T, and Ohgushi K (2010) Deformation microtextures in CaIrO<sub>3</sub> post-perovskite under high stress conditions using a laser-heated diamond anvil cell. *Journal of Physics: Conference Series* 215: 012097.

- Miyajima N, Ohgushi K, Ichihara M, and Yagi T (2006) Crystal morphology and dislocation microstructures of  $\text{CaIrO}_3$ : A TEM study of an analogue of the  $\text{MgSiO}_3$  post-perovskite phase. *Geophysical Research Letters* 33: L12302. <http://dx.doi.org/10.1029/2005GL025001>.
- Miyajima N, Yagi T, and Ichihara M (2009) Dislocation microstructures of  $\text{MgSiO}_3$  perovskite at a high pressure and temperature condition. *Physics of the Earth and Planetary Interiors* 174: 153–158.
- Mondt JC (1977) SH waves: Theory and observations for epicentral distances greater than 90 degrees. *Physics of the Earth and Planetary Interiors* 15: 46–59.
- Monnereau M and Yuen DA (2007) Topology of the postperovskite phase transition and mantle dynamics. *Proceedings of the National Academy of Sciences of the United States of America* 104: 9156–9161.
- Monnereau M and Yuen DA (2010) Seismic imaging of the D'' and constraints on the core heat flux. *Physics of the Earth and Planetary Interiors* 180: 258–270.
- Montagner J-P and Kennett BLN (1996) How to reconcile body-wave and normal-mode reference Earth models. *Geophysical Journal International* 125: 229–248.
- Montague NL, Kellogg LH, and Manga M (1998) High Rayleigh number thermochemical models of a dense boundary layer in D''. *Geophysical Research Letters* 25: 2345–2348.
- Montelli R, Nolet G, Dahlen FA, Masters G, Engdahl ER, and Hung SH (2004) Finite-frequency tomography reveals a variety of plumes in the mantle. *Science* 303: 338–343.
- Mookherjee M (2011) Mid-mantle anisotropy: Elasticity of aluminous phases in subducted MORB. *Geophysical Research Letters* 38: L14302. <http://dx.doi.org/10.1029/2011GL047923>.
- Moore MM, Garnero EJ, Lay T, and Williams Q (2003) Shear wave splitting and waveform complexity for lowermost mantle structures with low-velocity lamellae and transverse isotropy. *Journal of Geophysical Research* 109: B02319. <http://dx.doi.org/10.1029/2003JB002546>.
- Morelli A and Dziewonski AM (1987) Topography of the core–mantle boundary and lateral heterogeneity of the liquid core. *Nature* 325: 678–683.
- Morelli A and Dziewonski AM (1993) Body wave travel times and a spherically symmetric P and S-wave velocity model. *Geophysical Journal International* 112: 178–194.
- Mori J and Helmberger DV (1995) Localized boundary layer below the mid-Pacific velocity anomaly identified from a PnP precursor. *Journal of Geophysical Research* 100: 20359–20365.
- Mosca I, Cobden L, Deuss A, Ritsema J, and Trampert J (2012) Seismic and mineralogical structures of the lower mantle from probabilistic tomography. *Journal of Geophysical Research* 117: B06304. <http://dx.doi.org/10.1029/2011JB008851>.
- Mosenfelder JL, Asimow PD, and Ahrens TJ (2007) Thermodynamic properties of  $\text{Mg}_2\text{SiO}_4$  liquid at ultra-high pressures for shock measurements to 200 GPa on forsterite and wadsleyite. *Journal of Geophysical Research* 112: B06208.
- Mosenfelder JL, Asimow PD, Frost DJ, Rubie DC, and Ahrens TJ (2009) The  $\text{MgSiO}_3$  system at high pressure: Thermodynamic properties of perovskite, postperovskite, and melt from global inversion of shock and static compression data. *Journal of Geophysical Research* 114: B01203. <http://dx.doi.org/10.1029/2008JB005900>.
- Muirhead KJ and Hales AL (1980) Evidence for P-wave discontinuities at depths greater than 650 km in the mantle. *Physics of the Earth and Planetary Interiors* 23: 304–313.
- Mula AH and Müller G (1980) Ray parameters of diffracted long period P and S-waves and the velocities at the base of the mantle. *Pure and Applied Geophysics* 188: 1270–1290.
- Murakami M and Bass JD (2011) Evidence of denser  $\text{MgSiO}_3$  glass above 133 gigapascal (GPa) and implications for remnants of ultradense silicate melt from a deep magma ocean. *Proceedings of the National Academy of Sciences of the United States of America* 108(42): 17286–17289.
- Murakami M, Hirose K, Kawamura K, Sata N, and Ohishi Y (2004) Post-perovskite phase transition in  $\text{MgSiO}_3$ . *Science* 304: 855–858.
- Murakami M, Hirose K, Sata N, and Ohishi Y (2005) Post-perovskite phase transition and mineral chemistry in the pyrolytic lowermost mantle. *Geophysical Research Letters* 32: L03304. <http://dx.doi.org/10.1029/2004GL021956>.
- Murakami M, Ohishi Y, Hirao N, and Hirose K (2009) Elasticity of  $\text{MgO}$  to 130 GPa: Implications for lower mantle mineralogy. *Earth and Planetary Science Letters* 277(1–2): 123–129.
- Murakami M, Ohishi Y, Hirao N, and Hirose K (2012) A perovskitic lower mantle inferred from high-pressure, high-temperature sound velocity data. *Nature* 485: 90–94.
- Murakami M, Sinogeikin SV, Bass JD, Sata N, Ohishi Y, and Hirose K (2007) Sound velocity of  $\text{MgSiO}_3$  post-perovskite phase: A constraint on the D'' discontinuity. *Earth and Planetary Science Letters* 259(1–2): 18–23.
- Murakami M, Sinogeikin SV, Hellwig H, Bass JD, and Li J (2007) Sound velocity of  $\text{MgSiO}_3$  perovskite to Mbar pressure. *Earth and Planetary Science Letters* 256(1–2): 47–54. <http://dx.doi.org/10.1016/j.epsl.2007.01.011>.
- Myers SC, Johannesson G, and Simmons NA (2011) Global-scale P wave tomography optimized for prediction of teleseismic and regional travel times for Middle East events: 1. Data set development. *Journal of Geophysical Research* 116: B04304.
- Nakada M, Iriguchi C, and Karato S-I (2012) The viscosity structure of the D'' layer of the Earth's mantle inferred from the analysis of Chandler wobble and tidal deformation. *Physics of the Earth and Planetary Interiors* 208–209: 11–24.
- Nakada M and Karato S-I (2012) Low viscosity of the bottom of the Earth's mantle inferred from the analysis of Chandler wobble and tidal deformation. *Physics of the Earth and Planetary Interiors* 192–193: 68–80.
- Nakagawa T and Tackley PJ (2004) Effects of a perovskite–post perovskite phase change near core–mantle boundary in compressible mantle convection. *Geophysical Research Letters* 31: L16611. <http://dx.doi.org/10.1029/2004GL020648>.
- Nakagawa T and Tackley PJ (2005) The interaction between the post-perovskite phase change and thermo-chemical boundary layer near the core–mantle boundary. *Earth and Planetary Science Letters* 238: 204–216.
- Nakagawa T and Tackley PJ (2006) Three-dimensional structures and dynamics in the deep mantle: Effects of post-perovskite phase change and deep mantle layering. *Geophysical Research Letters* 33: L12S11. <http://dx.doi.org/10.1029/2006GL025719>.
- Nakagawa T and Tackley PJ (2008) Lateral variations in CMB heat flux and deep mantle seismic velocity caused by a thermal-chemical-phase boundary layer in 3D spherical convection. *Earth and Planetary Science Letters* 271: 348–358.
- Nakagawa T and Tackley PJ (2011) Effects of low-viscosity post-perovskite on thermochemical mantle convection in a 3-D spherical shell. *Geophysical Research Letters* 38: L04309. <http://dx.doi.org/10.1029/2010GL046494>.
- Nakajima Y, Frost DJ, and Rubin DC (2012) Ferrous iron partitioning between magnesium silicate perovskite and ferropericlase and the composition of perovskite in the Earth's lower mantle. *Journal of Geophysical Research* 117: B08201. <http://dx.doi.org/10.1029/2012JB009151>.
- Naryina O, Dubrovinsky LS, Samuel H, et al. (2011) Chemically homogeneous spin transition zone in Earth's lower mantle. *Physics of the Earth and Planetary Interiors* 185: 107–111.
- Nataf H-C and Houard S (1993) Seismic discontinuity at the top of D'': A world-wide feature? *Geophysical Research Letters* 20: 2371–2374.
- Nebel O, Münker C, Nebel-Jacobsen YJ, Kleine T, Mezger K, and Mortimer N (2007) Hf–Nd–Pb isotope evidence from Permian arc rocks for the long-term presence of the Indian-Pacific mantle boundary in the SW Pacific. *Earth and Planetary Science Letters* 254: 377–392.
- Ni S, Ding X, and Helmberger DV (2000) Constructing synthetics from deep earth tomographic models. *Geophysical Journal International* 140: 71–82.
- Ni S and Helmberger DV (2003a) Seismological constraints on the South African superplume; could be the oldest distinct structure on earth. *Earth and Planetary Science Letters* 206: 119–131.
- Ni S and Helmberger DV (2003b) Ridge-like lower mantle structure beneath South Africa. *Journal of Geophysical Research* 108(B2): 2094. <http://dx.doi.org/10.1029/2001JB001545>.
- Ni S, Helmberger DV, and Tromp J (2005) Three-dimensional structure of the Africa superplume from waveform modeling. *Geophysical Journal International* 161: 283–294.
- Ni S, Tan E, Gurnis M, and Helmberger DV (2002) Sharp sides to the African superplume. *Science* 296: 1850–1852.
- Nishio-Hamane D, Fujino K, Seto Y, and Nagai T (2007) Effect of the incorporation of  $\text{FeAlO}_3$  into  $\text{MgSiO}_3$  perovskite on the post-perovskite transition. *Geophysical Research Letters* 34: L12307. <http://dx.doi.org/10.1029/2007GL029991>.
- Nishio-Hamane D, Seto Y, Fujino K, and Nagai T (2008) Effect of  $\text{FeAlO}_3$  incorporation into  $\text{MgSiO}_3$  on the bulk modulus of perovskite. *Physics of the Earth and Planetary Interiors* 166: 219–225.
- Nishio-Hamane D and Yagi T (2009) Equations of state for postperovskite phases in the  $\text{MgSiO}_3$ – $\text{FeSiO}_3$ – $\text{FeAlO}_3$  system. *Physics of the Earth and Planetary Interiors* 175: 145–150.
- Nishiyama N, Yagi T, Ono S, Gotou H, Harada T, and Kikegawa T (2007) Effect of incorporation of iron and aluminum on the thermoelastic properties of magnesium silicate perovskite. *Physical Chemistry of Minerals* 34: 131–143. <http://dx.doi.org/10.1007/s00269-006-0134-6>.
- Niu F and Kawakatsu H (1997) Depth variation of the mid-mantle seismic discontinuity. *Geophysical Research Letters* 24: 429–432.
- Niu F and Perez AM (2004) Seismic anisotropy in the lower mantel: A comparison of waveform splitting of SKS and SKKS. *Geophysical Research Letters* 31: L24612. <http://dx.doi.org/10.1029/2004GL021196>.
- Niwa K, Miyajima N, Seto Y, Ohgushi K, Gotou H, and Yagi T (2012) In situ observation of shear stress-induced perovskite to post-perovskite phase transition in  $\text{CaIrO}_3$  and

- the development of its deformation texture in a diamond-anvil cell up to 30 GPa. *Physics of the Earth and Planetary Interiors* 194–195: 10–17.
- Niwa K, Yagi T, and Ohgushi K (2011) Elasticity of CaIrO<sub>3</sub> with perovskite and postperovskite structure. *Physical Chemistry of Minerals* 38: 21–31.
- Niwa K, Yagi T, Ohgushi K, Merkel S, Miyajima N, and Kikegawa T (2007) Lattice preferred orientation in CaIrO<sub>3</sub> perovskite and postperovskite formed by plastic deformation under pressure. *Physical Chemistry of Minerals* 34: 679–686. <http://dx.doi.org/10.1007/s00269-007-0182-6>.
- Nomura R, Hirose K, Sata N, and Ohishi Y (2010) Precise determination of post-stishovite phase transition boundary and implications for seismic heterogeneities in the mid-lower mantle. *Physics of the Earth and Planetary Interiors* 183: 104–109.
- Nomura R, Ozawa H, Tateno S, et al. (2011) Spin crossover and iron-rich silicate melt in the Earth's deep mantle. *Nature* 473: 199–202. <http://dx.doi.org/10.1038/nature09940>.
- Nowacki A, Walker AM, Wookey J, and Kendall J-M (2012) Evaluating post-perovskite as a cause of D'' anisotropy in regions of paleo-subduction. *Geophysical Journal International*. <http://dx.doi.org/10.1093/gji/ggs068>.
- Nowacki A, Wookey J, and Kendall J-M (2010) Deformation of the lowermost mantle from seismic anisotropy. *Nature* 467: 1091–1094.
- Nowacki A, Wookey J, and Kendall J-M (2011) New advances in using seismic anisotropy, mineral physics and geodynamics to understand deformation in the lower mantle. *Journal of Geodynamics* 52: 205–228.
- Obayashi M and Fukao Y (1997) P and PcP travel time tomography for the core–mantle boundary. *Journal of Geophysical Research* 102: 17825–17841.
- Oganov AR, Glass CW, and Ono S (2006) High-pressure phases of CaCO<sub>3</sub>: Crystal structure prediction and experiment. *Earth and Planetary Science Letters* 241: 95–103. <http://dx.doi.org/10.1016/j.epsl.2005.10.014>.
- Oganov AR, Maronak R, Laio A, Raiteri P, and Parrinello M (2005) Anisotropy of Earth's D'' layer and stacking faults in the MgSiO<sub>3</sub> post-perovskite phase. *Nature* 438: 1142–1144.
- Oganov AR and Ono S (2004) Theoretical and experimental evidence for a post-perovskite phase of MgSiO<sub>3</sub> in Earth's D'' layer. *Nature* 430: 445–448.
- Oganov AR, Ono S, Ma Y, Glass CW, and Garcia A (2008) Novel high-pressure structures of MgCO<sub>3</sub>, CaCO<sub>3</sub> and CO<sub>2</sub> and their role in Earth's lower mantle. *Earth and Planetary Science Letters* 273: 38–47. <http://dx.doi.org/10.1016/j.epsl.2008.06.005>.
- Ohta K, Hirose K, Ichiki M, Shimizu K, Sata N, and Ohishi Y (2010) Electrical conductivities of pyrolytic mantle and MORB materials up to the lowermost mantle conditions. *Earth and Planetary Science Letters* 289: 497–502. <http://dx.doi.org/10.1016/j.epsl.2009.11.042>.
- Ohta K, Hirose K, Lay T, Sata N, and Ohishi Y (2008) Phase transitions in pyrolytic and MORB at lowermost mantle conditions: Implications for a MORB-rich pile above the core–mantle boundary. *Earth and Planetary Science Letters* 267: 107–117.
- Ohta K, Hirose K, Onoda S, and Shimizu K (2007) The effect of iron spin transition on electrical conductivity of (Mg,Fe)O magnesiowüstite. *Proceedings of the Japanese Academy, Series B* 83: 97–100.
- Ohta K, Hirose K, Shimizu K, Sata N, and Ohishi Y (2010) The electrical resistance measurements of (Mg,Fe)SiO<sub>3</sub> perovskite at high pressures and implications for electronic spin transition of iron. *Physics of the Earth and Planetary Interiors* 180: 154–158.
- Ohta K, Onoda S, Hirose K, et al. (2008) The electrical conductivity of post-perovskite in Earth's D'' layer. *Science* 320: 89–91.
- Ohta K, Yagi T, Taketoshi N, et al. (2012) Lattice thermal conductivity of MgSiO<sub>3</sub> perovskite and post-perovskite at the core–mantle boundary. *Earth and Planetary Science Letters* 349–350: 109–115.
- Okada T, Yagi T, Niwa K, and Kikegawa T (2010) Lattice-preferred orientations in post-perovskite-type MgGeO<sub>3</sub> formed by transformations from different pre-phases. *Physics of the Earth and Planetary Interiors* 180: 195–202. <http://dx.doi.org/10.1016/j.pepi.2009.08.002>.
- Okano K and Suetsugu D (1992) Search for lower mantle high velocity zones beneath the deepest Kurile and Mariana earthquakes. *Geophysical Research Letters* 19: 745–748.
- Ono S, Kikegawa T, and Ohishi Y (2006) Equation of state of CaIrO<sub>3</sub>-type MgSiO<sub>3</sub> up to 144 GPa. *American Mineralogist* 91: 475–478. <http://dx.doi.org/10.2138/am.2006.2118>.
- Ono S and Oganov AR (2005) In situ observations of phase transition between perovskite and CaIrO<sub>3</sub>-type phase in MgSiO<sub>3</sub> and pyrolytic mantle composition. *Earth and Planetary Science Letters* 236: 914–931.
- Ono S, Oganov AR, Koyama T, and Shimizu H (2006) Stability and compressibility of the high-pressure phases of Al<sub>2</sub>O<sub>3</sub> up to 200 GPa: Implications for the electrical conductivity of the base of the lower mantle. *Earth and Planetary Science Letters* 246: 326–335.
- Otsuka K and Karato S-I (2012) Deep penetration of molten iron into the mantle caused by a morphological instability. *Nature* 492: 243–246.
- Ozawa H, Hirose K, Mitome M, Bando Y, Sata N, and Ohishi Y (2008) Chemical equilibrium between ferropericlase and molten iron to 134 GPa and implications for iron content at the bottom of the mantle. *Geophysical Research Letters* 35: L05308. <http://dx.doi.org/10.1029/2007GL032648>.
- Panero WR, Akber-Knutson S, and Stixrude L (2006) Al<sub>2</sub>O<sub>3</sub> incorporation in MgSiO<sub>3</sub> perovskite and ilmenite. *Earth and Planetary Science Letters* 252: 152–161.
- Pankow KL and Lay T (1999) Constraints on the Kurile slab from shear wave residual sphere analysis. *Journal of Geophysical Research* 104: 7255–7278.
- Panning MP, Lekić V, and Romanowicz BA (2010) Importance of crustal corrections in the development of a new global model of radial anisotropy. *Journal of Geophysical Research* 115: B12325. <http://dx.doi.org/10.1029/2010JB007520>.
- Panning MP and Romanowicz B (2004) Inferences on flow at the base of Earth's mantle based on seismic anisotropy. *Science* 303: 351–353.
- Panning M and Romanowicz B (2006) A three-dimensional radially anisotropic model of shear velocity in the whole mantle. *Geophysical Journal International* 167: 361–379. <http://dx.doi.org/10.1111/j.1365-246X.2006.03100.x>.
- Persch ST, Vidale JE, and Earle PS (2001) Absence of short-period ULVZ precursors to Pcp and Scp from two regions of the CMB. *Geophysical Research Letters* 28: 387–390.
- Persson K, Bengtsson A, Ceder G, and Morgan D (2006) *Ab initio* study of the composition dependence of the pressure-induced spin transition in the (Mg<sub>1-x</sub>Fe<sub>x</sub>)O system. *Geophysical Research Letters* 33: L16306. <http://dx.doi.org/10.1029/2006GL026621>.
- Phipps Morgan J and Shearer PM (1993) Seismic constraints on mantle flow and topography of the 660-km discontinuity: Evidence for whole mantle convection. *Nature* 365: 506–511.
- Pulliam J and Sen MK (1998) Seismic anisotropy in the core–mantle transition zone. *Geophysical Journal International* 135: 113–128.
- Pulliam J and Stark P (1993) Bumps on the core–mantle boundary: Are they facts or artifacts? *Journal of Geophysical Research* 98: 1943–1956.
- Randall MJ (1971) A revised travel-time table for S. *Geophysical Journal of the Royal Astronomical Society* 22: 229–234.
- Reasoner C and Revenaugh J (1999) Short-period P-wave constraints on D'' reflectivity. *Journal of Geophysical Research* 104: 955–961.
- Reasoner C and Revenaugh J (2000) ScP constraints on ultralow-velocity zone density and gradient thickness beneath the Pacific. *Journal of Geophysical Research* 105: 28173–28182.
- Ren Y, Stutzmann E, van der Hilst RD, and Besse J (2007) Understanding seismic heterogeneities in the lower mantle beneath the Americas from seismic tomography and plate tectonic history. *Journal of Geophysical Research* 112: B01302. <http://dx.doi.org/10.1029/2005JB004154>.
- Resovsky J and Trampert J (2003) Using probabilistic seismic tomography to test mantle velocity-density relationships. *Earth and Planetary Science Letters* 215: 121–130.
- Restivo A and Helffrich G (2006) Core–mantle boundary structure investigated using SKS and SKKS polarization anomalies. *Geophysical Journal International* 165: 288–302. <http://dx.doi.org/10.1111/j.1365-246X.2006.02901.x>.
- Revenaugh JS and Jordan TH (1991) Mantle layering from ScS reverberations, 2. The transition zone. *Journal of Geophysical Research* 96: 19763–19780.
- Revenaugh JS and Meyer R (1997) Seismic evidence of partial melt within a possibly ubiquitous low-velocity layer at the base of the mantle. *Science* 277: 670–673.
- Richards MA and Hager BH (1984) Geoid anomalies in a dynamic Earth. *Journal of Geophysical Research* 89: 5987–6002.
- Ricolleau A, Fei Y, Cottrell E, et al. (2009) Density profile of pyrolite under the lower mantle conditions. *Geophysical Research Letters* 36: L06302. <http://dx.doi.org/10.1029/2008GL036759>.
- Ricolleau A, Perrillat JP, Fiquet G, et al. (2010) Phase relations and equation of state of a natural MORB: Implications for the density profile of subducted oceanic crust in the Earth's lower mantle. *Journal of Geophysical Research* 115: B08202. <http://dx.doi.org/10.1029/2009JB006709>.
- Ritsema J (2000) Evidence for shear wave anisotropy in the lowermost mantle beneath the Indian Ocean. *Geophysical Research Letters* 27: 1041–1044.
- Ritsema J, Deuss A, van Heijst HJ, and Woodhouse JH (2011) S40RTS: A degree-40 shear-velocity model for the mantle from new Rayleigh wave dispersion, teleseismic traveltimes and normal-mode splitting function measurements. *Geophysical Journal International* 184: 1223–1236. <http://dx.doi.org/10.1111/j.1365-246X.2010.04884.x>.
- Ritsema J, Lay T, Garnero EJ, and Benz H (1998a) Seismic anisotropy in the lowermost mantle beneath the Pacific. *Geophysical Research Letters* 25: 1229–1232.
- Ritsema J, Ni S, Helmberger DV, and Crotwell HP (1998b) Evidence for strong shear velocity reductions and velocity gradients in the lower mantle beneath Africa. *Geophysical Research Letters* 25: 4245–4248.

- Ritsema J, McNamara AK, and Bull AL (2007) Tomographic filtering of geodynamical models. *Journal of Geophysical Research* 112: B01303. <http://dx.doi.org/10.1029/2006JB004566>
- Ritsema J and van Heijst HJ (2000) Seismic imaging of structural heterogeneity in Earth's mantle: Evidence for large-scale mantle flow. *Science Progress* 83: 243–259.
- Ritsema J, van Heijst HJ, and Woodhouse JH (1999) Complex shear wave velocity structure imaged beneath Africa and Iceland. *Science* 286: 1925–1928.
- Robertson GS and Woodhouse JH (1996) Ratio of relative S to P velocity heterogeneity in the lower mantle. *Journal of Geophysical Research* 101: 20041–20052.
- Rodgers A and Wahr J (1993) Inference of core–mantle boundary topography from ISC PcP and PKP traveltimes. *Geophysical Journal International* 115: 991–1011.
- Rokosky JM, Lay T, and Garnero EJ (2006) Small-scale lateral variations in azimuthally anisotropic D'' structure beneath the Cocos Plate. *Earth and Planetary Science Letters* 248: 411–425.
- Rokosky JM, Lay T, Garnero EJ, and Russell SA (2004) High-resolution investigation of shear wave anisotropy in D'' beneath the Cocos Plate. *Geophysical Research Letters* 31: L07605. <http://dx.doi.org/10.1029/2003GL018902>.
- Romanowicz B (2001) Can we resolve 3D density heterogeneity in the lower mantle? *Geophysical Research Letters* 28: 1107–1110.
- Rondenay S, Cormier VF, and Van Ark EM (2010) SKS and SPdKS sensitivity to two-dimensional ultralow-velocity zones. *Journal of Geophysical Research* 115: B04311. <http://dx.doi.org/10.1029/2009JB006733>.
- Rondenay S and Fischer KM (2003) Constraints on localized core–mantle boundary structure from multichannel, broadband SKS coda analysis. *Journal of Geophysical Research* 108: 2537. <http://dx.doi.org/10.1029/2003JB002518>.
- Ross AR, Thybo H, and Solidilov LN (2004) Reflection seismic profiles of the core–mantle boundary. *Journal of Geophysical Research* 109: B08303. <http://dx.doi.org/10.1029/2003JB002515>.
- Rost S and Earle PS (2010) Identifying regions of strong scattering at the core–mantle boundary from analysis of PKKP precursor energy. *Earth and Planetary Science Letters* 297: 616–626.
- Rost S and Garnero EJ (2006) Detection of an ultralow velocity zone at the core–mantle boundary using diffracted PKP<sub>b</sub>w waves. *Journal of Geophysical Research* 111: B07309. <http://dx.doi.org/10.1029/2005JB003850>.
- Rost S, Garnero EJ, and Stefan W (2010) Thin and intermittent ultralow-velocity zones. *Journal of Geophysical Research* 115: B06312. <http://dx.doi.org/10.1029/2009JB006981>.
- Rost S, Garnero EJ, Thorne MS, and Hutko AR (2010) On the absence of an ultralow-velocity zone in the North Pacific. *Journal of Geophysical Research* 115: B04312. <http://dx.doi.org/10.1029/2009JB006420>.
- Rost S, Garnero EJ, and Williams Q (2006) Fine-scale ultralow-velocity zone structure from high-frequency seismic array data. *Journal of Geophysical Research* 111: B09310. <http://dx.doi.org/10.1029/2005JB004088>.
- Rost S, Garnero EJ, and Williams Q (2008) Seismic array detection of subducted oceanic crust in the lower mantle. *Journal of Geophysical Research* 113: B06303. <http://dx.doi.org/10.1029/2007JB005263>.
- Rost S, Garnero EJ, Williams Q, and Manga M (2005) Seismological constraints on a possible plume root at the core–mantle boundary. *Nature* 435: 666–669.
- Rost S and Revenaugh J (2001) Seismic detection of rigid zones at the top of the core. *Science* 294: 1911–1914.
- Rost S and Revenaugh J (2003) Small-scale ultralow-velocity zone structure imaged by ScP. *Journal of Geophysical Research* 108: 2056. <http://dx.doi.org/10.1029/2001JB001627>.
- Rost S and Thomas C (2010) High resolution CMB imaging from migration of short-period core reflected phases. *Physics of the Earth and Planetary Interiors* 183: 143–150.
- Runge CE, Kubo A, Kiefer B, et al. (2006) Equation of state of MgGeO<sub>3</sub> perovskite to 65 GPa: Comparison with the post-perovskite phase. *Physical Chemistry of Minerals* 33: 699–709.
- Russell SA, Lay T, and Garnero EJ (1998) Seismic evidence for small-scale dynamics in the lowermost mantle at the root of the Hawaiian hotspot. *Nature* 396: 255–258.
- Russell SA, Lay T, and Garnero EJ (1999) Small-scale lateral shear velocity and anisotropy heterogeneity near the core–mantle boundary beneath the central Pacific imaged using broadband ScS-waves. *Journal of Geophysical Research* 104: 13183–13199.
- Russell SA, Reasoner C, Lay T, and Revenaugh J (2001) Coexisting shear-and compressional-wave seismic velocity discontinuities beneath the central Pacific. *Geophysical Research Letters* 28: 2281–2284.
- Sacks S (1966) Diffracted waves studies of the earth's core: 1. Amplitudes, core size, and rigidity. *Journal of Geophysical Research* 71: 1173–1181.
- Saha S, Bengtson A, Crispin KL, VanOrman JA, and Morgan D (2011) Effects of spin transition on diffusion of Fe<sup>2+</sup> in ferropericlase in Earth's lower mantle. *Physical Review B* 85: 184102.
- Saha S, Bengtson A, and Morgan D (2013) Effect of anomalous compressibility on Fe diffusion in ferropericlase throughout the spin crossover in the lower mantle. *Earth and Planetary Science Letters* 326: 1–5.
- Saiika A, Boffa Ballaran T, and Frost DJ (2009) The effect of Fe and Al substitution on the compressibility of MgSiO<sub>3</sub>-perovskite determined through single-crystal x-ray diffraction. *Physics of the Earth and Planetary Interiors* 173: 153–161. <http://dx.doi.org/10.1016/j.pepi.2008.11.006>.
- Sakai T, Kondo T, Ohtani E, et al. (2006) Interaction between iron and post-perovskite at core–mantle boundary and core signature in plume source region. *Geophysical Research Letters* 33: L15317. <http://dx.doi.org/10.1029/2006GL026868>.
- Sakai T, Ohtani E, Terasaki H, et al. (2009a) Fe–Mg partitioning between perovskite and ferropericlase. *American Mineralogist* 94: 921–925. <http://dx.doi.org/10.2138/am-2009.3123>.
- Sakai T, Ohtani E, Terasaki H, et al. (2009b) Fe–Mg partitioning between postperovskite and ferropericlase in the lowermost mantle. *Physical Chemistry of Minerals* 37(487–496): 1–10.
- Saltzer RL, van der Hilst RD, and Kárasoñ H (2001) Comparing P and S-wave heterogeneity in the mantle. *Geophysical Research Letters* 28: 1335–1338.
- Samuel H and Tosi N (2012) The influence of post-perovskite strength on the Earth's mantle thermal and chemical evolution. *Earth and Planetary Science Letters* 323–324: 50–59.
- Scherbaum F, Krüger F, and Weber M (1997) Double beam imaging: Mapping lower mantle heterogeneities using combinations of source and receiver arrays. *Journal of Geophysical Research* 102: 507–522.
- Schlüterhardt J, Schweitzer J, and Müller G (1985) Evidence against a discontinuity at the top of D''. *Geophysical Journal of the Royal Astronomical Society* 81: 295–306.
- Schmerr N, Garnero E, and McNamara A (2010) Deep mantle plumes and convective upwelling beneath the Pacific Ocean. *Earth and Planetary Science Letters* 294: 143–151.
- Schubert BSA, Bunge H-P, and Ritsema J (2009) Tomographic filtering of high-resolution mantle circulation models: Can seismic heterogeneity be explained by temperature alone? *Geochemistry, Geophysics, Geosystems* 10: Q05W03. <http://dx.doi.org/10.1029/2009GC002401>.
- Schwartz SY, Lay T, and Grand SP (1991) Seismic imaging of subducted slabs: Trade-offs with deep path and near-receiver effects. *Geophysical Research Letters* 18: 1265–1268.
- Seagle CT, Heinz DL, Campbell AJ, Prakapenka VB, and Wanless ST (2008) Melting and thermal expansion in the Fe–FeO system at high pressure. *Earth and Planetary Science Letters* 265: 655–665.
- Sengupta MK and Julian BR (1978) Radial variation of compressional and shear velocities in the Earth's lower mantle. *Geophysical Journal of the Royal Astronomical Society* 54: 185–219.
- Sengupta MK and Toksoz MN (1976) Three-dimensional model of seismic velocity variation in the Earth's mantle. *Geophysical Research Letters* 3: 84–86.
- Shahnas MH, Peltier WR, Wu Z, and Wentzcovitch R (2011) The high-pressure electronic spin transition in iron: Potential impacts upon mantle mixing. *Journal of Geophysical Research* 116: B08205. <http://dx.doi.org/10.1029/2010JB007965>.
- Shearer PM (1993) Global mapping of upper mantle reflectors from long-period SS precursors. *Geophysical Journal International* 115: 878–904.
- Shieh SR, Dorfman SM, Kubo A, Prakapenka VB, and Duffy TS (2011) Synthesis and equation of state of post-perovskites in the (Mg,Fe)<sub>3</sub>Al<sub>2</sub>Si<sub>3</sub>O<sub>12</sub> system. *Earth and Planetary Science Letters* 312: 422–428.
- Shieh SR, Duffy TS, Kubo A, et al. (2006) Equation of state of the post-perovskite phase synthesized from a natural (Mg,Fe)SiO<sub>3</sub> orthopyroxene. *Proceedings of the National Academy of Sciences of the United States of America* 103: 3039–3043.
- Shim SH (2008) The post-perovskite transition. *Annual Reviews of Earth and Planetary Sciences* 36: 569–599.
- Shim S-H, Bengtson A, Morgan D, et al. (2009) Electronic and magnetic structures of the postperovskite-type Fe<sub>2</sub>O<sub>3</sub>—Implications for planetary magnetic records and deep interior transitions. *Proceedings of the National Academy of Sciences of the United States of America* 106: 5508–5512. <http://dx.doi.org/10.1073/pnas.0808549106>.
- Shim S-H, Catalli K, Hustoft J, et al. (2008) Crystal structure and thermoelastic properties of (Mg<sub>0.91</sub>Fe<sub>0.09</sub>)SiO<sub>3</sub> postperovskite up to 135 GPa and 2700 K. *Proceedings of the National Academy of Sciences of the United States of America* 105: 7382–7386.
- Shim SH, Duffy TS, Jeanloz R, and Shen G (2004) Stability and crystal structure of MgSiO<sub>3</sub> perovskite to the core–mantle boundary. *Geophysical Research Letters* 31: L10603. <http://dx.doi.org/10.1029/2004GL019639>.

- Shim SH, Duffy TH, and Shen GY (2001) Stability and structure of  $\text{MgSiO}_3$  perovskite to 2300-kilometer depth in the Earth's mantle. *Science* 293: 2437–2440.
- Shim S-H, Kubo A, and Duffy TS (2007) Raman spectroscopy of perovskite and post-perovskite phases of  $\text{MgGeO}_3$  to 123 GPa. *Earth and Planetary Science Letters* 260: 166–178.
- Sidorin I, Gurnis M, and Helmberger DV (1999) Evidence for a ubiquitous seismic discontinuity at the base of the mantle. *Science* 286: 1326–1331.
- Sidorin I, Gurnis M, Helmberger DV, and Ding X (1998) Interpreting D'' seismic structure using synthetic waveforms computed from dynamic models. *Earth and Planetary Science Letters* 163: 31–41.
- Silver PG and Bina CR (1993) An anomaly in the amplitude ratio of SKKS/SKS in the range 100–108° from portable teleseismic data. *Geophysical Research Letters* 20: 1135–1138.
- Simmons NA, Forte AM, Boschi L, and Grand SP (2010) GyPSuM: A joint tomographic model of mantle density and seismic wave speeds. *Journal of Geophysical Research* 115: B12310. <http://dx.doi.org/10.1029/2010JB007631>.
- Simmons NA, Forte AM, and Grand SP (2007) Thermochemical structure and dynamics of the African superplume. *Geophysical Research Letters* 34: L02301. <http://dx.doi.org/10.1029/2006GL028009>.
- Simmons NA, Forte AM, and Grand SP (2009) Joint seismic, geodynamic and mineral physical constraints on three-dimensional mantle heterogeneity: Implications for the relative importance of thermal versus compositional heterogeneity. *Geophysical Journal International* 177: 1284–1304. <http://dx.doi.org/10.1111/j.1365-246X.2009.04133.x>.
- Simmons NA and Grand SP (2002) Partial melting in the deepest mantle. *Geophysical Research Letters* 29. <http://dx.doi.org/10.1029/2001GL013716>.
- Simmons NA, Myers SC, and Johannesson G (2011) Global-scale P wave tomography optimized for prediction of teleseismic and regional travel times for Middle East events: 2. Tomographic inversion. *Journal of Geophysical Research* 116: B04305. <http://dx.doi.org/10.1029/2010JB007969>.
- Simmons NA, Myers SC, Johannesson G, and Matzel E (2012) LLNL-G3Dv3: Global P wave tomography model for improved regional and teleseismic travel time prediction. *Journal of Geophysical Research* 117: B10302. <http://dx.doi.org/10.1029/2012JB009525>.
- Sinmyo R, Hirose K, Muto S, Ohishi Y, and Yasuhara A (2011) The valence state and partitioning of iron in the Earth's lowermost mantle. *Journal of Geophysical Research* 116: B07205. <http://dx.doi.org/10.1029/2010JB008179>.
- Sinmyo R, Hirose K, Nishio-Hamane D, et al. (2008) Partitioning of iron between perovskite/post-perovskite and ferropericlase in the lower mantle. *Journal of Geophysical Research* 113: B11204. <http://dx.doi.org/10.1029/2008JB005730>.
- Sinmyo R, Hirose K, O'Neill HSC, and Okunishi E (2006) Ferric iron in Al-bearing post-perovskite. *Geophysical Research Letters* 33: L12S13. <http://dx.doi.org/10.1029/2006GL025858>.
- Sinmyo R, Ozawa H, Hirose K, et al. (2008) Ferric iron content in  $(\text{Mg}, \text{Fe})\text{SiO}_3$  perovskite and post-perovskite at deep lower mantle conditions. *American Mineralogist* 93: 1899–1902.
- Sleep NH (1988) Gradual entrainment of a chemical layer at the base of the mantle by overlying convection. *Geophysical Journal* 95: 437–447.
- Soldati G, Boschi L, and Forte AM (2012) Tomography of core–mantle boundary and lowermost mantle coupled by geodynamics. *Geophysical Journal International* 189: 730–746. <http://dx.doi.org/10.1111/j.1365-246X.2012.05413.x>.
- Spera FJ, Yuen DA, and Giles G (2006) Tradeoffs in chemical and thermal variations in the post-perovskite phase transition: Mixed phase regions in the deep lower mantle? *Physics of the Earth and Planetary Interiors* 159: 234–246. <http://dx.doi.org/10.1016/j.pepi.2006.07.007>.
- Speziale S, Lee VE, Clark SM, Lin JF, Pasternak MP, and Jeanloz R (2007) Effects of Fe spin transition on the elasticity of  $(\text{Mg}, \text{Fe})\text{O}$  magnesiowüstites and implications for the seismological properties of the Earth's lower mantle. *Journal of Geophysical Research* 112: B10212. <http://dx.doi.org/10.1029/2006JB004730>.
- Speziale S, Milner A, Lee VE, Clark SM, Pasternak MP, and Jeanloz R (2005) Iron spin transition in Earth's mantle. *Proceedings of the National Academy of Sciences of the United States of America* 102(50): 17918–17922.
- Speziale S, Zha C-S, Duffy TS, Hemley RJ, Mao HK, and Jeanloz R (2007) Quasihydrostatic compression of magnesium oxide to 52 GPa: Implications for the pressure–volume–temperature equation of state. *Journal of Geophysical Research* 106: 515–528.
- Sreenivasan B and Gubbins D (2011) On mantle-induced heat flow variations at the inner core boundary. *Physics of the Earth and Planetary Interiors* 187: 336–341.
- Stacey FD and Loper DE (1983) The thermal boundary layer interpretation of D'' and its role as a plume source. *Physics of the Earth and Planetary Interiors* 33: 45–55.
- Stackhouse S and Brodholt JP (2007) High-temperature elasticity of  $\text{MgSiO}_3$  post-perovskite. In: Hirose K, Brodholt JP, Lay T, and Yuen D (eds.) *Post-perovskite: The Last Mantle Phase Transition*, pp. 99–113. Washington, DC: American Geophysical Union.
- Stackhouse S, Brodholt J, Dobson D, and Price GD (2006) Electronic spin transitions and the seismic properties of ferrous iron-bearing  $\text{MgSiO}_3$  post-perovskite. *Geophysical Research Letters* 33: L12S03. <http://dx.doi.org/10.1029/2005GL025589>.
- Stackhouse S, Brodholt JP, and Price GD (2005) High temperature elastic anisotropy of the perovskite and post-perovskite polymorphs of  $\text{Al}_2\text{O}_3$ . *Geophysical Research Letters* 32: L132305. <http://dx.doi.org/10.1029/2005GL0223163>.
- Stackhouse S, Brodholt JP, and Price GD (2006) Elastic anisotropy of  $\text{FeSiO}_3$  end-members of the perovskite and post-perovskite phases. *Geophysical Research Letters* 33: L01304. <http://dx.doi.org/10.1029/2006GL023887>.
- Stackhouse S, Brodholt J, and Price GD (2007) Electronic spin transitions in iron-bearing  $\text{MgSiO}_3$  perovskite. *Earth and Planetary Science Letters* 253(1–2): 282–290. <http://dx.doi.org/10.1016/j.epsl.2006.10.035>.
- Stackhouse S, Brodholt JP, Price GD, Wooley J, and Kendall JM (2005) The effect of temperature on the acoustic anisotropy of the perovskite and post-perovskite polymorphs of  $\text{MgSiO}_3$ . *Earth and Planetary Science Letters* 230: 1–10.
- Stackhouse S, Stixrude L, and Karki BB (2010) Thermal conductivity of periclase ( $\text{MgO}$ ) from first principles. *Physical Review Letters* 104: 208501.
- Steinberger B and Torsvik T (2012) A geodynamic model of plumes from the margins of large low shear velocity provinces. *Geochemistry, Geophysics, Geosystems* 13: Q01W09.
- Stixrude L (1998) Elastic constants and anisotropy of  $\text{MgSiO}_3$  perovskite, periclase, and  $\text{SiO}_2$  at high pressure. In: Gurnis M, Wyession ME, Knittle E, and Buffett BA (eds.) *The Core–Mantle Boundary Region*, pp. 83–86. Washington, DC: American Geophysical Union.
- Stixrude L, de Koker N, Sun N, Mookherjee M, and Karki BB (2009) Thermodynamics of silicate liquids in the deep Earth. *Earth and Planetary Science Letters* 278: 226–232.
- Stixrude L, Lithgow-Bertelloni C, Kiefer B, and Fumagalli P (2007) Phase stability and shear softening in  $\text{CaSiO}_3$  perovskite at high pressure. *Physical Review B* 75: 024108.
- Stolten S and Tronnes RG (2007) The perovskite to post-perovskite transition in  $\text{CaIrO}_3$ : Clapeyron slope and changes in bulk and shear moduli by density functional theory. *Physics of the Earth and Planetary Interiors* 164: 50–62.
- Sturhahn W, Jackson JM, and Lin J-F (2005) The spin state of iron in minerals in Earth's lower mantle. *Geophysical Research Letters* 32: L12307. <http://dx.doi.org/10.1029/2005GL022802>.
- Stutzmann E, Vinnik L, Ferreira A, and Singh S (2000) Constraint on the S-wave velocity at the base of the mantle. *Geophysical Research Letters* 27: 1571–1574.
- Styles E, Goes S, van Keken PE, Ritsema J, and Smith H (2011) Synthetic images of dynamically predicted plumes and comparison with a global tomographic model. *Earth and Planetary Science Letters* 311: 351–363.
- Su WJ and Dziewonski AM (1997) Simultaneous inversion for 3-D variations in shear and bulk velocity in the mantle. *Physics of the Earth and Planetary Interiors* 100: 135–156.
- Su W, Woodward RL, and Dziewonski AM (1994) Degree 12 model of shear velocity heterogeneity in the mantle. *Journal of Geophysical Research* 99: 6945–6980.
- Sueda Y, Irfune T, Yamada A, Inoue T, Liu X, and K-I Funakoshi (2006) The phase boundary between  $\text{CaSiO}_3$  perovskite and  $\text{Ca}_2\text{SiO}_4 + \text{CaSi}_2\text{O}_5$  determined by in situ x-ray observations. *Geophysical Research Letters* 33: L10307. <http://dx.doi.org/10.1029/2006GL025772>.
- Sumita I and Olson P (2000) Thermal convection experiments in a rapidly rotating hemispherical shell. *Science* 286: 1547–1549.
- Sun D and Helmberger D (2008) Lower mantle tomography and phase change mapping. *Journal of Geophysical Research* 113: B10305. <http://dx.doi.org/10.1029/2007JB005289>.
- Sun D, Helmberger D, and Gurnis M (2010) A narrow, mid-mantle plume below southern Africa. *Geophysical Research Letters* 37: L09302. <http://dx.doi.org/10.1029/2009GL042339>.
- Sun D, Helmberger D, Ni S, and Bower D (2009) Direct measures of lateral velocity variation in the deep Earth. *Journal of Geophysical Research* 114: B05303. <http://dx.doi.org/10.1029/2008JB005873>.
- Sun D, Song AT-R, and Helmberger D (2006) Complexity of D'' in the presence of slab-debris and phase changes. *Geophysical Research Letters* 33: L12S07. <http://dx.doi.org/10.1029/2005GL025384>.
- Sun D, Song X, Zheng S, and Helmberger DV (2007) Evidence for a chemical-thermal structure at base of mantle from sharp lateral P-wave variations beneath Central America. *Proceedings of the National Academy of Sciences of the United States of America* 104: 26–30.
- Sun D, Tan E, Helmberger DV, and Gurnis M (2007) Seismological support for the metastable superplume model, sharp features, and phase changes within the lower

- mantle. *Proceedings of the National Academy of Sciences of the United States of America* 104: 9151–9155.
- Sze EKM and van der Hilst RD (2003) Core mantle boundary topography from short period  $PcP$ ,  $PKP$ , and  $PKKP$  data. *Physics of the Earth and Planetary Interiors* 135: 27–46.
- Tackley PJ (1998) Three-dimensional simulations of mantle convection with a thermochemical basal boundary layer: D''? In: Gurnis M, Wysession ME, Knittle E, and Buffett BA (eds.) *The Core–Mantle Boundary Region*, pp. 231–253. Washington, DC: American Geophysical Union.
- Tackley PJ (2012) Dynamics and evolution of the deep mantle resulting from thermal, chemical, phase and melting effects. *Earth-Science Reviews* 110: 1–25.
- Tackley PJ, Nakagawa T, and Hernlund JW (2007) Influence of the post-perovskite transition on thermal and thermo-chemical mantle convection. *Post-Perovskite: The Last Mantle Phase Transition, Geophysical Monograph Series*, vol. 174, 229–247.
- Takahashi F, Tsunakawa H, Matsushima M, Mochizuki N, and Honkura Y (2008) Effects of thermally heterogeneous structure in the lowermost mantle on the geomagnetic field strength. *Earth and Planetary Science Letters* 272: 738–746.
- Takei Y and Suetsugu D (1989) A high velocity zone in the lower mantle under the Japan subduction zone inferred from precise measurements of P-wave arrival times. *Journal of Physics of the Earth* 37: 225–231.
- Takeuchi N (2007) Whole mantle SH velocity model constrained by waveform inversion based on three-dimensional Born kernels. *Geophysical Journal International* 169: 1153–1163.
- Takeuchi N (2009) A low-velocity conduit throughout the mantle in the robust component of a tomography model. *Geophysical Research Letters* 36: L07306. <http://dx.doi.org/10.1029/2009GL037590>.
- Takeuchi N (2012) Detection of ridge-like structures in the Pacific Large Low-Shear-Velocity Province. *Earth and Planetary Science Letters* 319–310: 55–64.
- Takeuchi N, Morita Y, Xuyen ND, and Zung NQ (2008) Extent of the low-velocity region in the lowermost mantle beneath the western Pacific detected by the Vietnamese Broadband Seismograph Array. *Geophysical Research Letters* 35: L05307. <http://dx.doi.org/10.1029/2008GL033197>.
- Takeuchi N and Obara K (2010) Fine-scale topography on the D'' discontinuity and its correlation to volumetric velocity fluctuations. *Physics of the Earth and Planetary Interiors* 183: 126–135.
- Tan E and Gurnis M (2005) Metastable superplumes and mantle compressibility. *Geophysical Research Letters* 32: L20307. <http://dx.doi.org/10.1029/2005GL024190>.
- Tan E and Gurnis M (2007) Compressible thermochemical convection and application to lower mantle structures. *Journal of Geophysical Research* 112: B06304. <http://dx.doi.org/10.1029/2006JB004505>.
- Tan E, Leng W, and Zhong S (2011) On the location of plumes and lateral movement of thermochemical structures with high bulk modulus in the 3-d compressible mantle. *Geochemistry, Geophysics, Geosystems* 12: Q07005.
- Tanaka S (2002) Very low shear wave velocity at the base of the mantle under the South Pacific superswell. *Earth and Planetary Science Letters* 203: 879–893.
- Tanaka S (2010) Constraints on the core–mantle boundary topography from P4KP-PcP differential travel times. *Journal of Geophysical Research* 115: B04310. <http://dx.doi.org/10.1029/2009JB006563>.
- Tanaka S, Suetsugu D, Shiobara H, et al. (2009) On the vertical extent of the large low shear velocity province beneath the South Pacific Superswell. *Geophysical Research Letters* 36: L07305. <http://dx.doi.org/10.1029/2009GL037568>.
- Tange Y, Kuwayama Y, Irfune T, Funakoshi K-i, and Ohishi Y (2012)  $P$ – $V$ – $T$  equation of state of  $MgSiO_3$  perovskite based on the  $MgO$  pressure scale: A comprehensive reference for mineralogy of the lower mantle. *Journal of Geophysical Research* 117: B06201. <http://dx.doi.org/10.1029/2011JB008988>.
- Tange Y, Takahashi E, Nishihara Y, Funakoshi K, and Sata N (2009) Phase relations in the system  $MgO$ – $FeO$ – $SiO_2$  to 50 GPa and 2000 °C: An application of experimental techniques using multianvil apparatus with sintered diamond anvils. *Journal of Geophysical Research* 114: B02214. <http://dx.doi.org/10.1029/2008JB005891>.
- Tarits P and Mandéa M (2010) The heterogeneous electrical conductivity structure of the lower mantle. *Physics of the Earth and Planetary Interiors* 183: 115–125.
- Tateno S, Hirose K, Sata N, and Ohishi Y (2005) Phase relations in  $Mg_3Al_2Si_3O_{12}$  to 180 GPa: Effect of Al on post-perovskite phase transition. *Geophysical Research Letters* 32: L15306. <http://dx.doi.org/10.1029/2005GL023309>.
- Tateno S, Hirose K, Sata N, and Ohishi Y (2006) High-pressure behavior of  $MnGeO_3$  and  $CdGeO_3$  and the post-perovskite phase transition. *Physical Chemistry of Minerals* 32: 721–725.
- Tateno S, Hirose K, Sata N, and Ohishi Y (2007) Solubility of  $FeO$  in  $(Mg,Fe)SiO_3$  perovskite and the post-perovskite phase transition. *Physics of the Earth and Planetary Interiors* 160: 319–325.
- Tateno S, Hirose K, Sata N, and Ohishi Y (2009) Determination of post-perovskite phase transition boundary up to 4400 K and implications for thermal structure in D'' layer. *Earth and Planetary Science Letters* 277: 130–136.
- Tateno S, Hirose K, Sata N, and Ohishi Y (2010) Structural distortion of  $CaSnO_3$  perovskite under pressure and the quenchable post-perovskite phase as a low pressure analogue to  $MgSiO_3$ . *Physics of the Earth and Planetary Interiors* 181: 54–59.
- Terasaki H, Frost DJ, Rubie DC, and Langenhorst F (2007) Interconnectivity of Fe–O–S liquid in polycrystalline silicate perovskite at lower mantle conditions. *Physics of the Earth and Planetary Interiors* 161: 170–176.
- Thomas C, Garnero EJ, and Lay T (2004a) High-resolution image of lowermost mantle structure under the Cocos Plate. *Journal of Geophysical Research* 109: B08307. <http://dx.doi.org/10.1029/2004JB003013>.
- Thomas C, Kendall J-M, and Lowman J (2004b) Lower-mantle seismic discontinuities and the thermal morphology of subducted slabs. *Earth and Planetary Science Letters* 225: 105–113.
- Thomas C, Heesom T, and Kendall JM (2002) Investigating the heterogeneity of the D'' region beneath the northern Pacific using a seismic array. *Journal of Geophysical Research* 107(B11): 2274. <http://dx.doi.org/10.1029/2000JB000021>.
- Thomas C and Kendall JM (2002) The lowermost mantle beneath northern Asia: (2) Evidence for D'' anisotropy. *Geophysical Journal International* 151: 296–308.
- Thomas C, Kendall J-M, and Helffrich G (2009) Probing two low-velocity regions with  $PKP$  b-caustic amplitudes and scattering. *Geophysical Journal International* 178: 503–512.
- Thomas CW, Liu Q, Agee CB, Asimow PD, and Lange RA (2012) Multi-technique equation of state for  $Fe_2SiO_4$  melt and the density of Fe-bearing silicate melts from 0 to 161 GPa. *Journal of Geophysical Research* 117: B10206. <http://dx.doi.org/10.1029/2012JB009403>.
- Thomas C and Weber M (1997) P velocity heterogeneities in the lower mantle determined with the German Regional Seismic Network: Improvement of previous models and results of 2D modeling. *Physics of the Earth and Planetary Interiors* 101: 105–117.
- Thomas C, Weber M, Agnon A, and Hofstetter A (1998) A low velocity lamella in D''. *Geophysical Research Letters* 25: 2885–2888.
- Thomas C, Weber M, Wicks CW, and Scherbaum F (1999) Small scatterers in the lower mantle observed at German broadband arrays. *Journal of Geophysical Research* 104: 15073–15088.
- Thomas C, Wooley J, Brodholt J, and Fieseler T (2011) Anisotropy as cause for polarity reversals of D'' reflections. *Earth and Planetary Science Letters* 307: 369–376.
- Thomas C, Wooley J, and Simpson M (2007) D'' anisotropy beneath Southeast Asia. *Geophysical Research Letters* 34: L04301. <http://dx.doi.org/10.1029/2006GL028965>.
- Thorne MS and Garnero EJ (2004) Inferences on ultralow-velocity zone structure from a global analysis of SPdKS waves. *Journal of Geophysical Research* 109: B08301. <http://dx.doi.org/10.1029/2004JB003010>.
- Thorne MS, Garnero EJ, and Grand SP (2004) Geographic correlation between hot spots and deep mantle lateral shear-wave velocity gradients. *Physics of the Earth and Planetary Interiors* 146: 47–63.
- Thorne MS, Garnero EJ, Jahnke G, Igel H, and McNamara AK (2013) Mega ultra low velocity zone and mantle flow. *Earth and Planetary Science Letters* 364: 59–67. <http://dx.doi.org/10.1016/j.epsl.2012.12.034>.
- Thorne MS, Lay T, Garnero EJ, Jahnke G, and Igel H (2007) Seismic imaging of the laterally varying D'' region beneath the Cocos Plate. *Geophysical Journal International* 170: 635–648. <http://dx.doi.org/10.1111/j.1365-246X.2006.03279.x>.
- Tibuleac IM and Herrin E (1999) Lower mantle lateral heterogeneity beneath the Caribbean Sea. *Science* 285: 1711–1715.
- Tilman FJ, McKenzie D, and Priesley KF (1998) P and S-wave scattering from mantle plumes. *Journal of Geophysical Research* 103: 21145–21163.
- Tkalcic H and Romanowicz B (2002) Short scale heterogeneity in the lowermost mantle: Insights form  $PcP$ -P and  $Scs$ -S data. *Earth and Planetary Science Letters* 201: 57–68.
- To A, Fukao Y, and Tsuboi S (2011) Evidence for a thick and localized ultra low shear velocity zone at the base of the mantle beneath the central Pacific. *Physics of the Earth and Planetary Interiors* 184: 119–133.
- To A and Romanowicz B (2009) Finite frequency effects on global S diffracted traveltimes. *Geophysical Journal International* 179: 1645–1657. <http://dx.doi.org/10.1111/j.1365-246X.2009.04359.x>.
- To A, Romanowicz B, Capdeville Y, and Takeuchi N (2005) 3D effects of sharp boundaries at the borders of the African and Pacific Superplumes: Observation and modeling. *Earth and Planetary Science Letters* 233: 237–253.
- Toksöz MN, Minear JW, and Julian BR (1971) Temperature field and geophysical effects of a downgoing slab. *Journal of Geophysical Research* 76: 1113–1138.
- Torsvik TH, Smethurst MA, Burke K, and Steinberger B (2006) Large Igneous Provinces generated from the margins of the large low-velocity provinces in the deep mantle. *Geophysical Journal International* 167: 1447–1460. <http://dx.doi.org/10.1111/j.1365-246X.2006.03158.x>.

- Torsvik T, Smethurst MA, Burke K, and Steinberger B (2008) Long term stability in deep mantle structure: Evidence from the 300 Ma Skagerrak-Centered Large Igneous Province (the SCLIP). *Earth and Planetary Science Letters* 267: 444–452.
- Tosi N, Čadek O, Martinec Z, Yuen DA, and Kaufmann G (2009) Is the long-wavelength geoid sensitive to the presence of post-perovskite above the core–mantle boundary? *Geophysical Research Letters* 36: L05303. <http://dx.doi.org/10.1029/2008GL036902>.
- Tosi N, Yuen DA, and Čadek O (2010) Dynamical consequences in the lower mantle with the post-perovskite phase change and strongly depth-dependent thermodynamic and transport properties. *Earth and Planetary Science Letters* 298: 229–243.
- Trampert J, Deschamps F, Resovsky J, and Yuen D (2004) Probabilistic tomography maps chemical heterogeneities throughout the lower mantle. *Science* 306: 853–856.
- Trønnes RG (2009) Structure, mineralogy and dynamics of the lowermost mantle. *Mineralogy and Petrology*, <http://dx.doi.org/10.1007/s00710-009-0068-z>.
- Tschauner O, Kiefer B, Liu H, Sinogeikin S, Somayazulu M, and Luo S-N (2008) Possible structural polymorphism in Al-bearing magnesium silicate post-perovskite. *American Mineralogist* 93: 533–539.
- Tsuchiya T (2011) Elasticity of subducted basaltic crust at the lower mantle pressures: Insights on the nature of deep mantle heterogeneity. *Physics of the Earth and Planetary Interiors* 188: 142–149.
- Tsuchiya T and Tsuchiya J (2006) Effect of impurity on the elasticity of perovskite and post-perovskite: Velocity contrast across the post-perovskite transition in (Mg,Fe,Al)(Si,Al)O<sub>3</sub>. *Geophysical Research Letters* 33: L12S04. <http://dx.doi.org/10.1029/2006GL025706>.
- Tsuchiya T and Tsuchiya J (2007) High-pressure–high-temperature phase relations of MgGeO<sub>3</sub>: First-principles calculations. *Physical Review B* 76: 092105. <http://dx.doi.org/10.1103/PhysRevB.76.092105>.
- Tsuchiya J and Tsuchiya T (2008) Postperovskite phase equilibria in the MgSiO<sub>3</sub>–Al<sub>2</sub>O<sub>3</sub> system. *Proceedings of the National Academy of Sciences of the United States of America* 105: 19160–19164.
- Tsuchiya T, Tsuchiya J, Umemoto K, and Wentzcovitch RM (2004a) Phase transition in MgSiO<sub>3</sub> perovskite in the Earth's lower mantle. *Earth and Planetary Science Letters* 224: 241–248.
- Tsuchiya T, Tsuchiya J, Umemoto K, and Wentzcovitch RM (2004b) Elasticity of post-perovskite MgSiO<sub>3</sub>. *Geophysical Research Letters* 31: L14603. <http://dx.doi.org/10.1029/2004GL020278>.
- Tsuchiya T, Wentzcovitch RM, da Silva CRS, and de Gironcoli S (2006) Spin transition in magnesiowüstite in Earth's lower mantle. *Physical Review Letters* 96(19): 198501–198504. <http://dx.doi.org/10.1103/PhysRevLett.96.198501>.
- Tsuchiya T, Wentzcovitch RM, da Silva CRS, de Gironcoli S, and Tsuchiya J (2006) Pressure induced high spin to low spin transition in magnesiowüstite. *Physica Status Solidi* 243(9): 2111–2116. <http://dx.doi.org/10.1002/pssb.200666814>.
- Tsujino N and Nishihara Y (2010) Effect of pressure on grain-growth kinetics of ferropericlase to lower mantle conditions. *Geophysical Research Letters* 37: L14304. <http://dx.doi.org/10.1029/2010GL043491>.
- Uhrhammer R (1978) S-wave travel times for a spherically averaged earth. *Geophysical Journal of the Royal Astronomical Society* 55: 283–309.
- Umemoto K, Hsu H, and Wentzcovitch RM (2010) Effect of site degeneracies on the spin crossovers in (Mg,Fe)SiO<sub>3</sub> perovskite. *Physics of the Earth and Planetary Interiors* 180: 209–214.
- Umemoto K, Wentzcovitch RM, Weidner DJ, and Parise JB (2006) NaMgF<sub>3</sub>: A low-pressure analog of MgSiO<sub>3</sub>. *Geophysical Research Letters* 33: L15304. <http://dx.doi.org/10.1029/2006GL026348>.
- Umemoto K, Wentzcovitch RM, Yu YG, and Requist R (2008) Spin transition in (Mg,Fe)SiO<sub>3</sub> perovskite under pressure. *Earth and Planetary Science Letters* 276(1–2): 198–206.
- Usui Y, Hiramatsu Y, Furumoto M, and Kanao M (2005) Thick and anisotropic D'' layer beneath Antarctic Ocean. *Geophysical Research Letters* 32: L13311. <http://dx.doi.org/10.1029/2005GL022622>.
- Usui Y, Hiramatsu Y, Furumoto M, and Kanao M (2008) Evidence of seismic anisotropy and a lower temperature condition in the D'' layer beneath Pacific Antarctic Ridge in the Antarctic Ocean. *Physics of the Earth and Planetary Interiors* 167: 205–216.
- Usui Y, Tsuchiya J, and Tsuchiya T (2010) Elastic, vibrational, and thermodynamic properties of MgGeO<sub>3</sub> postperovskite investigated by first principles simulation. *Journal of Geophysical Research* 115: B03201. <http://dx.doi.org/10.1029/2009JB006468>.
- Valenzuela R and Wysession ME (1998) Illuminating the base of the mantle with core-diffracted waves. In: Gurnis M, Wysession ME, Knittle E, and Buffett BA (eds.) *The Core–Mantle Boundary Region*, pp. 57–72. Washington, DC: American Geophysical Union.
- van den Berg AP, de Hoop MV, Yuen DA, Duchkov A, van der Hilst RD, and Jacobs MGH (2010) Geodynamical modeling and multiscale seismic expression of thermo-chemical heterogeneity and phase transitions in the lowermost mantle. *Physics of the Earth and Planetary Interiors* 180: 244–257. <http://dx.doi.org/10.1016/j.pepi.2010.02.008>.
- van der Hilst RD, de Hoop MV, Wang P, Shim SH, Ma P, and Tenorio L (2007) Seismostratigraphy and thermal structure of Earth's core–mantle boundary region. *Science* 315: 1813–1817.
- van der Hilst RD and Kárasoň H (1999) Compositional heterogeneity in the bottom 1000 kilometers of Earth's mantle: Toward a hybrid convection model. *Science* 283: 1885–1888.
- van der Hilst RD, Widjiantoro S, and Engdahl ER (1997) Evidence for deep mantle circulation from global tomography. *Nature* 386: 578–584.
- Vanacore E, Niu F, and Kawakatsu H (2006) Observations of the mid-mantle discontinuity beneath Indonesia from S to P converted waveforms. *Geophysical Research Letters* 33: L04302. <http://dx.doi.org/10.1029/2005GL025106>.
- Vanpeteghem CB, Angel RJ, Ross N, et al. (2006) Al, Fe substitution in the MgSiO<sub>3</sub> perovskite structure: A single-crystal x-ray diffraction study. *Physics of the Earth and Planetary Interiors* 155(1–2): 96–103.
- Vanpeteghem CB, Zhao J, Angle RJ, Ross NL, and Bolfan-Casanova N (2006) Crystal structure and equation of state of MgSiO<sub>3</sub> perovskite. *Geophysical Research Letters* 33: L03306. <http://dx.doi.org/10.1029/2005GL024955>.
- Vasco DW and Johnson LR (1998) Whole Earth structure estimated from seismic arrival times. *Journal of Geophysical Research* 103: 2633–2671.
- Velimsky J (2010) Electrical conductivity in the lower mantle: Constraints from CHAMP satellite data by time-domain EM induction modeling. *Physics of the Earth and Planetary Interiors* 180: 111–117.
- Velimsky J, Benesova N, and Cizkova H (2012) On the detectability of 3-D postperovskite distribution in D'' by electromagnetic induction. *Physics of the Earth and Planetary Interiors* 202–203: 71–77.
- Vidale JE and Hedlin MAH (1998) Evidence for partial melt at the core–mantle boundary north of Tonga from the strong scattering of seismic waves. *Nature* 391: 628–684.
- Vinnik LP, Breger L, and Romanowicz B (1998) Anisotropic structure at the base of the Earth's mantle. *Nature* 393: 564–567.
- Vinnik LP, Farra V, and Romanowicz B (1989) Observational evidence for diffracted SV in the shadow of the Earth's core. *Geophysical Research Letters* 16: 519–522.
- Vinnik LP, Niu F, and Kawakatsu H (1998) Broadband converted phases from midmantle discontinuities. *Earth, Planets and Space* 50: 987–997.
- Vinnik LP, Oreshin SI, Speziale S, and Weber M (2010) Mid-mantle layering from SKS receiver functions. *Geophysical Research Letters* 37: L24302. <http://dx.doi.org/10.1029/2010GL045323>.
- Vinnik LP, Romanowicz B, LeStunff Y, and Makeyeva L (1995) Seismic anisotropy in the D'' layer. *Geophysical Research Letters* 22: 1657–1660.
- Walker AM, Forte AM, Wooley J, Nowacki A, and Kendall J-M (2011) Elastic anisotropy of D'' predicted from global models of mantle flow. *Geochemistry, Geophysics, Geosystems* 12. <http://dx.doi.org/10.1029/2011GC003732>.
- Walte N, Heidelbach F, Miyajima N, and Frost D (2007) Texture development and TEM analysis of deformed CaIrO<sub>3</sub>: Implications for the D'' layer at the core–mantle boundary. *Geophysical Research Letters* 34: L08306. <http://dx.doi.org/10.1029/2007GL029407>.
- Walte NP, Heidelbach F, Miyajima N, Frost DJ, Rubie DC, and Dobson DP (2009) Transformation textures in post-perovskite: Understanding mantle flow in the D'' layer of the Earth. *Geophysical Research Letters* 36: L04302. <http://dx.doi.org/10.1029/2008GL036840>.
- Wang P, De Hoop MV, and van der Hilst RD (2008) Imaging of the lowermost mantle (D'') and the core–mantle boundary with SKKS coda waves. *Geophysical Journal International* 175: 103–115. <http://dx.doi.org/10.1111/j.1365-246X.2008.03861.x>.
- Wang P, De Hoop MV, van der Hilst RD, Ma P, and Tenorio L (2006) Imaging of structure at and near the core–mantle boundary using a generalized radon transform: 1. Construction of image gathers. *Journal of Geophysical Research* 111: B12304.
- Wang F, Tange Y, Irfune T, and Funakoshi K-i (2012) P–V–T equation of state of stishovite up to mid-lower mantle conditions. *Journal of Geophysical Research* 117: B06209. <http://dx.doi.org/10.1029/2011JB009100>.
- Wang Y and Wen L (2004) Mapping the geometry and geographic distribution of a very low velocity province at the base of the Earth's mantle. *Journal of Geophysical Research* 109: B10305. <http://dx.doi.org/10.1029/2003JB002674>.
- Wang Y and Wen L (2007a) Geometry and P and S velocity structures of the “African Anomaly” *Journal of Geophysical Research* 112: B05313. <http://dx.doi.org/10.1029/2006JB004483>.
- Wang Y and Wen L (2007b) Complex seismic anisotropy at the border of a very low velocity province at the base of the Earth's mantle. *Journal of Geophysical Research* 112: B09305. <http://dx.doi.org/10.1029/2006JB004719>.

- Weber M (1993) P and S-wave reflections from anomalies in the lowermost mantle. *Geophysical Journal International* 115: 183–210.
- Weber M (1994) Lamellae in D''? An alternative model for lower mantle anomalies. *Geophysical Research Letters* 21: 2531–2534.
- Weber M and Davis JP (1990) Evidence of a laterally variable lower mantle structure from P and S-waves. *Geophysical Journal International* 102: 231–255.
- Wen L (2000) Intense seismic scattering near the Earth's core–mantle boundary beneath the Comoros hotspot. *Geophysical Research Letters* 27: 3627–3630.
- Wen L (2001) Seismic evidence for a rapidly-varying compositional anomaly at the base of the Earth's mantle beneath Indian ocean. *Earth and Planetary Science Letters* 194: 83–95.
- Wen L (2006) A compositional anomaly at the Earth's core–mantle boundary as an anchor to the relatively slowly moving surface hotspots and as source to the DUPAL anomaly. *Earth and Planetary Science Letters* 246: 138–148.
- Wen L and Helmberger DV (1998) Ultra-low velocity zones near the core–mantle boundary from broadband PKP precursors. *Science* 279: 1701–1703.
- Wen L, Silver P, James D, and Kuehnel R (2001) Seismic evidence for a thermochemical boundary layer at the base of the Earth's mantle. *Earth and Planetary Science Letters* 189: 141–153.
- Wenk H-R, Cottaar S, Tomé CN, McNamara A, and Romanowicz B (2011) Deformation in the lowermost mantle: From polycrystal plasticity to seismic anisotropy. *Earth and Planetary Science Letters* 306: 33–45.
- Wentzcovitch RM, Fusto J, Wu Z, da Silva C, Yuen D, and Kohlstedt D (2009) Anomalous compressibility of ferropericlase throughout the iron spin crossover. *Proceedings of the National Academy of Sciences of the United States of America* 106: 8447–8452.
- Wentzcovitch RM, Karki BB, Cococcioni M, and de Gironcoli S (2004) Thermoelastic properties of  $MgSiO_3$ -perovskite: Insights on the nature of the Earth's lower mantle. *Physical Review Letters* 92: 018501-1–018501-4.
- Wentzcovitch RM, Tsuchiya T, and Tsuchiya J (2006)  $MgSiO_3$  postperovskite at D'' conditions. *Proceedings of the National Academy of Sciences of the United States of America* 103: 543–546.
- Wicks JK, Jackson JM, and Sturhahn W (2010) Very low sound velocities in iron-rich ( $Mg,Fe$ )O: Implications for the core–mantle boundary region. *Geophysical Research Letters* 37: L15304. <http://dx.doi.org/10.1029/2010GL043689>.
- Widjiantoro S and van der Hilst RD (1996) Mantle structure beneath Indonesia inferred from high-resolution tomographic imaging. *Geophysical Journal International* 130: 167–182.
- Widmer R, Masters G, and Gilbert F (1991) Spherically symmetric attenuation within the Earth from normal mode data. *Geophysical Journal International* 104: 541–553.
- Williams Q (1998) The temperature contrast across D''. In: Gurnis M, Wysession ME, Knittle E, and Buffett BA (eds.) *The Core–Mantle Boundary Region*, pp. 73–81. Washington, DC: American Geophysical Union.
- Williams Q and Garnero EJ (1996) Seismic evidence for partial melt at the base of the Earth's mantle. *Science* 273: 1528–1530.
- Williams Q, Revenaugh J, and Garnero EJ (1998) A correlation between ultra-low basal velocities in the mantle and hot spots. *Science* 281: 564–569.
- Willis AP, Sreenivasan B, and Gubbins D (2007) Thermal core–mantle interaction: Exploring regimes for 'locked' dynamo action. *Physics of the Earth and Planetary Interiors* 165: 83–92.
- Wookey J and Kendall J-M (2007) Seismic anisotropy of post-perovskite and the lowermost mantle. In: Hirose K, Brodholt J, Lay T, and Yuen D (eds.) *Post-Perovskite: The Last Mantle Phase Transition*. *Geophysical Monograph Series*, vol. 174, pp. 171–189. Washington, DC: AGU, 984.
- Wookey J and Kendall J-M (2008) Constraints on lowermost mantle mineralogy and fabric beneath Siberia from seismic anisotropy. *Earth and Planetary Science Letters* 275: 32–42. <http://dx.doi.org/10.1016/j.epsl.2008.07.049>.
- Wookey J, Kendall J-M, and Rümpker G (2005) Lowermost mantle anisotropy beneath the north Pacific from differential S-ScS splitting. *Geophysical Journal International* 161: 829–838.
- Wookey J, Stackhouse S, Kendall J-M, Brodholt J, and Price GD (2005) Efficacy of the post-perovskite phase as an explanation for lowermost-mantle seismic properties. *Nature* 438: 1004–1007.
- Wright C and Kuo B-Y (2007) The P-wavespeed structure in the lowermost 700 km of the mantle below the central part of the Indian Ocean. *Physics of the Earth and Planetary Interiors* 161: 243–266.
- Wright C and Lyons JA (1975) Seismology,  $dT/dA$  and deep mantle convection. *Geophysical Journal of the Royal Astronomical Society* 40: 115–138.
- Wright C, Muirhead KJ, and Dixon AE (1985) The P-wave velocity structure near the base of the mantle. *Journal of Geophysical Research* 90: 623–634.
- Wu Z, Justo JF, da Silva CRS, de Gironcoli S, and Wentzcovitch RM (2009) Anomalous thermodynamic properties in ferropericlase throughout its spin crossover. *Physical Review B* 80: 014409. <http://dx.doi.org/10.1103/PhysRevB.80.014409>.
- Wu W, Ni S, and Zeng X (2012) Evidence for P'P' asymmetrical scattering at near nodal distances. *Geophysical Research Letters* 39: L11306. <http://dx.doi.org/10.1029/2012GL052179>.
- Wu X, Qin S, Gu T-T, Yang J, and Manthilake G (2011) Structural and elastic properties of  $CaGeO_3$  perovskite at high pressures. *Physics of the Earth and Planetary Interiors* 189: 151–156.
- Wu Z, Wentzcovitch RM, Umemoto K, Li B, Hirose K, and Zheng J-C (2008) Pressure–volume–temperature relations in MgO: An ultrahigh pressure–temperature scale for planetary sciences applications. *Journal of Geophysical Research* 113: B06204. <http://dx.doi.org/10.1029/2007JB005275>.
- Wysession ME (1996) Large-scale structure at the core–mantle boundary from diffracted waves. *Nature* 382: 244–248.
- Wysession ME, Fischer KM, Al-eqabi GI, Shore PJ, and Gurari I (2001) Using MOMA broadband array SCS-S data to image smaller-scale structures at the base of the mantle. *Geophysical Research Letters* 28: 867–870.
- Wysession ME, Langenhorst A, Fouch MJ, et al. (1999) Lateral variations in compressional/shear velocities at the base of the mantle. *Science* 284: 120–125.
- Wysession M, Lay T, Revenaugh J, et al. (1998) The D'' discontinuity and its implications. In: Gurnis M, Wysession ME, Knittle E, and Buffett BA (eds.) *The Core–Mantle Boundary Region*, pp. 273–298. Washington, DC: American Geophysical Union.
- Wysession ME and Okal EA (1989) Regional analysis of D'' velocities from the ray parameters of diffracted P profiles. *Geophysical Research Letters* 16: 1417–1420.
- Xu Y and Koper KD (2009) Detection of a ULVZ at the base of the mantle beneath the northwest Pacific. *Geophysical Research Letters* 36: L17301. <http://dx.doi.org/10.1029/2009GL039387>.
- Xu J, Yamazaki D, Katsura T, et al. (2011) Silicon and magnesium diffusion in a single crystal of  $MgSiO_3$  perovskite. *Journal of Geophysical Research* 116: B12205. <http://dx.doi.org/10.1029/2011JB008444>.
- Yamada A and Nakanishi I (1998) Short-wavelength lateral variation of a D'' P-wave reflector beneath the southwestern Pacific. *Geophysical Research Letters* 25: 4545–4548.
- Yamanaka T, Hirose K, Mao WL, et al. (2012) Crystal structures of  $(Mg_{1-x}Fe_x)SiO_3$  postperovskite at high pressures. *Proceedings of the National Academy of Sciences of the United States of America* 109: 1035–1040.
- Yamanaka T, Mao WL, Hemley RJ, and Shen G (2010) New structure and spin state of iron rich  $MgFeSiO_3$  post-perovskite. *Journal of Physics: Conference Series* 215: 012100.
- Yamazaki D and Karato S-I (2002) Fabric development in  $(Mg,Fe)$ O during large strain shear deformation: Implications for seismic anisotropy in Earth's lower mantle. *Physics of the Earth and Planetary Interiors* 131: 251–267.
- Yamazaki D and Karato S (2007) Lattice preferred orientation of lower mantle materials and seismic anisotropy in the D'' layer. In: Hirose K, Brodholt J, Lay T, and Yuen D (eds.) *Post-Perovskite: The Last Mantle Phase Transition*. *Geophysical Monograph Series*, vol. 174, pp. 69–78.
- Yamazaki D, Yoshino T, Matsuzaki T, Katsura T, and Yoneda A (2009) Texture of  $(Mg,Fe)SiO_3$  perovskite and ferro-periclase aggregate: Implications for rheology of the lower mantle. *Physics of the Earth and Planetary Interiors* 174: 138–144.
- Yamazaki D, Yoshino T, Ohfuji H, Ando J, and Yoneda A (2006) Origin of seismic anisotropy in the D'' layer inferred from shear deformation experiments on post-perovskite phase. *Earth and Planetary Science Letters* 252: 372–378.
- Yoshida M (2008) Core–mantle boundary topography estimated from numerical simulations of instantaneous flow. *Geochemistry, Geophysics, Geosystems* 9(7): Q07002. <http://dx.doi.org/10.1029/2008GC002008>.
- Yoshino T, Ito E, Katsura T, et al. (2011) Effect of iron content on electrical conductivity of ferropericlase with implications for the spin transition pressure. *Journal of Geophysical Research* 116: B04202. <http://dx.doi.org/10.1029/2010JB007801>.
- Yoshino T and Yamazaki D (2007) Grain growth kinetics of  $CaIrO_3$  perovskite and postperovskite, with implications for rheology of D'' layer. *Earth and Planetary Science Letters* 255: 485–493.
- Young CJ and Lay T (1987a) Evidence for a shear velocity discontinuity in the lower mantle beneath India and the Indian Ocean. *Physics of the Earth and Planetary Interiors* 49: 37–53.
- Young CJ and Lay T (1987b) Comment on "Wave propagation effects and the Earth's structure in the lower mantle". *Geophysical Research Letters* 14: 562–565.
- Young CJ and Lay T (1989) The core shadow zone boundary and lateral variations of the P velocity structure of the lowermost mantle. *Physics of the Earth and Planetary Interiors* 54: 64–81.
- Young CJ and Lay T (1990) Multiple phase analysis of the shear velocity structure in the D'' region beneath Alaska. *Journal of Geophysical Research* 95: 17385–17402.
- Youngs BAR and Houseman GA (2007) Topography on the D'' region from analysis of a thin dense layer beneath a convecting cell. *Physics of the Earth and Planetary Interiors* 160: 60–74.

- Yu YG, Hsu H, Cococcioni M, and Wentzcovitch RM (2012) Spin states and hyperfine interactions of iron incorporated in  $\text{MgSiO}_3$  post-perovskite. *Earth and Planetary Science Letters* 331–332: 1–7.
- Yu YG, Wentzcovitch RM, Tsuchiya T, Umemoto K, and Weidner DJ (2007) First principles investigation of the postspinel transition in  $\text{Mg}_2\text{SiO}_4$ . *Geophysical Research Letters* 34: L10306. <http://dx.doi.org/10.1029/2007GL029462>.
- Yuen DA, Matska C, Cadek O, and Kameyama M (2007) The dynamical influences from physical properties in the lower mantle and post-perovskite phase transition. *Post-Perovskite: The Last Mantle Phase Transition, Geophysics Monograph Series*, 174, pp. 249–270.
- Zhan D (2011) Shearing mechanism of  $\text{MgSiO}_3$  at conditions of the Earth's D'' layer. *Geophysical Research Letters* 38: L16319. <http://dx.doi.org/10.1029/2011GL048203>.
- Zhang L and Fei Y (2008) Melting behavior of (Mg,Fe)O solid solutions at high pressure. *Geophysical Research Letters* 35: L13302. <http://dx.doi.org/10.1029/2008GL034585>.
- Zhang Y and Guo G (2009) Partitioning of Si and O between liquid iron and silicate melt: A two-phase ab-initio molecular dynamics study. *Geophysical Research Letters* 36: L18305. <http://dx.doi.org/10.1029/2009GL039751>.
- Zhang L, Meng Y, and Mao WL (2012) Effect of pressure and composition on lattice parameters and unit-cell volume of (Fe,Mg) $\text{SiO}_3$  post-perovskite. *Earth and Planetary Science Letters* 317–318: 120–125.
- Zhang F and Oganov AR (2006) Valence state and spin transitions of iron in Earth's mantle silicates. *Earth and Planetary Science Letters* 249(3–4): 436–443. <http://dx.doi.org/10.1016/j.epsl.2006.07.023>.
- Zhang FW and Oganov AR (2007) Mechanisms of  $\text{Al}^{3+}$  incorporation in  $\text{MgSiO}_3$  post-perovskite at high pressures. *Earth and Planetary Science Letters* 248: 69–76.
- Zhang Y, Ritsema J, and Thorne MS (2009) Modeling the ratios of SKKS and SKS amplitudes with ultra-low velocity zones at the core–mantle boundary. *Geophysical Research Letters* 36: L19303. <http://dx.doi.org/10.1029/2009GL040030>.
- Zhao D (2001) Seismic structure and origin of hotspots and mantle plumes. *Earth and Planetary Science Letters* 192: 251–265.
- Zhao D (2004) Global tomographic images of mantle plumes and subducting slabs: Insight into deep Earth dynamics. *Physics of the Earth and Planetary Interiors* 146: 3–34.
- Zhong S (2006) Constraints on thermochemical convection of the mantle from plume heat flux, plume excess temperature, and upper mantle temperature. *Journal of Geophysical Research* 111: B04409. <http://dx.doi.org/10.1029/2005JB003972>.
- Zhou H-W and Anderson DL (1989) Search for deep slabs in the northwest Pacific mantle. *Proceedings of the National Academy of Sciences of the United States of America* 86: 8602–8606.
- Zhou H-W, Anderson DL, and Clayton RW (1990) Modeling of residual spheres for subduction zone earthquakes, 1: Apparent slab penetration signatures in the NW Pacific caused by deep diffuse mantle anomalies. *Journal of Geophysical Research* 95: 6799–6827.
- Zou Z, Leyton F, and Koper KD (2007) Partial melt in the lowermost mantle near the base of a plume. *Geophysical Journal International* 168: 809–817. <http://dx.doi.org/10.1111/j.1365-246X.2006.03266.x>.